FRACTURE DENSITY AND BRITTLENESS OF THE MESOZOIC FORMATIONS EXPOSED ON THE CANADIAN ESCARPMENT OF EASTERN NEW MEXICO

by

SCOTT ALEXANDER MOORE

Presented to the Faculty of the Graduate School of

The University of Texas at Arlington in Partial Fulfillment

of the Requirements

for the Degree of

MASTER OF SCIENCE IN PETROLEUM GEOSCIENCE

THE UNIVERSITY OF TEXAS AT ARLINGTON

AUGUST 2018

Acknowledgements

I would like to thank my thesis committee; Dr. John Wickham, Dr. Xinbao Yu, and Dr. Richard McMullen. Especially Dr. Wickham for his guidance and time invested advising me through this process. I would also like to thank my parents, James and Jeanne Moore, for all of the support they have provided me and always pushing intellectual curiosity. Without them constantly pushing me in different directions, academic and non-academic, I would not have ever known geology to be my passion in life.

May 03, 2018

Abstract

FRACTURE DENSITY AND BRITTLENESS OF THE MESOZOIC FORMATIONS EXPOSED ON THE CANADIAN ESCARPMENT OF EASTERN NEW MEXICO

Scott Alexander Moore, MS

The University of Texas at Arlington, 2018

Supervising Professor: John S. Wickham

Production of hydrocarbons from tight and unconventional reservoirs has become so prevalent, the need to understand rock fracture mechanics has become increasingly important. A specific research goal is the need to understand fracture density and brittleness and what can affect the two. Fracture density is defined as the fracture surface area per unit volume and is calculated from strain energies and material properties of the rocks. Brittleness has been defined as the fracture density at a particular strain state (Wickham et al., 2013).

There are three goals for this study. One is to use the dimensionless geomechanical fracture density equation, $\frac{F_d K_{IC}^2}{4\mu^2(1+\nu)} = A\frac{\upsilon}{1-2\upsilon} + B$, to test whether the strain conditions were constant in the sampled stratigraphic layers. If strain conditions were constant, then the data will plot as a straight line with a positive slope where A is the slope of the line and B is the intercept. A and B are estimates of the strain state as a function of the strain invariants.

Another goal is to compare a brittleness equation commonly used in the industry, $B_{19} = \frac{E_n + v_n}{2}$ (Equation 1), and the geomechanical equation, $F_d = \frac{4\mu^2(1+v)}{K_{IC}^2}\left[A\frac{v}{1-2v} + B\right]$(Equation 4). All layers were ranked according to their brittleness using the two equations. If the two methods are equivalent, the ranking should be the same. The advantage of the geomechanical equation (Equation 4) is that the results are based on established fracture mechanics equations and not intuitive relationships.

A third goal is to directly measure fracture toughness using a method recommended by the International Society of Rock Mechanics, the Cracked Chevron Notched Brazilian Disc Test (CCNBD) and compare those measured values with values calculated using an equation that correlates fracture toughness with Young's Modulus (Whittaker, 1993) and see if the two methods correlate with one another.

Fracture density measurements were taken at a road-cut in the Tucumcari Basin on the Canadian Escarpment in East Central New Mexico. The road-cut is located on NM Highway 104 and is about 30 miles east of Las Vegas, NM. Samples were collected and brought back to UTA to measure density, fracture toughness, and dynamic material properties (Poisson's Ratio, Young's Modulus, and Shear Modulus) calculated from P and S wave velocities.

Results show that the measured stratigraphic layers were subject to constant strain, the fracture density brittlness and the Jin et al., (2014) brittleness calculations did not correlate, and that the fracture toughness values obtained from the CCNBD did correlate well with the values obtained for fracture toughness using the Young's Modulus correlation equation (Whittaker et al., 1993).

Table of Contents

List of Illustrations

List of Tables

Chapter 1

Introduction

Over the past decade, the oil and gas industry has evolved through the emergence of new drilling and completion technologies that now allow companies to access and exploit oil and gas reserves that weren't previously accessible through standard drilling and completions practices. Hydraulic fracturing in horizontally drilled wells has created a new batch of questions to be answered and problems to be solved. Brittleness of rocks is an important variable in the oil and gas industry due to the rise of production through hydraulic fracturing in unconventional reservoirs. Another problem related to hydraulic fracturing is the definition of brittleness. There are many definitions of brittleness and not one is exactly the same (Jackson, Mehl, and Neuendorf, 2005; Jin et al, 2014; Kahraman and Altindag, 2004; Mullen et al., 2012; Wickham et al, 2013). In this thesis. brittleness is defined as fracture density at a particular strain state; this can be calculated from an equation based on geomechanical principles. The other definitions seem to be based on intuitive relationships.

As exploration and production companies continue making new discoveries and look back at older fields, research in this area will become critical for companies to understand how to produce hydrocarbons in an economic fashion.

In addition, fracture toughness of rocks is an important material property that has not been previously used in the industry to estimate brittleness. Using Fracture density (fracture surface area per unit volume) as the definition of brittleness, fracture toughness as well as the other material properties of the rock, such as Poisson's Ratio, Young's Modulus, and the Shear Modulus. Are all included (Wickham et al., 2013).

At this time, brittleness does not have a standard definition. Other ways used to predict brittleness are based on internal friction angle, Young's Modulus, Poisson's Ratio, and mineralogy. The Young's Modulus and Poisson's Ratio brittleness is often used in the industry and is defined by the following equation from Jin et al., (2014):

$$B_{19} = \frac{E_n + \upsilon_n}{2} \text{......Equation 1}$$

where E_n and υ_n are normalized dynamic Young's Modulus and Poisson's Ratio, and are defined as:

$$E_n = \frac{E - E_{min}}{E_{max} - E_{min}} \text{......Equation 2}$$

$$\upsilon_n = \frac{\upsilon_{max} - \upsilon}{\upsilon_{max} - \upsilon_{min}} \text{......Equation 3}$$

where E_{min} and E_{max} are the minimum and maximum dynamic Young's Modulus for the stratigraphic column (Triassic through Cretaceous in this case), ν_{min} and ν_{max} are the minimum and maximum for Poisson's Ratio for the column and are all constants. E and ν are Young's Modulus and Poisson's Ratio for the particular layers being measured and are variables. Equation 1 indicates the sample with highest Young's Modulus and lowest Poisson's Ratio has higher brittleness and is derived from the assumption that brittle materials experience both less axial strain and lateral strain (Jin et al., 2014).

In this thesis the fracture density and Young's Modulus/Poisson's Ratio definitions of brittleness are compared using the Mesozoic outcrops described in Ch 4.

Chapter 2

Purpose and Expected Results

The purpose of this study is to use the following geomechanical fracture density equation:

$$F_d = \frac{4\mu^2(1+\upsilon)}{K_{IC}^2}[A\frac{\upsilon}{1-2\upsilon} + B] \text{……. Equation 4}$$

to predict fracture density-brittleness at a particular strain state measured by A and B (See Table 1 for definitions of each variable). This equation assumes linear elasticity and that energy to create new fracture surface area comes from the elastic strain in the rock volume (Wickham, et al., 2013). By applying progressive uniaxial strain to samples with different material properties and using this equation, a brittleness graph can be created that shows the rock with largest fracture density at a particular strain state and therefore most brittle. The geomechanical measure of brittleness can then be compared to Equation 1. The purpose of brittleness evaluation is to identify formations of low, medium, and high brittleness, so that companies can better appraise a rock's potential for hydraulic fracturing (Rickman, et al., 2008). Using the geomechanical equation, brittleness is defined as the fracture density of a material at a specified strain state, so given two materials under the same strain state, the material with the higher fracture density is most brittle. Using Equation 1, the rock with the highest

Young's Modulus and the lowest Poisson's Ratio is most brittle. All layers will be ranked for brittleness using the two equations (Equations 1 and 4). If the two methods are equivalent, the ranking should be the same. Since the equations differ in the material properties that they use, we do not expect them to give the same results.

Another purpose is to use Equation 5, the dimensionless form of Equation 4, to test whether the strain conditions are constant from layer to layer or whether the ultimate strength has been reached.

$$\frac{F_d K_{IC}^2}{4\mu^2(1+\nu)} = A\frac{\upsilon}{1-2\upsilon} + B \ldots\ldots \text{ Equation 5}$$

Refer to Table 1 for definition of variables used. If strain conditions are constant and within the yield portion of the stress-strain curve, then the data will plot as a straight line with a positive slope where A and B are related to the strain invariants.

A third goal is to compare fracture toughness values obtained through the Cracked Chevron Notched Brazilian Disc Test method (CCNBD) with values obtained through a series of correlation equations from Whittaker et al., (1993). Because the CCNBD is a direct measure of fracture toughness we expect this to provide a test of the accuracy of the correlation equations and more accurate values for fracture toughness.

Chapter 3

Theoretical Formulation

Fracture density and brittleness are defined as fracture area per volume in units of $(\text{Length})^{-1}$. Table 1 lists all of the symbols used and their meaning.

Table 1 - Explanation of symbols used.

Symbol	Meaning
U	Energy
U_V	Strain energy in volume V
A	Area
G	Energy release rate
σ	Stress
ε	Strain
F_d	Fracture Density
U_a	Energy per fracture area created
μ	Elastic Shear Modulus

ν	Poisson's Ratio
E	Young's Modulus
ρ	Mass Density
V_p	Compressional wave velocity – P Wave velocity
V_s	Shear wave velocity – S Wave velocity
I_1	First strain invariant
I_2	Second strain invariant
$K_{IC}, K_{IIC}, K_{IIIC}$	Critical stress intensity factors for Mode I, II, III fractures for fracture toughness

Strain energy density is the area under a stress-strain curve:

$$U_v = \int_{t_0}^{\varepsilon_1} \sigma_x d\varepsilon_x \text{......Equation 6}$$

A.A. Griffith (1921) developed a fracture criteria based on strain energy and G.C. Sih (1985) has expanded on this creating a more comprehensive theory summarized as follows:

“The strain energy density theory in its most basic form can be formulated from the basic hypothesis that the surface and volume energy density of each material element are related by the rate of change of volume with surface.” (Sih 1985 p. 167).

Shown as a differential equation as:

$$\left(\frac{dA}{dV}\right)\left(\frac{dU}{dA}\right) = (\frac{dU}{dV})\text{……Equation 7}$$

where A is the fracture surface area, V is volume, and U is the strain energy. However, for this study, the integrated form over a volume element is used:

$$(F_d)(U_a) = (U_v)\text{……Equation 8}$$

where F_d = Fracture density (the fracture surface area in the volume of rock); U_a = energy per fracture area, which is considered a material property; U_v = strain energy in the volume of rock. U_a also accounts for all of the energy that goes into producing a new fracture surface area, energy dissipated as heat, acoustic emissions, and other crack growth in the process zone. U_a takes into account the energy associated with damage and plastic deformation emphasized by Busetti et al., (2012). U_v is understood to be the elastic strain energy associated with a volume. Below the elastic yield point U_v might be associated with closing cracks and a reduction of fracture density, while above the yield point U_v might be associated with increasing volume, fracture density, and plastic deformation. Additionally, above the yield point, the assumption is that the matrix material away from the fracture and damage zones continues to behave elastically, building elastic strain energy. Some of that elastic energy, U_v, is converted into fracture energy, so in this approach it should not matter whether the material yields in tension or compression. The important result of this theory is that fracture density measured over some volume of rock is a function of the strain energy in that same volume of rock at the time the fractures formed.

Strain energy density is expressed as:

$$U_v = \frac{1}{2}\left(\sigma_{xx}\varepsilon_{xx} + \sigma_{yy}\varepsilon_{yy} + \sigma_{zz}\varepsilon_{zz}\right) + (\sigma_{xy}\varepsilon_{xy} + \sigma_{yz}\varepsilon_{yz} + \sigma_{zx}\varepsilon_{zx}) \ldots\ldots \text{Equation 9}$$

The assumption is made that up to the yield point all strain energy is elastic, and above the yield point, the matrix material away from the damage zones is also deforming elastically. Some of the elastic strain energy in the matrix is now used to create more fracture surface instead of elastic distortion. Another assumption is that U_a, the energy per fracture area, is constant for a particular rock type since it is related to fracture toughness, which tends to be constant for a particular material. Linear elasticity is also assumed, so substituting the equations for linear elasticity into Equation 9, the strain energy density in a particular rock volume of constant elastic properties is:

$U_v = \frac{v\mu}{1-2v}(\varepsilon_{xx} + \varepsilon_{yy} + \varepsilon_{zz})^2 + \mu\left(\varepsilon_{xx}^2 + \varepsilon_{yy}^2 + \varepsilon_{zz}^2\right) + 2\mu(\varepsilon_{xy}^2 + \varepsilon_{yz}^2 +$

$\varepsilon_{xz}^2)$……Equation 10

where U_v is the elastic strain energy (some of which can be used to create fracture surface area), Nu (v) is Poisson's ratio, and Mu (μ) is the Shear Modulus. Written in terms of the strain invariants, Equation 10 becomes:

$$U_v = \mu(A\frac{v}{1-2v} + B) \text{……Equation 11}$$

The strain invariants are as follows:

$$I_1 = \varepsilon_1 + \varepsilon_2 + \varepsilon_3$$

$$I_2 = \varepsilon_1\varepsilon_2 + \varepsilon_2\varepsilon_3 + \varepsilon_3\varepsilon_1$$

Rewriting A and B in Equation 11 in terms of the strain invariants gives:

$$A = I_1^2 = \varepsilon_1^2 + \varepsilon_2^2 + \varepsilon_3^2(\varepsilon_1\varepsilon_2 + \varepsilon_2\varepsilon_3 + \varepsilon_3\varepsilon_1)$$

$$B = \varepsilon_1^2 + \varepsilon_2^2 + \varepsilon_3^2 = I_1^2 - 2I_2$$

Substitute Equation 11 into Equation 8 and we get:

$$F_d = \frac{\mu}{U_a}(A\frac{v}{1-2v} + B) \text{……Equation 12}$$

And rewriting Equation 12 yields the dimensionless form:

$$\frac{F_d U_a}{\mu} = (A\frac{v}{1-2v} + B)\text{......Equation 13}$$

If the strain state represented by A and B is constant, then the measurements of fracture density and the material properties should plot as a straight line with a positive slope.

U_a, the fracture surface energy, is related to the critical energy release rate G_c. For brittle-elastic materials, the following equation can be derived (Bakers T., 2005):

$$G_c = 2U_a\text{......Equation 14}$$

There is a critical stress intensity factor associated with each mode of fracturing. The critical stress intensity factor is dependent on sample geometry, size and location of the crack, and the magnitude and distribution of load on the material. Irwin (1985) showed the equivalence of the energy release rate and the stress intensity factor, which is expressed as:

$$G_c = \frac{K_{IC}^2}{2\mu(1+v)} + \frac{K_{IIC}^2}{2\mu(1+v)} + \frac{K_{IIIC}^2}{2\mu}\text{......Equation 15}$$

Since we measure joints in the field, we assume Mode 1 fractures (opening mode fractures) dominate, so Equation 15 can be simplified to:

$$G_c = \frac{K_{IC}^2}{2\mu(1+v)} \ldots\ldots \text{Equation 16}$$

Combining Equations 14 and 16 gives:

$$U_a = \frac{K_{IC}^2}{4\mu(1+v)} \ldots\ldots \text{Equation 17}$$

Equation 12 becomes:

$$F_d = \frac{4\mu^2(1+v)}{K_{IC}^2}\left(A\frac{v}{1-2v} + B\right) \ldots\ldots \text{Equation 18}$$

And Equation 13 becomes:

$$\frac{F_d K_{IC}^2}{4\mu^2(1+v)} = \left(A\frac{v}{1-2v} + B\right) \ldots\ldots \text{Equation 19}$$

(Derivations from Wickham, et al, 2013).

Chapter 4

Geologic Background

The study area is located in the Tucumcari Basin on the Canadian Escarpment in East Central New Mexico along NM Highway 104 about 30 miles east of Las Vegas, NM (Figure 1). All the stratigraphic units used in this study are Triassic through lower Cretaceous in age (Figure 2). The following is an overview of each of the formations found in the area surrounding Las Vegas, New Mexico.

Triassic

The Chinle Formation lies conformably above the Santa Rosa Sandstone. Baltz (1972) divided the formation into three members in the Las Vegas area: a lower shale member, middle sandstone member, and an upper shale member. The Chinle was deposited in fluvial channels and floodplains, which is shown by fluvial cross-stratification, ancient channels, and lithology of its members. There are also numerous deposits of petrified wood in the middle sandstone member, (Lessard and Bejnar, 1976).

Jurassic

There are three Jurassic units in the Las Vegas area. The Entrada Sandstone, Todilto Limestone, and the Morrison Formation. The Entrada Sandstone is a pale orange sandstone that lies unconformably over the Chinle Formation. It has also been referred to as the Exeter and Ocate Sandstone. It is a fine- to medium-grained, feldspathic quartz arenite, varies from thin to thick beds, and contains some cross laminations (Lessard and Bejnar, 1976). The Entrada Sandstone was deposited in a lacustrine environment in the Las Vegas area and in an eolian environment in the Tucumcari Basin area.

The Todilto Limestone lies conformably on the Entrada Sandstone. It contains limy siltstone and shale and is medium to dark gray and thinly bedded. It was deposited in a lacustrine environment with little influence from terrestrial sedimentation (Lessard and Bejnar, 1976).

The Morrison Formation overlies the Todilto Limestone both conformably and unconformably and is divided into three members in the Las Vegas area. The lower member contains thin, alternating beds of claystone, siltstone, dolostone, limestone, and quartz arenite. It also contains bentonite and channel deposits. The middle member contains thick quartz arenites that alternate with mudstones and quartz rudites, with cross-stratification and channeling. Alternating claystones, siltstones, and arenites containing channeling and cross-stratification make up the upper member. In the Las Vegas area, the Morrison Formation is a fluvial unit that was deposited in channels, lakes, and floodplains (Lessard and Bejnar, 1976). In the Tucumcari Basin the Morrison is made up of thick sandstones and conglomerates (Wanek, 1962).

Cretaceous

The Dakota Group overlies the Morrison paraconformably, meaning there is no apparent erosion - the beds lie parallel to one another (non-depositional unconformity). In the Las Vegas area, the Dakota Group is divided into three units: a lower sandstone, middle shale, and upper sandstone. The Lower Sandstone is a pale, grayish-orange to very light gray, conglomeratic to fine-grained, cross-stratified, quartz arenite that was deposited on a piedmont plain at the foot of mountains with sediment deposited by shifting streams. The Middle Shale unit is silty, fine-grained, quartz arenite and black carbonaceous shale deposited on a swampy coastal plain. The Upper Sandstone is light to dark gray, fine- to medium grained quartz arenite containing carbonized wood fragments and was deposited in a beach/lagoon complex (Lessard and Bejnar, 1976).

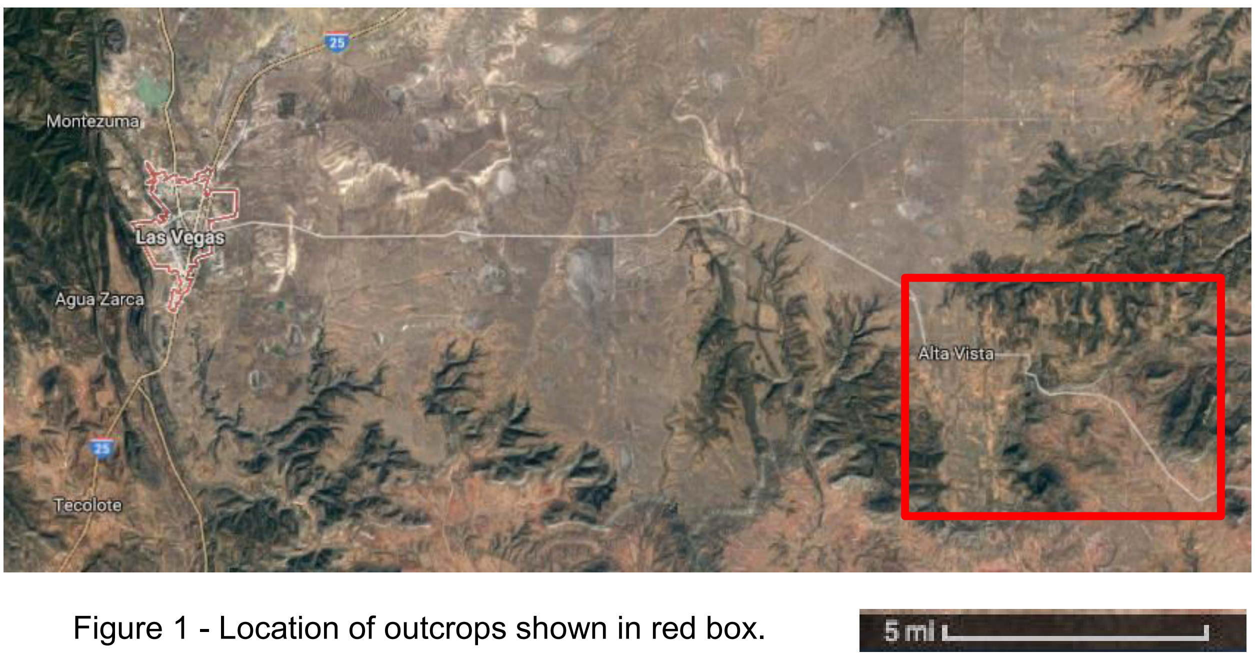

Figure 1 - Location of outcrops shown in red box.

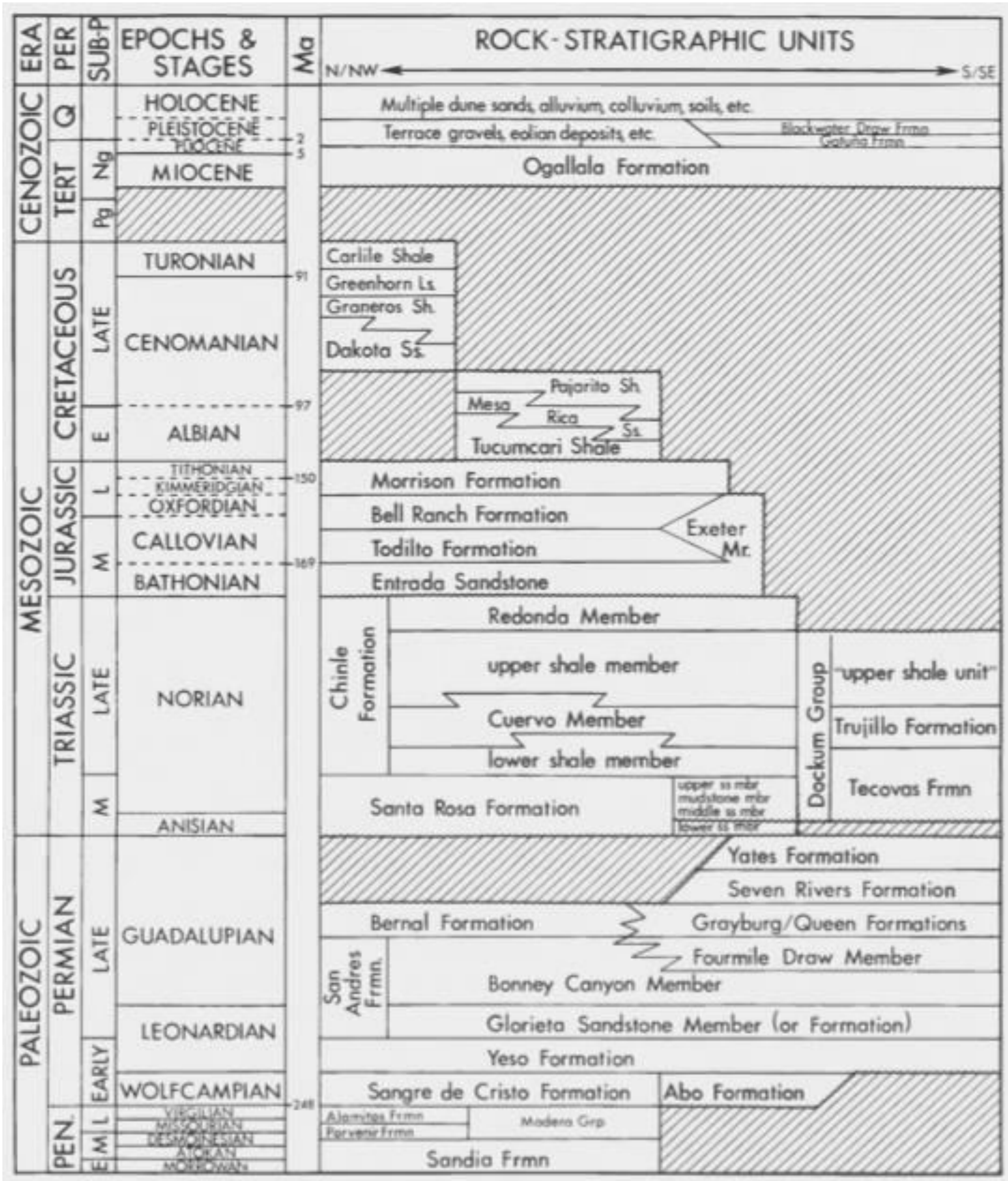

Figure 2 - Stratigraphic succession of road-cut formations. Relevant formations are Dakota Sandstone, Morrison Formation, Todilto Formation, Entrada Sandstone, Chinle Formation, and the Santa Rosa Formation, which are all Mesozoic in age. (Lucas and Kues, 1985).

Chapter 5

Methods and Data

Fracture densities were measured using scan lines on roadcuts located in the Tucumcari Basin on the Canadian Escarpment in East Central New Mexico. The road-cut studied is located on NM Highway 104 and is about 30 miles east of Las Vegas, NM (Figure 1). All the stratigraphic units used in this study are Triassic through lower Cretaceous in age (Figure 2). The outcrops are located in relatively close proximity to each other, so if each layer was subject to the same strain, then Equation 19 will plot as a straight line with a positive slope. This means the layers cannot be curved and must be deformed under extension. To avoid measuring fractures created by dynamite blasting areas around drill holes were avoided. Figure 3 shows the three different modes of fracturing:

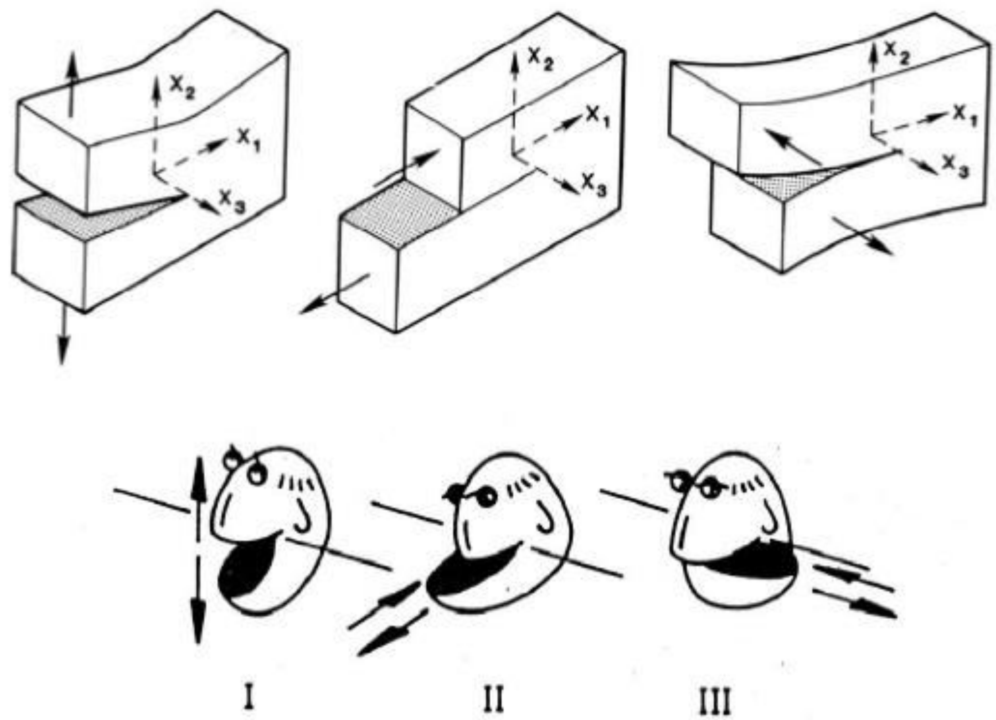

Figure 3 - Fracture modes from Kanninen and Popelar (1985): opening Mode I, sliding Mode II, and tearing Mode III.

Once fracture densities were measured, a rock sample was taken from each layer that was measured to bring back to UTA. Samples were cut in order to measure density, fracture toughness, and dynamic elastic properties in Dr. Griffith's Geomechanics Lab in the Geoscience Building and Dr. Yu's Materials Characterization Lab in the Engineering Complex.

5.1 Field Measurements

The method for measuring fracture density in outcrops in the field is described in Chiles et al., (2008). The following is a list of the measurements that were made:

1. GPS position of outcrop;
2. The distance at which the fracture intersects the scanline;
3. The length of the fracture in the layer;
4. Fracture orientation;
5. Thickness of the layer being measured;
6. Orientation of the layer;
7. Orientation of the scanline;
8. Orientation of the surface containing the scanline;
9. Any curvature or faults associated with the bed were noted if present.

Length of each scanline varies for each stratigraphic layer because it is dependent on fracture spacing within each layer. The scanline length needs to be long enough so there is an adequate statistical sample of the fractures. All of the outcrops measured were in the same locale in the Tucumcari Basin on the Canadian Escarpment in East Central New Mexico on NM Highway 104 about 30 miles east of Las Vegas, NM (Figure 1). The fracture densities for the field measurements were calculated using spreadsheets that take into account the strike, dip, bed thickness, scanline length, scanline trend and plunge, the length of the fractures and the spacing between the fractures. For joints measured on surfaces perpendicular to bedding, the length of the fractures was weighted by dividing by the bedding thickness. For fractures measured on bedding surfaces, the fractures were weighted by dividing by the longest fracture. All fractures then had a dimensionless value between 0 and 1. Fracture density was calculated by taking the sum of the fracture length weighting, which is the individual fracture length divided by the maximum value of the fracture lengths for all scanlines at that individual station. There is also an orientation bias. Joints perpendicular to the scan line are sampled correctly while those at angle are sampled less. This was corrected by finding the angle ξ between the vector represented by the scanline and the vector represented by the perpendicular to the joint. The weighted joint length was multiplied by the Cos ξ so the perpendicular fractures received a weight of 1 while the parallel fractures received a weight of zero.

The result was a series of weighted, dimensionless numbers between 0 and 1. These were added together for each scanline in a layer and divided by the total length of scanlines for that layer to get the fracture density in units of M^{-1}

5.1.1 Day 1; 5-21-17

The first set of beds measured, 5-21-17A, 5-21-17B, and 5-21-17C, were all in the Dakota Formation, which is Cretaceous in age, and were moderately sorted with grain size ranging from medium to coarse. Station 5-21-17A and station 5-21-17C were both measured parallel to the bedding plane. Station 5-21-17A, was measured on the top of the Dakota Formation (Figure 4). Bed thickness was approximately 40 feet, had a strike of 298 degrees and a dip of 5 degrees. The scanline was approximately 30 feet long. The average fracture length was 5.27 feet and fracture density was 0.45 m^{-1} (Table 2). The strike orientation of the joint sets were predominantly in the N-S, E-W directions (Figure 5).

Station 5-21-17B was measured on the base of the Dakota and had a bed thickness of approximately 15 feet, strike of 298 degrees, and dip of 5 degrees, while the strike of the outcrop was 80 degrees with a dip of 90 degrees (Figure 6). Fracture length averaged out at 2.59 feet and fracture density is 1.44 m^{-1} (Table 3) with a strike orientation of the joint sets mostly in the N-S direction (Figure 7).

Station 5-21-17C was also measured on the base of the Dakota and had a bed thickness of 5 feet with a strike of 340 degrees dipping at 12 degrees (Figure 8). Average fracture length was 1.92 feet and fracture density is 1.12 m^{-1} (Table 4) with joint set's strike orientation of N-S and E-W with lots of scatter (Figure 9). Samples from each bed were collected and brought back to perform various lab tests to obtain material property measurements.

Figure 4 - Dakota Sandstone. Measured parallel to bedding; Station 5-21-17A.

Table 2 - Fracture density measurements from the Dakota Sandstone; 5-21-17A.

Station	UTM Coordinates	Strike of Outcrop (Right Hand Rule)	Dip of Outcrop (Right Hand Rule)	Thickness of Bed (Ft)	Thickness of Bed (M)	Strike of Bed (Right Hand Rule)	Dip of Bed (Right Hand Rule)	Sample strike (right hand rule)	Sample dip (right hand rule)	Bed Curvature	Rock Description			
5-21-17A	527133; 393127	298	5	10.00	3.048	298	5	NA	NA	None	SS medium sorted			
	Scanline #	Start Ft	End ft	Trend Scanline	Plunge Scanline	scanline length (M)	Scanline Vector x = North	Scanline Vector y = East	Scanline Vector z = down		Dakota Fm			
	1	0	29	265	2	8.8392	-0.09	-1.00	0.03					
		Fracture Distance (Ft)	Fracture Distance (M)	Fracture Length (Ft)	Fracture Length Weighting	Fracture Strike	Fracture Dip	Fracture Vector x coord	Fracture Vector y coord	Fracture Vector z coord	Weighting factor for fracture density		New Weighting factor for fracture density	COS of angle between Scanline & Fracture Vector
5-21-17A	1	1.4	0.42672	15.00	0.63	160	85	0.34	0.94	0.09	0.65		0.067782033	-0.96
5-21-17A	1	6.4	1.95072	18	0.75	166	90	0.24	0.97	0.00	0.76		0.08375362	-0.99
5-21-17A	1	9.6	2.92608	18	0.75	164	84	0.27	0.96	0.10	0.77		0.082474124	-0.97
5-21-17A	1	9.4	2.86512	9.5	0.40	164	84	0.27	0.96	0.10	0.41		0.04352801	-0.97
5-21-17A	1	11.6	3.53568	14	0.58	166	80	0.24	0.96	0.17	0.60		0.063752117	-0.97
5-21-17A	1	14.5	4.4196	24	1.00	170	90	0.17	0.98	0.00	1.00		0.112633252	-1.00
5-21-17A	1	16.2	4.93776	1.03	0.04	188	90	-0.14	0.99	0.00	0.04		0.004727944	-0.97
5-21-17A	1	16.9	5.15112	1	0.04	174	90	0.10	0.99	0.00	0.04		0.004710261	-1.00
5-21-17A	1	18.6	5.66928	0.83	0.03	185	90	-0.09	1.00	0.00	0.04		0.003850709	-0.98
5-21-17A	1	19.3	5.88264	12	0.50	170	90	0.17	0.98	0.00	0.50		0.056316626	-1.00
5-21-17A	1	20	6.096	8	0.33	207	76	-0.44	0.86	0.24	0.41		0.030693322	-0.81
5-21-17A	1	21.3	6.49224	12	0.50	165	81	0.26	0.95	0.16	0.52		0.054678654	-0.97
5-21-17A	1	22.1	6.73608	1.5	0.06	168	90	0.21	0.98	0.00	0.06		0.007013796	-0.99
5-21-17A	1	23.2	7.07136	1.5	0.06	135	90	0.71	0.71	0.00	0.08		0.005413229	-0.77
5-21-17A	1	25.1	7.65048	12	0.50	167	90	0.22	0.97	0.00	0.51		0.055981583	-0.99
5-21-17A	1	24.9	7.58952	8	0.33	170	40	0.11	0.63	0.77	0.54		0.023124904	-0.61
5-21-17A	1	25.8	7.86384	0.5	0.02	170	90	0.17	0.98	0.00	0.02		0.002346526	-1.00
5-21-17A	1	26.7	8.13816	0.5	0.02	170	90	0.17	0.98	0.00	0.02		0.002346526	-1.00
5-21-17A	1	27	8.2296	4.7	0.20	172	90	0.14	0.99	0.00	0.20		0.022111256	-1.00
5-21-17A	1	28.1	8.56488	1.5	0.06	166	90	0.24	0.97	0.00	0.06		0.006979468	-0.99
5-21-17A	1	28.3	8.62584	0.83	0.03	120	90	0.87	0.50	0.00	0.06		0.002242748	-0.57
											Line 1 Fractures	0.70		
	Scanline #	Start Ft	End ft	Trend Scanline	Plunge Scanline	scanline length (M)	Scanline Vector x = North	Scanline Vector y = East	Scanline Vector z = down					
	2	0	24	165	5	7.3152	-0.96	0.26	0.09					
		Fracture Distance (Ft)	Fracture Distance (M)	Fracture Length (Ft)	Fracture Length Weighting	Fracture Strike	Fracture Dip	Fracture Vector x coord	Fracture Vector y coord	Fracture Vector z coord	Weighting factor for fracture density			COS of angle between Scanline & Fracture Vector
Sta 1	2	0	0	1.3	0.05	72	70	0.89	-0.29	0.34	0.06		0.006701414	-0.91
Sta 2	2	1.7	0.51816	1.7	0.07	80	90	0.98	-0.17	0.00	0.07		0.009609481	-0.99
Sta 2	2	5.4	1.64592	1.9	0.08	73	90	0.96	-0.29	0.00	0.08		0.010774466	-1.00
Sta 2	2	13.3	4.05384	2	0.08	120	90	0.87	0.50	0.00	0.12		0.00802457	-0.70
Sta 2	2	14.7	4.48056	5.6	0.23	82	80	0.98	-0.14	0.17	0.24		0.030576936	-0.96
Sta 2	2	22.2	6.76656	2	0.08	70	90	0.94	-0.34	0.00	0.08		0.011305272	-0.99
Sta 2	2	22.3	6.79704	1	0.04	108	90	0.95	0.31	0.00	0.05		0.004758808	-0.84
Sta 2	2	23	7.0104	4.8	0.20	90	90	1.00	0.00	0.00	0.21		0.02630824	-0.96
Sta 2	2	23.4	7.13232	4	0.17	85	88	1.00	-0.09	0.03	0.17		0.022269178	-0.98
											Line 2 Fractures	0.14		
											Outcrop Fracture Density without COS weighting factor (2)	0.447994561		

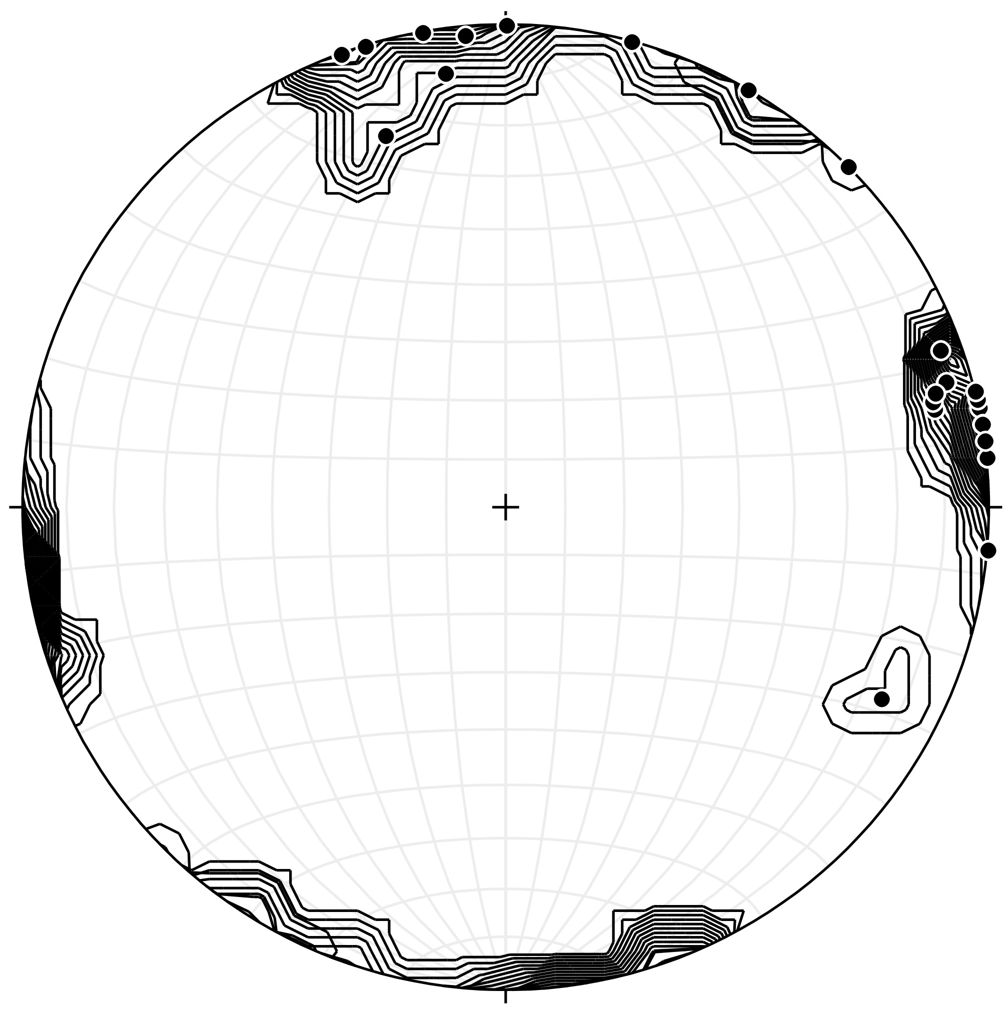

Figure 5 - Stereonet of poles to joints. North at top station; Station 5-21-17A.

Figure 6 - Dakota Sandstone. Bed measured outlined in red box; Station 5-21-17B.

Table 3 - Fracture Density measurements from the Dakota Sandstone; Station 5-21-17B.

Station	UTM Coordinates	Strike of Outcrop (Right Hand Rule)	Dip of Outcrop (Right Hand Rule)	Thickness of Bed (Ft)	Thickness of Bed (M)	Strike of Bed (Right Hand Rule)	Dip of Bed (Right Hand Rule)	Sample strike (right hand rule)	Sample dip (right hand rule)	Bed Curvature/faulting	Rock Description			
5-21-17B	527205;383127	91	90	7.00	2.1336	298	5	NA	NA	None/yes	SS - Lower Dakota			
	Scanline #	Start Ft	End ft	Trend Scanline	Plunge Scanline	scanline length (M)	Scanline Vector x = North	Scanline Vector y = East	Scanline Vector z = down					
	1	0	9.5	91	0	2.8956	-0.02	1.00	0.00					
		Fracture Distance (Ft)	Fracture Distance (M)	Fracture Length (Ft)	Fracture Length Weighting	Fracture Strike	Fracture Dip	Fracture Vector x coord	Fracture Vector y coord	Fracture Vector z coord	Weighting factor for fracture density		New Weighting factor for fracture density	COS of angle between Scanline & Fracture Vector
Max(Imax	1	1.9	0.57912	7.00	1.00	176	80	0.07	0.98	0.17	1.02		0.3388107	0.98
	1	2	0.6096	0.8	0.11	200	68	-0.32	0.87	0.37	0.13		0.034601052	0.88
	1	2.3	0.70104	2.5	0.36	172	87	0.14	0.99	0.05	0.36		0.121654376	0.99
	1	2.9	0.88392	0.6	0.09	174	82	0.10	0.98	0.14	0.09		0.029094984	0.98
	1	3.1	0.94488	2.5	0.36	180	85	0.00	1.00	0.09	0.36		0.122851787	1.00
	1	3.3	1.00584	2.1	0.30	208	83	-0.47	0.88	0.12	0.34		0.091625062	0.88
	1	5.2	1.58496	1.5	0.21	205	65	-0.38	0.82	0.42	0.26		0.061271784	0.83
	1	6.1	1.85928	0.5	0.07	195	57	-0.22	0.81	0.54	0.09		0.020073769	0.81
	1	6.2	1.88976	1.1	0.16	187	60	-0.11	0.86	0.50	0.18		0.046741329	0.86
	1	6.4	1.95072	0.9	0.13	175	81	0.09	0.98	0.16	0.13		0.043615432	0.98
	1	6.8	2.07264	0.5	0.07	168	71	0.20	0.92	0.33	0.08		0.02272623	0.92
	1	7.1	2.16408	0.25	0.04	190	76	-0.17	0.96	0.24	0.04		0.011830271	0.96
	1	7.25	2.2098	1.11	0.16	150	85	0.50	0.86	0.09	0.19		0.046762335	0.85
	1	9.1	2.77368	1.1	0.16	187	85	-0.12	0.99	0.09	0.16		0.053766857	0.99
											Line 1 Fractures	1.11		
	Scanline #	Start Ft	End ft	Trend Scanline	Plunge Scanline	scanline length (M)	Scanline Vector x = North	Scanline Vector y = East	Scanline Vector z = down					
	2	0	4.5	185	0	1.3716	-1.00	-0.09	0.00					
		Fracture Distance (Ft)	Fracture Distance (M)	Fracture Length (Ft)	Fracture Length Weighting	Fracture Strike	Fracture Dip	Fracture Vector x coord	Fracture Vector y coord	Fracture Vector z coord	Weighting factor for fracture density			COS of angle between Scanline & Fracture Vector
Sta 1	2	0	0	1.6	0.2285714	244	90	-0.90	0.44	0.00	0.27		0.142843361	0.86
Sta 2	2	1.6	0.48768	1.6	0.2285714	290	70	-0.88	-0.32	0.34	0.25		0.151259988	0.91
Sta 2	2	2	0.6096	2.4	0.3428571	270	87	-1.00	0.00	0.05	0.34		0.248676277	0.99
Sta 2	2	2.6	0.79248	1.5	0.2142857	266	70	-0.94	0.07	0.34	0.23		0.145001163	0.93
Sta 2	2	3.5	1.0668	1.1	0.1571429	266	76	-0.97	0.07	0.24	0.16		0.109797187	0.96
Sta 2	2	4.4	1.34112	2.9	0.4142857	260	86	-0.98	0.17	0.07	0.43		0.291042927	0.96
											Line 2 Fractures	1.16		
	Scanline #	Start Ft	End ft	Trend Scanline	Plunge Scanline	scanline length (M)	Scanline Vector x = North	Scanline Vector y = East	Scanline Vector z = down					
	3	0	13	98	0	3.9624	-0.14	0.99	0.00					
		Fracture Distance (Ft)	Fracture Distance (M)	Fracture Length (Ft)	Fracture Length Weighting	Fracture Strike	Fracture Dip	Fracture Vector x coord	Fracture Vector y coord	Fracture Vector z coord	Weighting factor for fracture density			COS of angle between Scanline & Fracture Vector
	3	0	0	2.9	0.4142857	170	90	0.17	0.98	0.00	0.44		0.09943599	0.95
	3	1	0.3048	1.3	0.1857143	170	78	0.17	0.96	0.21	0.20		0.043601127	0.93
	3	1.3	0.39624	0.5	0.0714286	170	73	0.17	0.94	0.29	0.08		0.016395184	0.91
	3	1.55	0.47244	1.4	0.2	148	85	0.53	0.84	0.09	0.26		0.038518545	0.76
	3	2.2	0.67056	3	0.4285714	173	85	0.12	0.99	0.09	0.45		0.104076554	0.96
	3	3.35	1.02108	2.9	0.4142857	165	80	0.25	0.95	0.17	0.46		0.094780541	0.91
	3	6.35	1.93548	5	0.7142857	140	84	0.64	0.76	0.10	1.07		0.119960673	0.67
	3	7.35	2.24028	7	1	176	85	0.07	0.99	0.09	1.03		0.245917993	0.97
	3	8.1	2.46888	1.75	0.25	85	30	0.50	-0.04	0.87	2.22		0.007096427	-0.11
	3	8.5	2.5908	0.5	0.0714286	171	60	0.14	0.86	0.50	0.09		0.01492934	0.83
	3	8.9	2.71272	2.8	0.4	170	75	0.17	0.95	0.26	0.44		0.09273673	0.92
	3	9	2.7432	0.5	0.0714286	168	64	0.19	0.88	0.44	0.08		0.015225082	0.84
	3	9.3	2.83464	0.5	0.0714286	177	90	0.05	1.00	0.00	0.07		0.017695394	0.98
	3	9.5	2.8956	3	0.4285714	175	90	0.09	1.00	0.00	0.44		0.105387435	0.97
	3	11	3.3528	2	0.2857143	171	87	0.16	0.99	0.05	0.30		0.068861164	0.95
	3	11.1	3.38328	2.5	0.3571429	171	78	0.15	0.97	0.21	0.38		0.084311024	0.94
	3	12	3.6576	3	0.4285714	181	82	-0.02	0.99	0.14	0.44		0.106308597	0.98
	3	12.6	3.84048	4.5	0.6428571	177	90	0.05	1.00	0.00	0.65		0.159258542	0.98
											Line 3 Fractures	1.62		
	Scanline #	Start Ft	End ft	Trend Scanline	Plunge Scanline	scanline length (M)	Scanline Vector x = North	Scanline Vector y = East	Scanline Vector z = down					
	4	0	4	175	0	1.2192	-1.00	0.09	0.00					
		Fracture Distance (Ft)	Fracture Distance (M)	Fracture Length (Ft)	Fracture Length Weighting	Fracture Strike	Fracture Dip	Fracture Vector x coord	Fracture Vector y coord	Fracture Vector z coord	Weighting factor for fracture density			COS of angle between Scanline & Fracture Vector
	4	0	0	7	1	272	90	-1.00	-0.03	0.00	1.01		0.814096253	0.99
Sta 4	4	1.8	0.54864	1.4	0.2	270	90	-1.00	0.00	0.00	0.20		0.163417765	1.00
Sta 4	4	2.5	0.762	1.3	0.1857143	267	82	-0.99	0.05	0.14	0.19		0.150750407	0.99
Sta 4	4	3.9	1.18872	7	1	280	85	-0.98	-0.17	0.09	1.04		0.789247201	0.96
											Line 4 Fractures	1.96		
											Outcrop Fracture Density without COS weighting factor (2)	1.440999311		

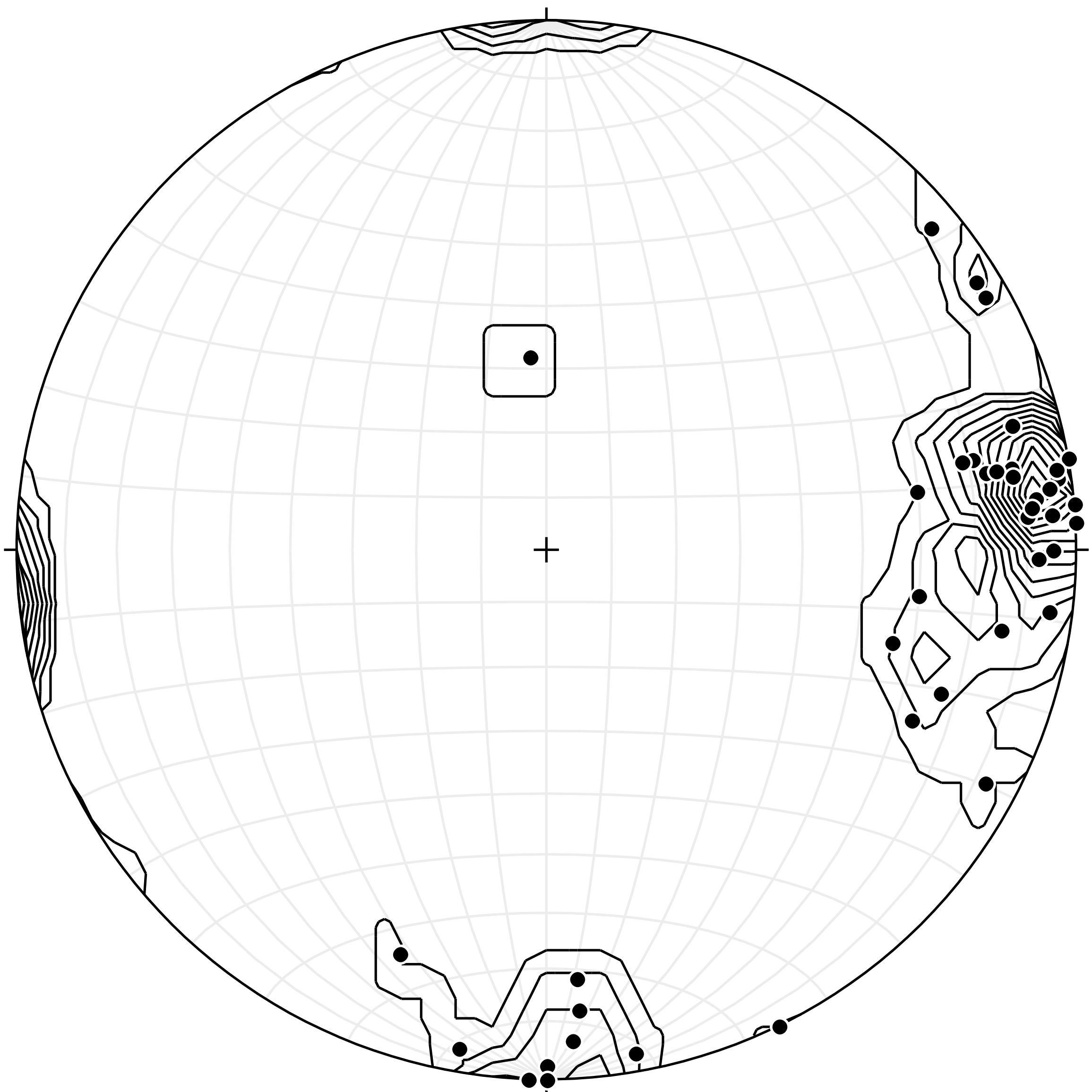

Figure 7 - Stereonet of poles to joints. Station 5-21-17B.

Figure 8 - Dakota Sandstone. Measured parallel to bedding; Station 5-21-17C.

Table 4 - Fracture Density measurements from the Dakota Sandstone; Station 5-21-17C.

Station	UTM Coordinates	Strike of Outcrop (Right Hand Rule)	Dip of Outcrop (Right Hand Rule)	Thickness of Bed (Ft)	Thickness of Bed (M)	Strike of Bed (Right Hand Rule)	Dip of Bed (Right Hand Rule)	Sample strike (right hand rule)	Sample dip (right hand rule)	Bed Curvature	Rock Description			
5-21-17C	527153; 3931300	340	12	5.00	1.524	340	12	NA	NA	None	SS			
	Scanline #	Start Ft	End ft	Trend Scanline	Plunge Scanline	scanline length (M)	Scanline Vector x = North	Scanline Vector y = East	Scanline Vector z = down		Base Dakota			
	1	0	18	115	4	5.4864	-0.42	0.90	0.07					
		Fracture Distance (Ft)	Fracture Distance (M)	Fracture Length (Ft)	Fracture Length Weighting	Fracture Strike	Fracture Dip	Fracture Vector x coord	Fracture Vector y coord	Fracture Vector z coord	Weighting factor for fracture density		New Weighting factor for fracture density	COS of angle between Scanline & Fracture Vector
5-21-17C	1	0	0	1.50	0.22	25	55	0.35	-0.74	0.57	0.28		0.031246219	-0.78
5-21-17C	1	1.4	0.42672	2	0.29	25	87	0.42	-0.91	0.05	0.30		0.053208905	-0.99
5-21-17C	1	2.2	0.67056	2	0.29	15	80	0.25	-0.95	0.17	0.31		0.051215987	-0.96
5-21-17C	1	3.5	1.0668	2	0.29	335	90	-0.42	-0.91	0.00	0.46		0.034374936	-0.64
5-21-17C	1	4.6	1.40208	0.5	0.07	75	90	0.97	-0.26	0.00	0.11		0.008593734	-0.64
5-21-17C	1	6.6	2.01168	1	0.15	24	90	0.41	-0.91	0.00	0.15		0.026734881	-1.00
5-21-17C	1	6.9	2.10312	0.2	0.03	350	90	-0.17	-0.98	0.00	0.04		0.004380654	-0.82
5-21-17C	1	7	2.1336	0.5	0.07	345	81	-0.26	-0.95	0.16	0.10		0.009969274	-0.74
5-21-17C	1	7.5	2.286	1.6	0.24	346	90	-0.24	-0.97	0.00	0.30		0.033248112	-0.78
5-21-17C	1	8	2.4384	1.8	0.26	60	90	0.87	-0.50	0.00	0.32		0.039425883	-0.82
5-21-17C	1	9.2	2.80416	0.5	0.07	65	86	0.90	-0.42	0.07	0.10		0.010151451	-0.76
5-21-17C	1	9.6	2.92608	0.5	0.07	4	80	0.07	-0.98	0.17	0.08		0.012129519	-0.91
5-21-17C	1	10.4	3.16992	6.5	0.96	325	65	-0.52	-0.74	0.42	2.26		0.073623304	-0.42
5-21-17C	1	14.6	4.45008	6.8	1.00	358	90	-0.03	-1.00	0.00	1.13		0.162007159	-0.89
5-21-17C	1	15.4	4.69392	2.8	0.41	354	90	-0.10	-0.99	0.00	0.48		0.064175319	-0.86
5-21-17C	1	15.6	4.75488	0.5	0.07	355	90	-0.09	-1.00	0.00	0.09		0.011578307	-0.86
5-21-17C	1	16.2	4.93776	1.4	0.21	355	90	-0.09	-1.00	0.00	0.24		0.032419258	-0.86
5-21-17C	1	17.7	5.39496	0.8	0.12	40	75	0.62	-0.74	0.26	0.13		0.019571081	-0.91
5-21-17C	1	18	5.4864	4	0.59	346	90	-0.24	-0.97	0.00	0.76		0.08312028	-0.78
											Line 1 Fracture Density	0.99		
	Scanline #	Start Ft	End ft	Trend Scanline	Plunge Scanline	scanline length (M)	Scanline Vector x = North	Scanline Vector y = East	Scanline Vector z = down					
	2	0	8.8	358	4	2.68224	1.00	-0.03	0.07					
		Fracture Distance (Ft)	Fracture Distance (M)	Fracture Length (Ft)	Fracture Length Weighting	Fracture Strike	Fracture Dip	Fracture Vector x coord	Fracture Vector y coord	Fracture Vector z coord	Weighting factor for fracture density			COS of angle between Scanline & Fracture Vector
5-21-17C	2	0.5	0.1524	0.5	0.07	255	90	-0.97	0.26	0.00	0.08		0.026645764	-0.97
5-21-17C	2	0.9	0.27432	0.9	0.13	270	90	-1.00	0.00	0.00	0.13		0.049193997	-1.00
5-21-17C	2	1.3	0.39624	1	0.15	318	90	-0.67	-0.74	0.00	0.23		0.035156185	-0.64
5-21-17C	2	1.6	0.48768	0.75	0.11	280	90	-0.98	-0.17	0.00	0.11		0.040123601	-0.98
5-21-17C	2	1.7	0.51816	1	0.15	299	75	-0.84	-0.47	0.26	0.18		0.044294017	-0.81
5-21-17C	2	1.9	0.57912	4	0.59	273	90	-1.00	-0.05	0.00	0.59		0.217940759	-0.99
5-21-17C	2	2.5	0.762	0.9	0.13	256	90	-0.97	0.24	0.00	0.14		0.048148321	-0.98
5-21-17C	2	2.7	0.82296	3	0.44	268	63	-0.89	0.03	0.45	0.51		0.1409874	-0.86
5-21-17C	2	4.1	1.24968	2	0.29	295	78	-0.89	-0.41	0.21	0.34		0.093744045	-0.85
5-21-17C	2	4.3	1.31064	0.5	0.07	298	65	-0.80	-0.43	0.42	0.10		0.020655839	-0.75
5-21-17C	2	4.5	1.3716	0.75	0.11	295	90	-0.91	-0.42	0.00	0.12		0.036549075	-0.89
5-21-17C	2	5	1.524	6.7	0.99	303	20	-0.29	-0.19	0.94	4.61		0.078586663	-0.21
5-21-17C	2	5.3	1.61544	0.5	0.07	252	90	-0.95	0.31	0.00	0.08		0.026287294	-0.96
5-21-17C	2	7.7	2.34696	1	0.15	105	90	0.97	0.26	0.00	0.15		0.052303477	0.95
5-21-17C	2	8.8	2.68224	5	0.74	106	90	0.96	0.28	0.00	0.78		0.260082165	0.95
											Line 2 Fracture Density	1.56		
											Outcrop Fracture Density without COS weighting factor (2)	1.177386573		

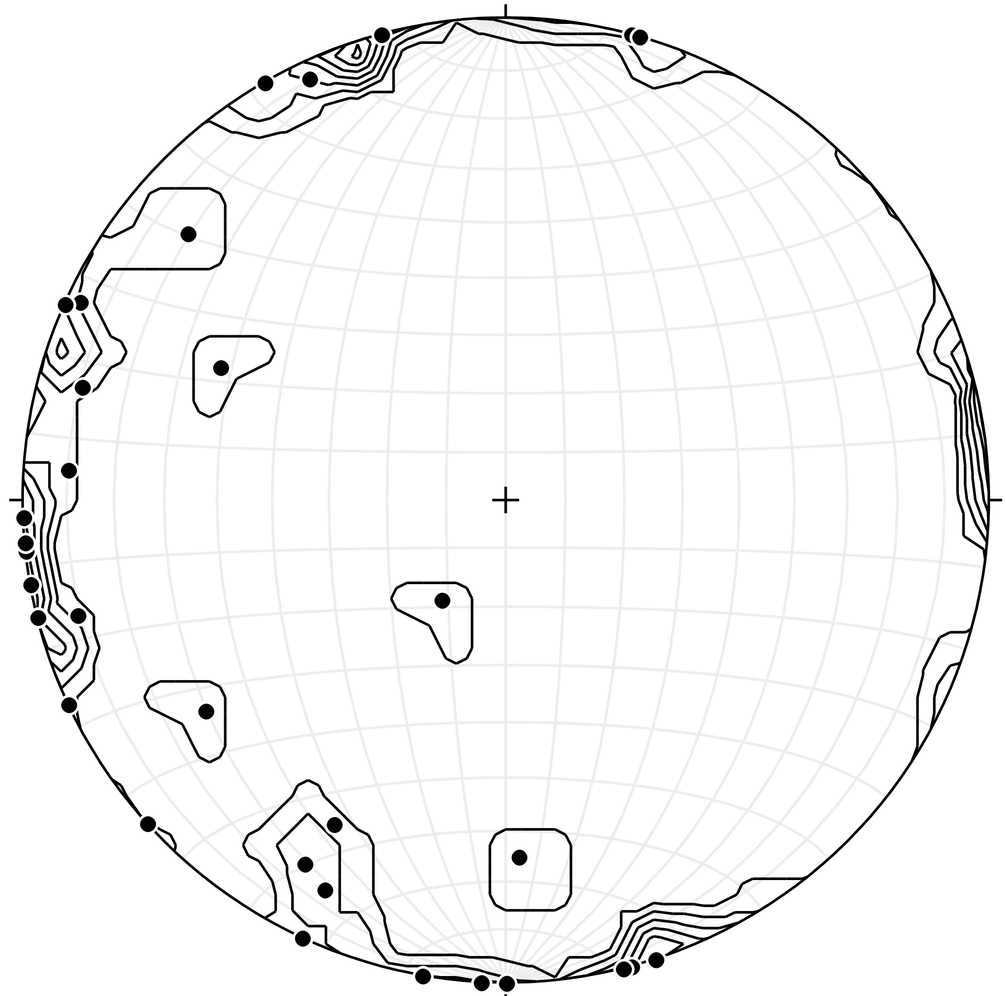

Figure 9 - Stereonet of poles to joints. Station 5-21-17C.

5.2.1 Day 2; 5-22-17

The second set of beds measured and sampled were all Jurassic in age. Station 5-22-17A was a sandstone unit and part of the Morrison Formation. Stations 5-22-17B and 5-22-17C were part of the Todilto Formation and are a micritic limestone and limy siltstone, respectively. Station 5-22-17A was measured in the Upper Morrison Formation and has a bed thickness of approximately 2.60 feet with a strike of 140 degrees and a dip of 12 degrees (Figure 10). Outcrop strike and dip was 180 degrees and 90 degrees, respectively. The average fracture length was 0.84 feet and the outcrop had a fracture density of 3.85 m^{-1} (Tables 5 and 6) with a strike orientation of the joint sets predominantly in the N-S direction with some scatter (Figure 11).

Station 5-22-17B was measured in the Todilto Formation (Figure 12). The bed thickness is approximately 2.6 feet and has a strike of 340 degrees and is dipping at 5 degrees, while the outcrop strike is 160 degrees with a dip of 90 degrees. The average fracture length is approximately 1.64 feet and the outcrop has a fracture density of 2.33 m^{-1} (Tables 7 and 8) with a strike orientation of the joint sets in the N-S direction and some in the E-W direction (Figure 13).

Station 5-22-17C was also measured in the Todilto, in a limy siltstone portion and had a bed thickness of about 5.5 feet with a strike of 340 degrees and a dip of 5 degrees (Figure 14). Outcrop strike was 153 degrees with a dip of 90 degrees. Average fracture length was approximately 3.6 feet and fracture density is 1.01 m^{-1} with strike orientation of joint sets in the N-S, E-W directions (Figure 15).

Figure 10 - Upper Morrison. Bed measured outlined in red box; Station 5-22-17A.

Table 5 - Fracture Density measurements from the Morrison Formation; Station 5-22-17A. Part 1.

Station	UTM Coordinates	Strike of Outcrop (Right Hand Rule)	Dip of Outcrop (Right Hand Rule)	Thickness of Bed (Ft)	Thickness of Bed (M)	Strike of Bed (Right Hand Rule)	Dip of Bed (Right Hand Rule)	Sample strike (right hand rule)	Sample dip (right hand rule)	Bed Curvature/faulting	Rock Description			
5-22-17A	527699-3931106	180	90	1.00	0.3048	140	12	NA	NA	None/no	Moderately sorted SS, Upper Morrison			
	Scanline #	Start Ft	End ft	Trend Scanline	Plunge Scanline	scanline length (M)	Scanline Vector x = North	Scanline Vector y = East	Scanline Vector z = down					
	1	0	2.4	180	0	0.73152	-1.00	0.00	0.00					
		Fracture Distance (Ft)	Fracture Distance (M)	Fracture Length (Ft)	Fracture Length Weighting	Fracture Strike	Fracture Dip	Fracture Vector x coord	Fracture Vector y coord	Fracture Vector z coord	Weighting factor for fracture density		New Weighting factor for fracture density	COS of angle between Scanline & Fracture Vector
	1	0.2	0.06096	1.00	1.00	258	70	-0.92	0.20	0.34	1.09		1.256504378	0.92
	1	2.4	0.73152	1	1.00	276	90	-0.99	-0.10	0.00	1.01		1.359527963	0.99
											Line 1 Fracture Density	2.73		
	Scanline #	Start Ft	End ft	Trend Scanline	Plunge Scanline	scanline length (M)	Scanline Vector x = North	Scanline Vector y = East	Scanline Vector z = down					
	2	2.4	3	276	0	0.18288	0.10	-0.99	0.00					
		Fracture Distance (Ft)	Fracture Distance (M)	Fracture Length (Ft)	Fracture Length Weighting	Fracture Strike	Fracture Dip	Fracture Vector x coord	Fracture Vector y coord	Fracture Vector z coord	Weighting factor for fracture density			COS of angle between Scanline & Fracture Vector
	2			0	0	0	0	0.00	0.00	1.00	0.00		0	0.00
											Line 1 Fracture Density	0.00		
	Scanline #	Start Ft	End ft	Trend Scanline	Plunge Scanline	scanline length (M)	Scanline Vector x = North	Scanline Vector y = East	Scanline Vector z = down					
	3	3	7	165	0	1.2192	-0.97	0.26	0.00					
		Fracture Distance (Ft)	Fracture Distance (M)	Fracture Length (Ft)	Fracture Length Weighting	Fracture Strike	Fracture Dip	Fracture Vector x coord	Fracture Vector y coord	Fracture Vector z coord	Weighting factor for fracture density			COS of angle between Scanline & Fracture Vector
	3	5.4	1.64592	1	1	71	65	0.86	-0.30	0.42	1.11		0.741551892	-0.90
	3	6.1	1.85928	0.8	0.8	266	78	-0.98	0.07	0.21	0.83		0.630036925	0.96
											Line 3 Fractures	1.48		
	Scanline #	Start Ft	End ft	Trend Scanline	Plunge Scanline	scanline length (M)	Scanline Vector x = North	Scanline Vector y = East	Scanline Vector z = down					
	4	7	8.7	88	0	0.51816	0.03	1.00	0.00					
		Fracture Distance (Ft)	Fracture Distance (M)	Fracture Length (Ft)	Fracture Length Weighting	Fracture Strike	Fracture Dip	Fracture Vector x coord	Fracture Vector y coord	Fracture Vector z coord	Weighting factor for fracture density			COS of angle between Scanline & Fracture Vector
	4	7	2.1336	0.8	0.8	163	90	0.29	0.96	0.00	0.83		1.4913167	0.97
	4	7.2	2.19456	1	1	184	90	-0.07	1.00	0.00	1.01		1.919333595	0.99
	4	7.8	2.37744	1	1	175	90	0.09	1.00	0.00	1.00		1.927260952	1.00
	4	7.9	2.40792	1	1	155	85	0.42	0.90	0.09	1.09		1.769727603	0.92
	4	8.1	2.46888	0.75	0.75	188	75	-0.13	0.96	0.26	0.79		1.376868982	0.95
	4	8.5	2.5908	0.25	0.25	193	79	-0.22	0.96	0.19	0.26		0.457474066	0.95
	4	8.7	2.65176	0.8	0.8	165	90	0.26	0.97	0.00	0.82		1.504353968	0.97
											Line 4 Fractures	10.81		
	Scanline #	Start Ft	End ft	Trend Scanline	Plunge Scanline	scanline length (M)	Scanline Vector x = North	Scanline Vector y = East	Scanline Vector z = down					
	5	8.7	9.5	164	0	0.24384	-0.96	0.28	0.00					
		Fracture Distance (Ft)	Fracture Distance (M)	Fracture Length (Ft)	Fracture Length Weighting	Fracture Strike	Fracture Dip	Fracture Vector x coord	Fracture Vector y coord	Fracture Vector z coord	Weighting factor for fracture density			COS of angle between Scanline & Fracture Vector
	5	8.7	2.65176	0.75	0.75	260	90	-0.98	0.17	0.00	0.75		3.058937916	0.99
	5	9	2.7432	0.5	0.5	238	65	-0.77	0.48	0.42	0.57		1.786415191	0.87
											Line 5 Fracturee	5.13		
	Scanline #	Start Ft	End ft	Trend Scanline	Plunge Scanline	scanline length (M)	Scanline Vector x = North	Scanline Vector y = East	Scanline Vector z = down					
	6	9.5	10.8	270	0	0.39624	0.00	-1.00	0.00					
		Fracture Distance (Ft)	Fracture Distance (M)	Fracture Length (Ft)	Fracture Length Weighting	Fracture Strike	Fracture Dip	Fracture Vector x coord	Fracture Vector y coord	Fracture Vector z coord	Weighting factor for fracture density			COS of angle between Scanline & Fracture Vector
	6	10.2	3.10896	0.4	0.4	169	90	0.19	0.98	0.00	4.59		0.087982781	0.09
	6	10.8	3.29184	1	1	167	90	0.22	0.97	0.00	19.11		0.132081456	0.05
											Line 6 Fracturee	3.53		
	Scanline #	Start Ft	End ft	Trend Scanline	Plunge Scanline	scanline length (M)	Scanline Vector x = North	Scanline Vector y = East	Scanline Vector z = down					
	7	10.8	12.9	155	0	0.64008	-0.91	0.42	0.00					
		Fracture Distance (Ft)	Fracture Distance (M)	Fracture Length (Ft)	Fracture Length Weighting	Fracture Strike	Fracture Dip	Fracture Vector x coord	Fracture Vector y coord	Fracture Vector z coord	Weighting factor for fracture density			COS of angle between Scanline & Fracture Vector
	7	11.7	3.56616	1	1	204	90	-0.41	0.91	0.00	1.56		1.004230111	0.64
	7	12.9	3.93192	1	1	178	90	0.03	1.00	0.00	4.13		0.377955717	0.24
											Line 7 Fracturee	3.12		

Table 6 - Fracture Density measurements from the Morrison Formation;

Station 5-22-17A. Part 2.

Scanline #	Start Ft	End ft	Trend Scanline	Plunge Scanline	scanline length (M)	Scanline Vector x = North	Scanline Vector y = East	Scanline Vector z = down					
8	12.9	15.8	125	0	0.88392	-0.57	0.82	0.00					
	Fracture Distance (Ft)	Fracture Distance (M)	Fracture Length (Ft)	Fracture Length Weighting	Fracture Strike	Fracture Dip	Fracture Vector x coord	Fracture Vector y coord	Fracture Vector z coord	Weighting factor for fracture density			COS of angle between Scanline & Fracture Vector
8	12.9	3.93192	1	1	262	83	-0.98	0.14	0.12	1.02		1.111963482	0.98
8	14	4.2672	1	1	177	90	0.05	1.00	0.00	4.45		0.254492549	0.22
8	14.6	4.45008	1	1	176	90	0.07	1.00	0.00	4.81		0.235215507	0.21
8	15.4	4.69392	1	1	199	90	-0.33	0.95	0.00	1.74		0.648900847	0.57
										Line 8 Fracturee	4.53		
Scanline #	Start Ft	End ft	Trend Scanline	Plunge Scanline	scanline length (M)	Scanline Vector x = North	Scanline Vector y = East	Scanline Vector z = down					
9	15.8	17	201	0	0.36576	-0.93	-0.36	0.00					
	Fracture Distance (Ft)	Fracture Distance (M)	Fracture Length (Ft)	Fracture Length Weighting	Fracture Strike	Fracture Dip	Fracture Vector x coord	Fracture Vector y coord	Fracture Vector z coord	Weighting factor for fracture density			COS of angle between Scanline & Fracture Vector
9	15.8	4.81584	1	1	273	90	-1.00	-0.05	0.00	1.06		2.58507922	0.95
9	16.3	4.96824	0.5	0.5	276	90	-0.99	-0.10	0.00	0.54		1.267475742	0.93
										Line 9 Fracturee	4.10		
Scanline #	Start Ft	End ft	Trend Scanline	Plunge Scanline	scanline length (M)	Scanline Vector x = North	Scanline Vector y = East	Scanline Vector z = down					
10	17	21	110	0	1.2192	-0.34	0.94	0.00					
	Fracture Distance (Ft)	Fracture Distance (M)	Fracture Length (Ft)	Fracture Length Weighting	Fracture Strike	Fracture Dip	Fracture Vector x coord	Fracture Vector y coord	Fracture Vector z coord	Weighting factor for fracture density			COS of angle between Scanline & Fracture Vector
10	17.5	5.334	1	1	200	72	-0.33	0.89	0.31	1.79		0.458511314	0.56
10	18.8	5.73024	1	1	178	90	0.03	1.00	0.00	4.13		0.198426752	0.24
10	19.2	5.85216	0.55	0.55	214	82	-0.55	0.82	0.14	0.73		0.342211404	0.76
10	19.5	5.9436	1	1	220	90	-0.64	0.77	0.00	1.21		0.679984886	0.83
10	19.7	6.00456	1	1	160	90	0.34	0.94	0.00	14.34		0.057214955	-0.07
10	20.4	6.21792	0.5	0.5	210	90	-0.50	0.87	0.00	0.70		0.295004839	0.72
10	20.8	6.33984	1	1	205	90	-0.42	0.91	0.00	1.52		0.538106159	0.66
										Line 10 Fracturee	4.96		
Scanline #	Start Ft	End ft	Trend Scanline	Plunge Scanline	scanline length (M)	Scanline Vector x = North	Scanline Vector y = East	Scanline Vector z = down					
11	21	24.4	131	0	1.03632	-0.66	0.75	0.00					
	Fracture Distance (Ft)	Fracture Distance (M)	Fracture Length (Ft)	Fracture Length Weighting	Fracture Strike	Fracture Dip	Fracture Vector x coord	Fracture Vector y coord	Fracture Vector z coord	Weighting factor for fracture density			COS of angle between Scanline & Fracture Vector
11	21	6.4008	1	1	270	90	-1.00	0.00	0.00	1.04		0.927572271	0.96
11	23.8	7.25424	0.8	0.8	184	90	-0.07	1.00	0.00	2.34		0.264026666	0.34
										Line 11 Fracturee	1.74		
Scanline #	Start Ft	End ft	Trend Scanline	Plunge Scanline	scanline length (M)	Scanline Vector x = North	Scanline Vector y = East	Scanline Vector z = down					
12	24.4	26.5	165	0	0.64008	-0.97	0.26	0.00					
	Fracture Distance (Ft)	Fracture Distance (M)	Fracture Length (Ft)	Fracture Length Weighting	Fracture Strike	Fracture Dip	Fracture Vector x coord	Fracture Vector y coord	Fracture Vector z coord	Weighting factor for fracture density			COS of angle between Scanline & Fracture Vector
12	24.4	7.43712	1	1	296	90	-0.90	-0.44	0.00	1.35		1.161018662	0.74
12	24.6	7.49808	0.9	0.9	245	90	-0.91	0.42	0.00	0.91		1.388763134	0.99
12	25.5	7.7724	0.9	0.9	205	90	-0.42	0.91	0.00	1.37		0.922467701	0.66
12	26.3	8.01624	0.9	0.9	205	90	-0.42	0.91	0.00	1.37		0.922467701	0.66
										Line 12 Fracturee	5.78		
										Outcrop Fracture Density without weighting factor (2)	3.850344179		

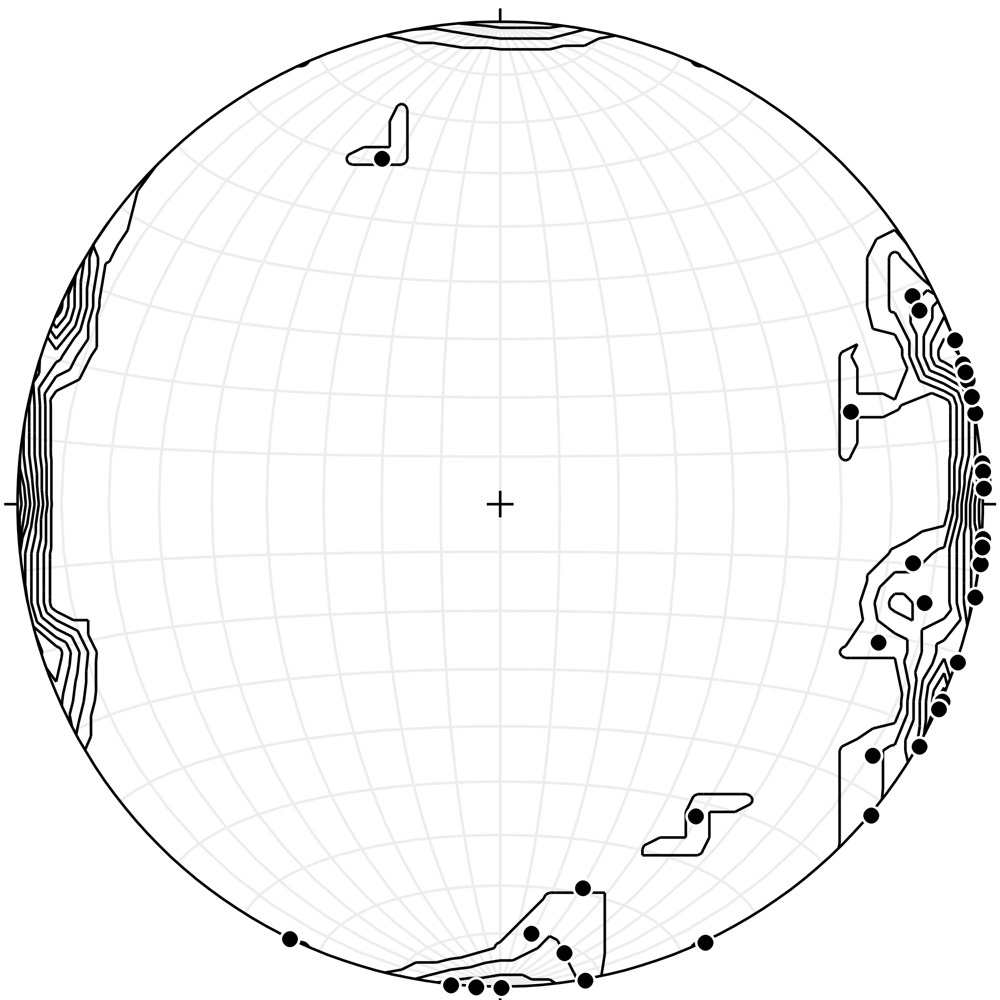

Figure 11 - Stereonet of poles to joints; Station 5-22-17A.

Figure 12 - Todilto Limestone. Bed measured outlined in red box; Station 5-22-17B.

Table 7 - Fracture Density measurements from the Todilto Limestone; Station 5-22-17B. Part 1.

Station	UTM Coordinates	Strike of Outcrop (Right Hand Rule)	Dip of Outcrop (Right Hand Rule)	Thickness of Bed (Ft)	Thickness of Bed (M)	Strike of Bed (Right Hand Rule)	Dip of Bed (Right Hand Rule)	Sample strike (right hand rule)	Sample dip (right hand rule)	Bed Curvature/faulting	Rock Description			
5-22-17B	527794: 3930740	160	90	2.60	0.79248	340	5	NA	NA	None/yes	Limestone - Micrite			
	Scanline #	Start Ft	End ft	Trend Scanline	Plunge Scanline	scanline length (M)	Scanline Vector x = North	Scanline Vector y = East	Scanline Vector z = down					
	1	0	6	176	0	1.8288	-1.00	0.07	0.00					
		Fracture Distance (Ft)	Fracture Distance (M)	Fracture Length (Ft)	Fracture Length Weighting	Fracture Strike	Fracture Dip	Fracture Vector x coord	Fracture Vector y coord	Fracture Vector z coord	Weighting factor for fracture density		New Weighting factor for fracture density	COS of angle between Scanline & Fracture Vector
	1	0	0	2.70	1.04	279	80	-0.97	-0.15	0.17	1.08		0.544878404	0.96
	1	3.7	1.12776	1.5	0.58	328	90	-0.53	-0.85	0.00	1.23		0.148102022	0.47
	1	6	1.8288	0.8	0.31	198	74	-0.30	0.91	0.28	0.85		0.06058533	0.36
											Line 1 Fractures	1.05		
	Scanline #	Start Ft	End ft	Trend Scanline	Plunge Scanline	scanline length (M)	Scanline Vector x = North	Scanline Vector y = East	Scanline Vector z = down					
	2	6.1	7.3	148	0	0.36576	-0.85	0.53	0.00					
		Fracture Distance (Ft)	Fracture Distance (M)	Fracture Length (Ft)	Fracture Length Weighting	Fracture Strike	Fracture Dip	Fracture Vector x coord	Fracture Vector y coord	Fracture Vector z coord	Weighting factor for fracture density			COS of angle between Scanline & Fracture Vector
	2	6.1	1.85928	2.8	1.0769231	184	90	-0.07	1.00	0.00	1.83		1.730641684	0.59
	2	7.1	2.16408	1.5	0.5769231	172	90	0.14	0.99	0.00	1.42		0.641556637	0.41
											Line 2 Fractures	4.52		
	Scanline #	Start Ft	End ft	Trend Scanline	Plunge Scanline	scanline length (M)	Scanline Vector x = North	Scanline Vector y = East	Scanline Vector z = down					
	3	7.3	9	98	0	0.51816	-0.14	0.99	0.00					
		Fracture Distance (Ft)	Fracture Distance (M)	Fracture Length (Ft)	Fracture Length Weighting	Fracture Strike	Fracture Dip	Fracture Vector x coord	Fracture Vector y coord	Fracture Vector z coord	Weighting factor for fracture density			COS of angle between Scanline & Fracture Vector
	3	7.3	2.22504	1.6	0.6153846	150	90	0.50	0.87	0.00	0.78		0.93586864	0.79
	3	7.4	2.25552	1	0.3846154	181	90	-0.02	1.00	0.00	0.39		0.73673869	0.99
	3	8.2	2.49936	1	0.3846154	184	83	-0.07	0.99	0.12	0.39		0.734944032	0.99
	3	9	2.7432	2.2	0.8461538	177	90	0.05	1.00	0.00	0.86		1.602994474	0.98
											Line 3 Fractures	4.31		
	Scanline #	Start Ft	End ft	Trend Scanline	Plunge Scanline	scanline length (M)	Scanline Vector x = North	Scanline Vector y = East	Scanline Vector z = down					
	4	9	11.1	177	0	0.64008	-1.00	0.05	0.00					
		Fracture Distance (Ft)	Fracture Distance (M)	Fracture Length (Ft)	Fracture Length Weighting	Fracture Strike	Fracture Dip	Fracture Vector x coord	Fracture Vector y coord	Fracture Vector z coord	Weighting factor for fracture density			COS of angle between Scanline & Fracture Vector
	4	9.1	2.77368	2	0.7692308	268	84	-0.99	0.03	0.10	0.77		1.195007385	0.99
	4	11.1	3.38328	2.1	0.8076923	262	90	-0.99	0.14	0.00	0.81		1.257059734	1.00
											Line 4 Fractures	2.46		
	Scanline #	Start Ft	End ft	Trend Scanline	Plunge Scanline	scanline length (M)	Scanline Vector x = North	Scanline Vector y = East	Scanline Vector z = down					
	5	11.1	13	115	0	0.57912	-0.42	0.91	0.00					
		Fracture Distance (Ft)	Fracture Distance (M)	Fracture Length (Ft)	Fracture Length Weighting	Fracture Strike	Fracture Dip	Fracture Vector x coord	Fracture Vector y coord	Fracture Vector z coord	Weighting factor for fracture density			COS of angle between Scanline & Fracture Vector
	5	11.7	3.56616	0.8	0.3076923	198	90	-0.31	0.95	0.00	0.31		0.5273498	0.99
	5	11.9	3.62712	0.8	0.3076923	193	90	-0.22	0.97	0.00	0.31		0.519699704	0.98
	5	12	3.6576	1	0.3846154	145	90	0.57	0.82	0.00	0.77		0.332068815	0.50
	5	12.5	3.81	2	0.7692308	165	87	0.26	0.96	0.05	1.01		1.01612341	0.76
											Line 5 Fracturee	3.06		

Table 8 - Fracture Density measurements from the Todilto Limestone; Station 5-22-17B. Part 2.

	Scanline #	Start Ft	End ft	Trend Scanline	Plunge Scanline	scanline length (M)	Scanline Vector x = North	Scanline Vector y = East	Scanline Vector z = down					
	6	13	17.4	175	0	1.34112	-1.00	0.09	0.00					
		Fracture Distance (Ft)	Fracture Distance (M)	Fracture Length (Ft)	Fracture Length Weighting	Fracture Strike	Fracture Dip	Fracture Vector x coord	Fracture Vector y coord	Fracture Vector z coord	Weighting factor for fracture density			COS of angle between Scanline & Fracture Vector
	6	13	3.9624	2.8	1.0769231	270	90	-1.00	0.00	0.00	2.55		0.339363635	0.42
	6	13.1	3.99288	1	0.3846154	282	40	-0.63	-0.13	0.77	2.66		0.041468139	0.14
	6	13.5	4.1148	0.75	0.2884615	322	86	-0.61	-0.79	0.07	0.64		0.097410962	-0.45
	6	14.1	4.29768	1	0.3846154	319	90	-0.66	-0.75	0.00	0.95		0.116646661	-0.41
	6	14.9	4.54152	2	0.7692308	281	90	-0.98	-0.19	0.00	3.18		0.138759966	0.24
											Line 6 Fracturee	2.17		
	Scanline #	Start Ft	End ft	Trend Scanline	Plunge Scanline	scanline length (M)	Scanline Vector x = North	Scanline Vector y = East	Scanline Vector z = down					
	7	17.4	18.7	93	0	0.39624	-0.05	1.00	0.00					
		Fracture Distance (Ft)	Fracture Distance (M)	Fracture Length (Ft)	Fracture Length Weighting	Fracture Strike	Fracture Dip	Fracture Vector x coord	Fracture Vector y coord	Fracture Vector z coord	Weighting factor for fracture density			COS of angle between Scanline & Fracture Vector
	7	17.4	5.30352	2	0.7692308	166	90	0.24	0.97	0.00	0.99		1.50869318	0.78
	7	17.7	5.39496	1.5	0.5769231	175	90	0.09	1.00	0.00	0.67		1.260927823	0.87
	7	18.3	5.57784	1.7	0.6538462	195	90	-0.26	0.97	0.00	0.66		1.625057444	0.98
	7	18.6	5.66928	1.6	0.6153846	156	90	0.41	0.91	0.00	0.94		1.018899236	0.66
	7	18.7	5.69976	2.5	0.9615385	182	90	-0.03	1.00	0.00	1.04		2.233749295	0.92
											Line 7 Fracturee	9.03		
	Scanline #	Start Ft	End ft	Trend Scanline	Plunge Scanline	scanline length (M)	Scanline Vector x = North	Scanline Vector y = East	Scanline Vector z = down					
	8	18.7	22.7	182	0	1.2192	-1.00	-0.03	0.00					
		Fracture Distance (Ft)	Fracture Distance (M)	Fracture Length (Ft)	Fracture Length Weighting	Fracture Strike	Fracture Dip	Fracture Vector x coord	Fracture Vector y coord	Fracture Vector z coord	Weighting factor for fracture density			COS of angle between Scanline & Fracture Vector
	8	22.7	6.91896	2	0.7692308	323	87	-0.60	-0.80	0.05	1.64		0.295798107	-0.47
											Line 8 Fracturee	0.63		
	Scanline #	Start Ft	End ft	Trend Scanline	Plunge Scanline	scanline length (M)	Scanline Vector x = North	Scanline Vector y = East	Scanline Vector z = down					
	9	22.7	27.1	150	0	1.34112	-0.87	0.50	0.00					
		Fracture Distance (Ft)	Fracture Distance (M)	Fracture Length (Ft)	Fracture Length Weighting	Fracture Strike	Fracture Dip	Fracture Vector x coord	Fracture Vector y coord	Fracture Vector z coord	Weighting factor for fracture density			COS of angle between Scanline & Fracture Vector
	9	23.5	7.1628	2	0.7692308	258	89	-0.98	0.21	0.02	1.28		0.345132521	0.60
	9	26.3	8.01624	1	0.3846154	259	62	-0.87	0.17	0.47	0.74		0.148837589	0.52
	9	27	8.2296	1	0.3846154	286	72	-0.91	-0.26	0.31	2.59		0.042667557	0.15
	9	27.1	8.26008	2.2	0.8461538	264	90	-0.99	0.10	0.00	1.64		0.324953358	0.52
											Line 9 Fracturee	1.78		
	Scanline #	Start Ft	End ft	Trend Scanline	Plunge Scanline	scanline length (M)	Scanline Vector x = North	Scanline Vector y = East	Scanline Vector z = down					
	10	27.1	27.6	254	0	0.1524	-0.28	-0.96	0.00					
		Fracture Distance (Ft)	Fracture Distance (M)	Fracture Length (Ft)	Fracture Length Weighting	Fracture Strike	Fracture Dip	Fracture Vector x coord	Fracture Vector y coord	Fracture Vector z coord	Weighting factor for fracture density			COS of angle between Scanline & Fracture Vector
	10	27.6	8.41248	2	0.7692308	189	80	-0.15	0.97	0.17	3.76		1.033479937	0.20
											Line 10 Fracturee	5.05		
											Outcrop Fracture Density without COS weighting factor (2)	2.333296625		

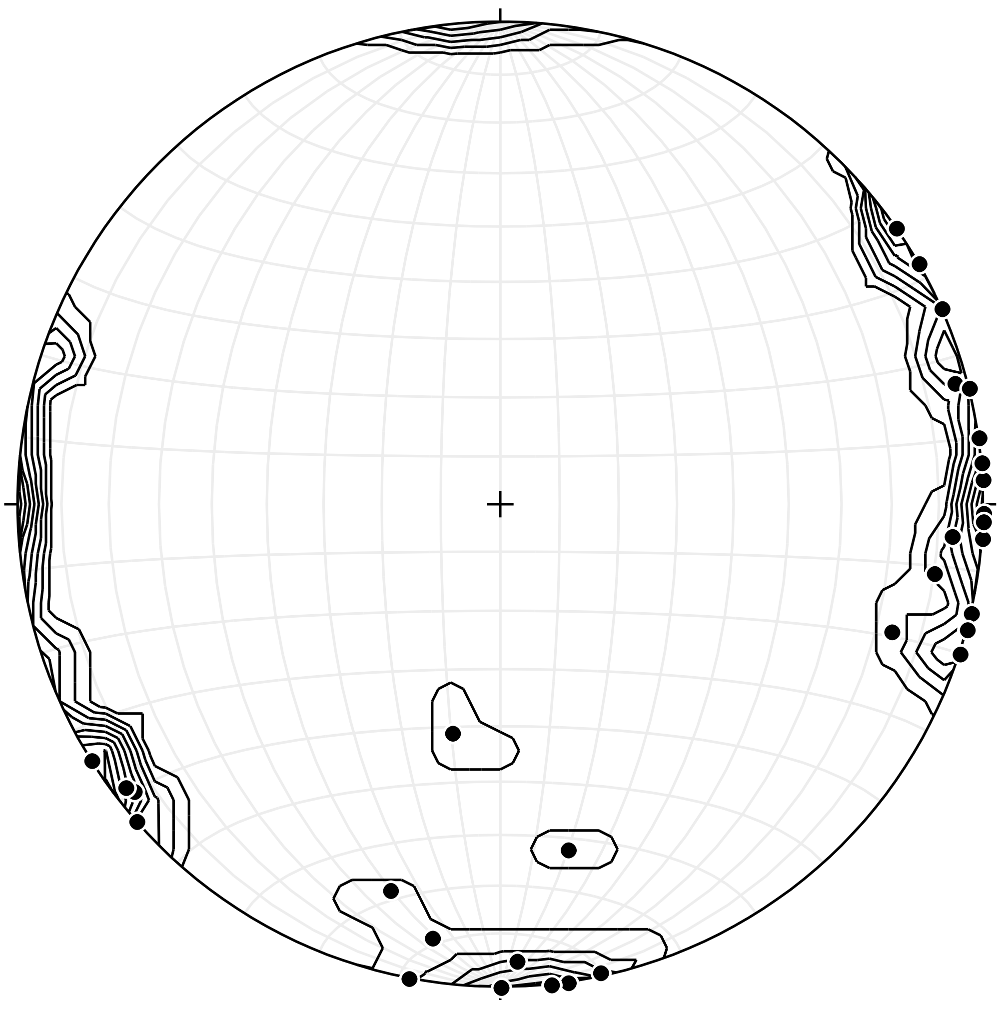

Figure 13 - Stereonet of poles to joints; Station 5-22-17B.

Figure 14 - Todilto Limestone. Bed measured outlined in red box; Station 5-22-17C.

Table 9 - Fracture Density measurements from the Todilto Limestone; Station 5-22-17C. Part 1.

Station	UTM Coordinates	Strike of Outcrop (Right Hand Rule)	Dip of Outcrop (Right Hand Rule)	Thickness of Bed (Ft)	Thickness of Bed (M)	Strike of Bed (Right Hand Rule)	Dip of Bed (Right Hand Rule)	Sample strike (right hand rule)	Sample dip (right hand rule)	Bed Curvature/faulting	Rock Description			
5-22-17C	527874; 3930537	153	90	5.50	1.6764	340	5	NA	NA	No	Siltstone			
	Scanline #	Start Ft	End ft	Trend Scanline	Plunge Scanline	scanline length (M)	Scanline Vector x = North	Scanline Vector y = East	Scanline Vector z = down					
	1	0	3	106	0	0.9144	-0.28	0.96	0.00					
		Fracture Distance (Ft)	Fracture Distance (M)	Fracture Length (Ft)	Fracture Length Weighting	Fracture Strike	Fracture Dip	Fracture Vector x coord	Fracture Vector y coord	Fracture Vector z coord	Weighting factor for fracture density		New Weighting factor for fracture density	COS of angle between Scanline & Fracture Vector
	1	0	0	5.50	1.00	161	90	0.33	0.95	0.00	1.22		0.895835569	0.82
	1	0.25	0.0762	1	0.18	168	90	0.21	0.98	0.00	0.21		0.175564224	0.88
	1	3	0.9144	4	0.73	164	90	0.28	0.96	0.00	0.86		0.6744994	0.85
											Line 1 Fractures	2.09		
	Scanline #	Start Ft	End ft	Trend Scanline	Plunge Scanline	scanline length (M)	Scanline Vector x = North	Scanline Vector y = East	Scanline Vector z = down					
	2	3	5.5	154	0	0.762	-0.90	0.44	0.00					
		Fracture Distance (Ft)	Fracture Distance (M)	Fracture Length (Ft)	Fracture Length Weighting	Fracture Strike	Fracture Dip	Fracture Vector x coord	Fracture Vector y coord	Fracture Vector z coord	Weighting factor for fracture density			COS of angle between Scanline & Fracture Vector
	2	4.1	1.24968	2.5	0.4545455	189	90	-0.16	0.99	0.00	0.79		0.342147719	0.57
	2	5.4	1.64592	3.5	0.6363636	272	90	-1.00	-0.03	0.00	0.72		0.737369739	0.88
											Line 2 Fractures	1.43		
	Scanline #	Start Ft	End ft	Trend Scanline	Plunge Scanline	scanline length (M)	Scanline Vector x = North	Scanline Vector y = East	Scanline Vector z = down					
	3	5.5	6.8	198	0	0.39624	-0.95	-0.31	0.00					
		Fracture Distance (Ft)	Fracture Distance (M)	Fracture Length (Ft)	Fracture Length Weighting	Fracture Strike	Fracture Dip	Fracture Vector x coord	Fracture Vector y coord	Fracture Vector z coord	Weighting factor for fracture density			COS of angle between Scanline & Fracture Vector
	3	6.7	2.04216	5	0.9090909	156	89	0.41	0.91	0.02	1.36		1.534948274	-0.67
											Line 3 Fractures	2.29		
	Scanline #	Start Ft	End ft	Trend Scanline	Plunge Scanline	scanline length (M)	Scanline Vector x = North	Scanline Vector y = East	Scanline Vector z = down					
	4	6.8	11	165	0	1.28016	-0.97	0.26	0.00					
		Fracture Distance (Ft)	Fracture Distance (M)	Fracture Length (Ft)	Fracture Length Weighting	Fracture Strike	Fracture Dip	Fracture Vector x coord	Fracture Vector y coord	Fracture Vector z coord	Weighting factor for fracture density			COS of angle between Scanline & Fracture Vector
	4	11	3.3528	5.5	1	287	76	-0.93	-0.28	0.24	1.22		0.642777031	0.82
											Line 4 Fractures	0.78		
	Scanline #	Start Ft	End ft	Trend Scanline	Plunge Scanline	scanline length (M)	Scanline Vector x = North	Scanline Vector y = East	Scanline Vector z = down					
	5	11	16	121	0	1.524	-0.52	0.86	0.00					
		Fracture Distance (Ft)	Fracture Distance (M)	Fracture Length (Ft)	Fracture Length Weighting	Fracture Strike	Fracture Dip	Fracture Vector x coord	Fracture Vector y coord	Fracture Vector z coord	Weighting factor for fracture density			COS of angle between Scanline & Fracture Vector
	5	12.7	3.87096	5.5	1	203	90	-0.39	0.92	0.00	1.01		0.649782197	0.99
	5	14.2	4.32816	1	0.1818182	188	90	-0.14	0.99	0.00	0.20		0.109819238	0.92
											Line 5 Fracturee	0.78		

Table 10 - Fracture Density measurements from the Todilto Limestone; Station 5-22-17C. Part 2.

	Scanline #	Start Ft	End ft	Trend Scanline	Plunge Scanline	scanline length (M)	Scanline Vector x = North	Scanline Vector y = East	Scanline Vector z = down					
	6	16	19.3	188	0	1.00584	-0.99	-0.14	0.00					
		Fracture Distance (Ft)	Fracture Distance (M)	Fracture Length (Ft)	Fracture Length Weighting	Fracture Strike	Fracture Dip	Fracture Vector x coord	Fracture Vector y coord	Fracture Vector z coord	Weighting factor for fracture density			COS of angle between Scanline & Fracture Vector
	6	16.4	4.99872	5	0.9090909	272	85	-1.00	-0.03	0.09	1.88		0.436509668	0.48
	6	13.1	3.99288	1	0.1818182	276	80	-0.98	-0.10	0.17	0.44		0.075232956	0.42
											Line 6 Fracturee	1.08		
	Scanline #	Start Ft	End ft	Trend Scanline	Plunge Scanline	scanline length (M)	Scanline Vector x = North	Scanline Vector y = East	Scanline Vector z = down					
	7	19.3	25	165	0	1.73736	-0.97	0.26	0.00					
		Fracture Distance (Ft)	Fracture Distance (M)	Fracture Length (Ft)	Fracture Length Weighting	Fracture Strike	Fracture Dip	Fracture Vector x coord	Fracture Vector y coord	Fracture Vector z coord	Weighting factor for fracture density			COS of angle between Scanline & Fracture Vector
	7	20.1	6.12648	2.5	0.4545455	280	74	-0.95	-0.17	0.28	1.32		0.090127702	0.34
	7	21	6.4008	2	0.3636364	256	80	-0.96	0.24	0.17	0.52		0.145751807	0.70
											Line 7 Fracturee	0.47		
	Scanline #	Start Ft	End ft	Trend Scanline	Plunge Scanline	scanline length (M)	Scanline Vector x = North	Scanline Vector y = East	Scanline Vector z = down					
	8	25.1	27.8	107	0	0.82296	-0.29	0.96	0.00					
		Fracture Distance (Ft)	Fracture Distance (M)	Fracture Length (Ft)	Fracture Length Weighting	Fracture Strike	Fracture Dip	Fracture Vector x coord	Fracture Vector y coord	Fracture Vector z coord	Weighting factor for fracture density			COS of angle between Scanline & Fracture Vector
	8	27.8	8.47344	5	0.9090909	182	86	-0.03	1.00	0.07	1.04		0.963803805	0.87
											Line 8 Fracturee	1.10		
	Scanline #	Start Ft	End ft	Trend Scanline	Plunge Scanline	scanline length (M)	Scanline Vector x = North	Scanline Vector y = East	Scanline Vector z = down					
	9	27.8	32	145	0	1.28016	-0.82	0.57	0.00					
		Fracture Distance (Ft)	Fracture Distance (M)	Fracture Length (Ft)	Fracture Length Weighting	Fracture Strike	Fracture Dip	Fracture Vector x coord	Fracture Vector y coord	Fracture Vector z coord	Weighting factor for fracture density			COS of angle between Scanline & Fracture Vector
	9	32	9.7536	5	0.9090909	280	85	-0.98	-0.17	0.09	2.55		0.253522465	0.36
											Line 9 Fracturee	0.71		
											Outcrop Fracture Density without COS weighting factor (2)	1.01		

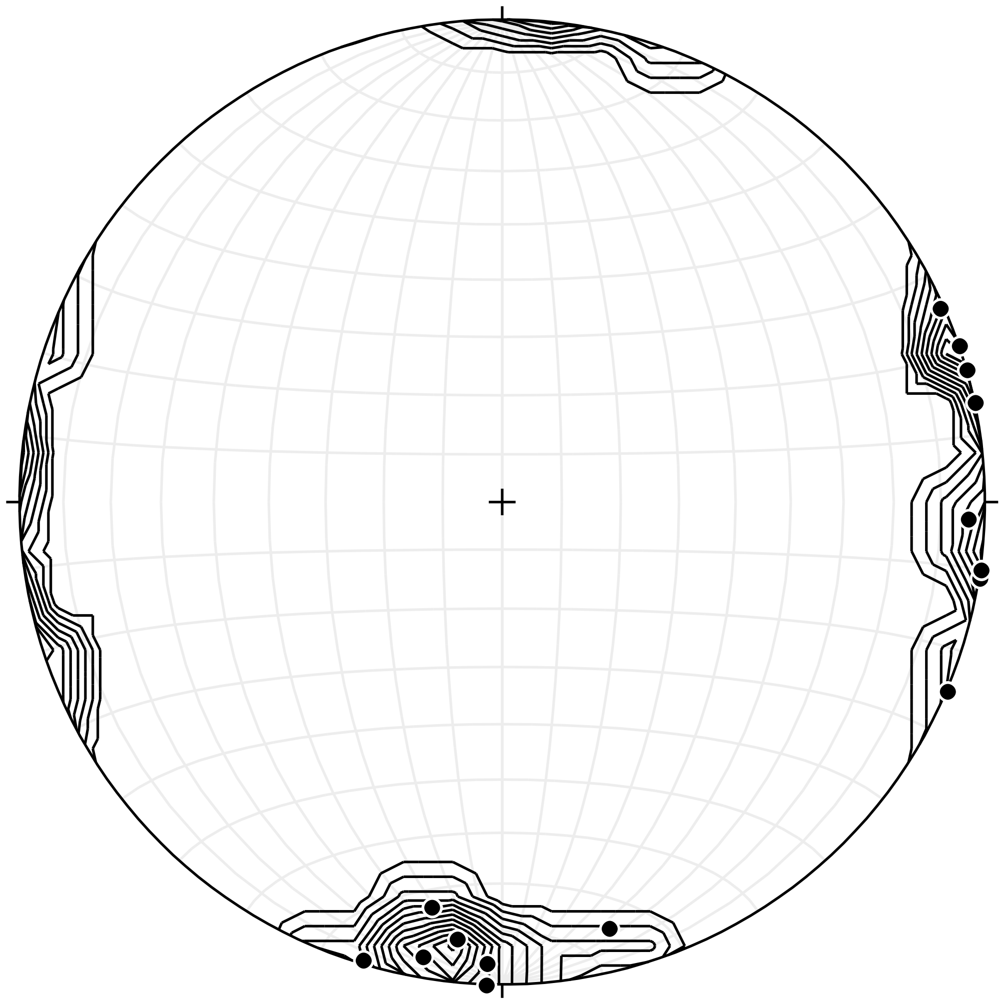

Figure 15 - Stereonet of poles to joints; Station 5-22-17C.

5.3.1 Day 3; 5-23-17

The third day consisted of measuring just the Entrada Formation, 5-23-17A, which is Jurassic in age and is a sandstone composed of mostly coarse grains. The outcrop was very large so getting an accurate measurement of the bed thickness was not possible, but we estimated it to be about 50 feet with an average fracture length of about 36 feet (Figure 16). Strike of the bed was 280 degrees with a dip of 5 degrees, while the strike of the outcrop was 119 degrees with a 90-degree dip. Most of the fractures went throughout the bed. The fracture density is 0.75 m^{-1} (Table 11) with strike orientation of the joint sets in the N-S, E-W directions (Figure 17).

Figure 16 - Entrada Sandstone. Bed measured outlined in red box.; Station 5-23-17A.

Table 11 - Fracture Density measurements from the Entrada Sandstone; Station 5-23-17A.

Station	UTM Coordinates	Strike of Outcrop (Right Hand Rule)	Dip of Outcrop (Right Hand Rule)	Thickness of Bed (Ft)	Thickness of Bed (M)	Strike of Bed (Right Hand Rule)	Dip of Bed (Right Hand Rule)	Sample strike (right hand rule)	Sample dip (right hand rule)	Bed Curvature/faulting	Rock Description			
5-23-17A	528183; 3930226	119	90	50.00	15.24	280	5	NA	NA	None	SS - Entrada			
	Scanline #	Start Ft	End ft	Trend Scanline	Plunge Scanline	scanline length (M)	Scanline Vector x = North	Scanline Vector y = East	Scanline Vector z = down					
	1	0	13	86	-12	3.9624	0.07	0.98	-0.21					
		Fracture Distance (Ft)	Fracture Distance (M)	Fracture Length (Ft)	Fracture Length Weighting	Fracture Strike	Fracture Dip	Fracture Vector x coord	Fracture Vector y coord	Fracture Vector z coord	Weighting factor for fracture density		New Weighting factor for fracture density	COS of angle between Scanline & Fracture Vector
	1	0	0	50.00	1.00	170	84	0.17	0.98	0.10	1.06		0.238675418	0.95
	1	0	0	50	1.00	260	80	-0.97	0.17	0.17	15.48		0.016300086	0.06
	1	13	3.9624	50	1.00	169	80	0.19	0.97	0.17	1.09		0.232183439	0.92
											Line 1 Fractures	0.76		
	Scanline #	Start Ft	End ft	Trend Scanline	Plunge Scanline	scanline length (M)	Scanline Vector x = North	Scanline Vector y = East	Scanline Vector z = down					
	2	13	14.6	169	0	0.48768	-0.98	0.19	0.00					
		Fracture Distance (Ft)	Fracture Distance (M)	Fracture Length (Ft)	Fracture Length Weighting	Fracture Strike	Fracture Dip	Fracture Vector x coord	Fracture Vector y coord	Fracture Vector z coord	Weighting factor for fracture density			COS of angle between Scanline & Fracture Vector
	2	14.6	4.45008	50	1	272	86	-1.00	-0.03	0.07	1.03		1.993103158	0.97
											Line 2 Fractures	2.05		
	Scanline #	Start Ft	End ft	Trend Scanline	Plunge Scanline	scanline length (M)	Scanline Vector x = North	Scanline Vector y = East	Scanline Vector z = down					
	3	14.6	25.3	108	-19	3.26136	-0.29	0.90	-0.33					
		Fracture Distance (Ft)	Fracture Distance (M)	Fracture Length (Ft)	Fracture Length Weighting	Fracture Strike	Fracture Dip	Fracture Vector x coord	Fracture Vector y coord	Fracture Vector z coord	Weighting factor for fracture density			COS of angle between Scanline & Fracture Vector
	3	15.5	4.7244	9	0.18	157	77	0.38	0.90	0.22	0.29		0.034332864	0.62
	3	25.3	7.71144	30	0.6	174	75	0.10	0.96	0.26	0.80		0.137993702	0.75
	3	25.3	7.71144	50	1	264	80	-0.98	0.10	0.17	3.10		0.098793186	0.32
											Line 3 Fractures	0.55		
											Outcrop Fracture Density without COS weighting factor (2)	0.749535755		

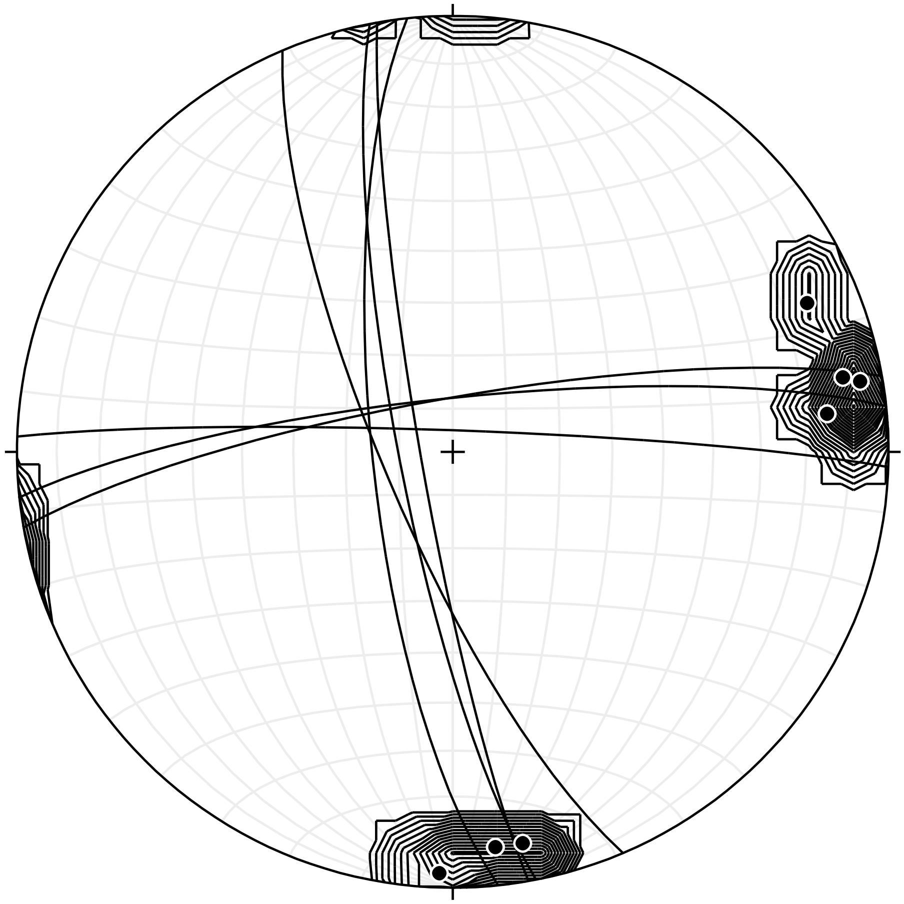

Figure 17 - Stereonet of poles to joints; Station 5-23-17A.

5.4.1 Day 4; 5-24-17

The fourth day of field work involved measuring four beds of Jurassic and Triassic age. The first bed measured, 5-24-17A, a Jurassic limestone above the Entrada (Figure 18). There was a normal fault with a few meters of offset approximately 100 meters from where the hand sample was taken. The bed had a strike of 126 degrees and a dip of 3 degrees. The bed was 1 foot thick with every fracture clearing the entire thickness of the bed. The fracture density is 7.67 m^{-1} (Table 12) with the orientation of joint sets mostly in the NW-SE direction (Figure 19).

Station 5-24-17A is in the Triassic Chinle Sandstone. The strike of the outcrop was 66 degrees with a dip of 90 degrees and the strike of the bed was 240 degrees with a dip of 10 degrees (Figure 20). The thickness of the bed was 6 feet with an average fracture length of 4.18 feet. The fracture density is 1.55 m^{-1} (Table 13) with the orientation of joint sets in the E-W direction with lots of scatter (Figure 21).

Station 5-24-17C lower Chinle, had a bed thickness of 7 feet with a strike of 100 degrees and a dip of 5 degrees. Strike of the outcrop was 94 degrees and the dip of the outcrop was 90 degrees (Figure 22). Most of the fractures made their way through the entire bed, but the average fracture length was 5.86 feet. The fracture density is 2.13 m^{-1} (Table 14) with the orientation of the joint sets in the N-S direction (Figure 23).

Station 5-24-17D the Santa Rosa Sandstone, had a bed thickness of approximately 5 feet with a strike of 85 degrees and a dip of 7 degrees (Figure 24) The outcrop strike was 84 degrees and the dip of the outcrop was 90 degrees. A majority of the fractures penetrated the thickness of the bed but the average fracture length was about 4.02 feet. Fracture density is 2.13 m^{-1} (Table 15 and 16) with the orientation of joint sets in the N-S direction with lots of scatter (Figure 25).

Table 17 is a summary of all fracture densities measured in the field using scanlines.

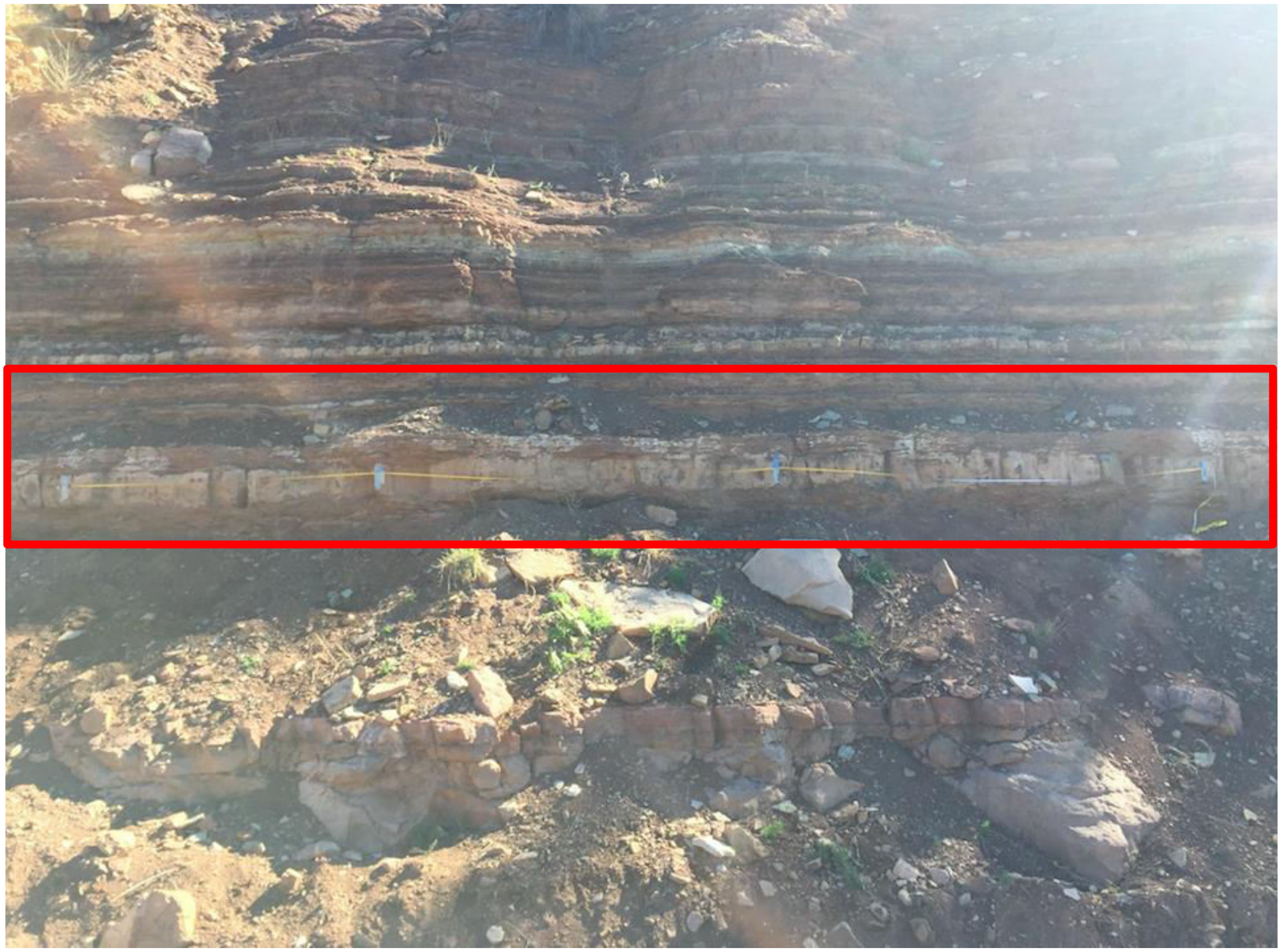

Figure 18 - Todilto Limestone. Measured bed outlined in red box; Station 5-24-17A.

Table 12 - Fracture Density measurements from the Limestone above the Entrada Sandstone; Station 5-24-17A.

Station	UTM Coordinates	Strike of Outcrop (Right Hand Rule)	Dip of Outcrop (Right Hand Rule)	Thickness of Bed (Ft)	Thickness of Bed (M)	Strike of Bed (Right Hand Rule)	Dip of Bed (Right Hand Rule)	Sample strike (right hand rule)	Sample dip (right hand rule)	Bed Curvature/faulting	Rock Description			
5-24-17A	528080; 3930292			1.00	0.3048	126	3	NA	NA	None/yes	Limestone above Entrada			
	Scanline #	Start Ft	End ft	Trend Scanline	Plunge Scanline	scanline length (M)	Scanline Vector x = North	Scanline Vector y = East	Scanline Vector z = down					
	1	0	10.7	130	0	3.26136	-0.64	0.77	0.00					
		Fracture Distance (Ft)	Fracture Distance (M)	Fracture Length (Ft)	Fracture Length Weighting	Fracture Strike	Fracture Dip	Fracture Vector x coord	Fracture Vector y coord	Fracture Vector z coord	Weighting factor for fracture density		New Weighting factor for fracture density	COS of angle between Scanline & Fracture Vector
	1	0	0	1.00	1.00	220	90	-0.64	0.77	0.00	1.00		0.306620551	1.00
	1	0	0	1	1.00	128	90	0.79	0.62	0.00			0.010700903	-0.03
	1	0.4	0.12192	1	1.00	233	90	-0.80	0.60	0.00	1.03		0.298761886	0.97
	1	0.9	0.27432	1	1.00	225	90	-0.71	0.71	0.00	1.00		0.305453767	1.00
	1	1.6	0.48768	1	1.00	220	90	-0.64	0.77	0.00	1.00		0.306620551	1.00
	1	2.5	0.762	1	1.00	237	90	-0.84	0.54	0.00	1.05		0.293222691	0.96
	1	3.1	0.94488	1	1.00	194	90	-0.24	0.97	0.00	1.11		0.275588726	0.90
	1	3.9	1.18872	1	1.00	192	90	-0.21	0.98	0.00	1.13		0.270729877	0.88
	1	4	1.2192	1	1.00	225	86	-0.71	0.71	0.07	1.01		0.304709697	0.99
	1	4.4	1.34112	1	1.00	155	85	0.42	0.90	0.09	2.38		0.12909034	0.42
	1	4.95	1.50876	1	1.00	286	89	-0.96	-0.28	0.02	2.46		0.124694819	0.41
	1	5	1.524	1	1.00	196	87	-0.28	0.96	0.05	1.10		0.279727928	0.91
	1	5.3	1.61544	1	1.00	163	83	0.29	0.95	0.12	1.85		0.165752747	0.54
	1	5.5	1.6764	1	1.00	116	85	0.90	0.44	0.09	4.15		0.073895954	-0.24
	1	5.6	1.70688	1	1.00	194	76	-0.23	0.94	0.24	1.15		0.267402563	0.87
	1	6.2	1.88976	1	1.00	190	77	-0.17	0.96	0.22	1.19		0.258735383	0.84
	1	6.9	2.10312	1	1.00	199	80	-0.32	0.93	0.17	1.09		0.281906089	0.92
	1	7	2.1336	1	1.00	227	85	-0.73	0.68	0.09	1.01		0.303176961	0.99
	1	7.7	2.34696	1	1.00	205	76	-0.41	0.88	0.24	1.07		0.287375114	0.94
	1	8.4	2.56032	1	1.00	215	90	-0.57	0.82	0.00	1.00		0.305453767	1.00
	1	8.7	2.65176	1	1.00	119	90	0.87	0.48	0.00	5.24		0.058505959	-0.19
	1	8.9	2.71272	1	1.00	229	84	-0.75	0.65	0.10	1.02		0.301186524	0.98
	1	10	3.048	1	1.00	197	84	-0.29	0.95	0.10	1.09		0.280699534	0.92
	1	10.4	3.16992	1	1.00	127	89	0.80	0.60	0.02	19.11		0.016044836	-0.05
	1	10.7	3.26136	1	1.00	224	86	-0.69	0.72	0.07	1.00		0.305128546	1.00
											Line 1 Fractures	7.67		
											Outcrop Fracture Density without COS weighting factor (2)	7.665513773		

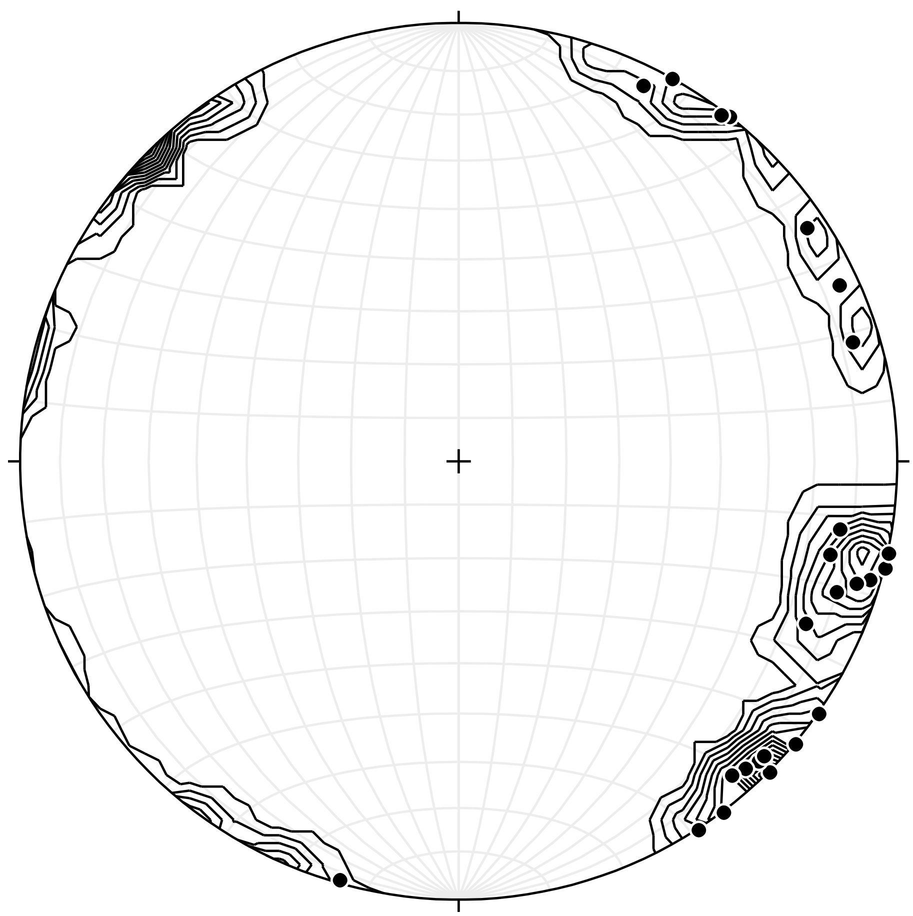

Figure 19 - Stereonet of poles to joints; Station 5-24-17A.

Figure 20 - Chinle Sandstone. Bed outlined in red box; Station 5-24-17B.

Table 13 - Fracture Density measurements from the Chinle Sandstone; Station 5-24-17B.

UTM Coordinates	Strike of Outcrop (Right Hand Rule)	Dip of Outcrop (Right Hand Rule)	Thickness of Bed (Ft)	Thickness of Bed (M)	Strike of Bed (Right Hand Rule)	Dip of Bed (Right Hand Rule)	Sample strike (right hand rule)	Sample dip (right hand rule)	Bed Curvature/faulting	Rock Description			
528614; 3930127	66	90	6.00	1.8288	240	10	NA	NA	None	Triassic SS below entrada			
Scanline #	Start Ft	End ft	Trend Scanline	Plunge Scanline	scanline length (M)	Scanline Vector x = North	Scanline Vector y = East	Scanline Vector z = down					
1	0	25	66	0	7.62	0.41	0.91	0.00					
	Fracture Distance (Ft)	Fracture Distance (M)	Fracture Length (Ft)	Fracture Length Weighting	Fracture Strike	Fracture Dip	Fracture Vector x coord	Fracture Vector y coord	Fracture Vector z coord	Weighting factor for fracture density		New Weighting factor for fracture density	COS of angle between Scanline & Fracture Vector
1	0	0	6.00	1.00	110	73	0.90	0.33	0.29	1.51		0.087179147	0.66
1	0.7	0.21336	3.00	0.50	165	85	0.26	0.96	0.09	0.51		0.064562329	0.98
1	1.7	0.51816	3	0.50	213	89	-0.54	0.84	0.02	0.92		0.035732026	0.54
1	2	0.6096	1	0.17	111	90	0.93	0.36	0.00	0.24		0.015466028	0.71
1	3.3	1.00584	6	1.00	134	90	0.72	0.69	0.00	1.08		0.121677671	0.93
1	9	2.7432	2	0.33	101	83	0.97	0.19	0.12	0.59		0.024903809	0.57
1	9.3	2.83464	6	1.00	159	81	0.35	0.92	0.16	1.01		0.129440256	0.99
1	12.5	3.81	5	0.83	94	90	1.00	0.07	0.00	1.78		0.051342034	0.47
1	13.4	4.08432	2	0.33	119	87	0.87	0.48	0.05	0.42		0.034888058	0.80
1	14.1	4.29768	3	0.50	97	55	0.81	0.10	0.57	1.19		0.027683366	0.42
1	16	4.8768	6	1.00	115	79	0.89	0.41	0.19	1.35		0.097223548	0.74
1	16.9	5.15112	3	0.50	131	75	0.73	0.63	0.26	0.57		0.057442657	0.88
1	17.2	5.24256	3	0.50	141	70	0.59	0.73	0.34	0.55		0.05955862	0.91
1	18	5.4864	2	0.33	209	90	-0.48	0.87	0.00	0.55		0.026326116	0.60
1	20.1	6.12648	6	1.00	165	84	0.26	0.96	0.10	1.02		0.128907832	0.98
1	23.9	7.28472	6	1.00	162	65	0.28	0.86	0.42	1.11		0.118286475	0.90
1	25.3	7.71144	8	1.33	208	87	-0.47	0.88	0.05	2.17		0.107579656	0.61
										Line 1 Fractures	1.55		
										Outcrop Fracture Density without COS weighting factor (2)	1.552930884		

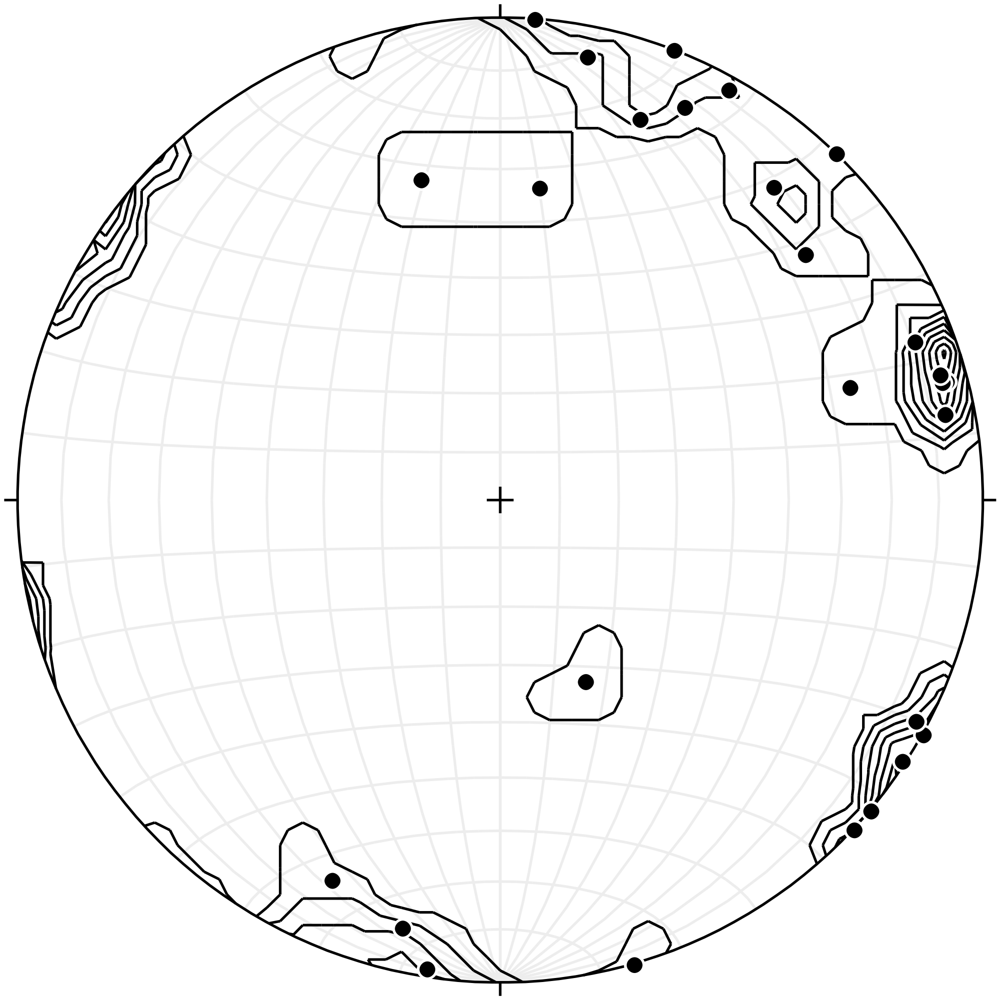

Figure 21 - Stereonet of poles to joints; Station 5-24-17B.

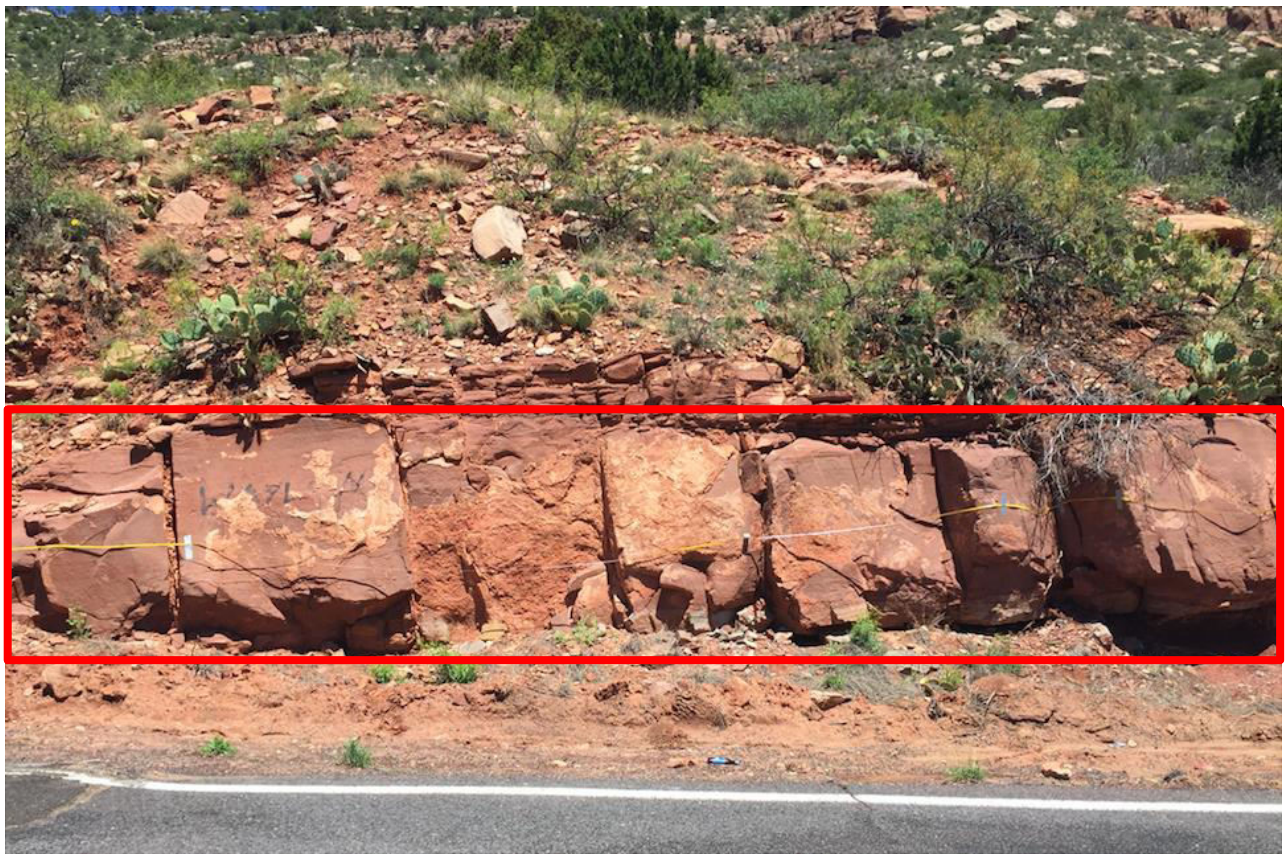

Figure 22 – Lower Chinle Sandstone. Bed measured outlined in red box; Station 5-24-17C.

Table 14 - Fracture Density measurements from the Lower Chinle Sandstone; Station 5-24-17C.

Strike of Outcrop (Right Hand Rule)	Dip of Outcrop (Right Hand Rule)	Thickness of Bed (Ft)	Thickness of Bed (M)	Strike of Bed (Right Hand Rule)	Dip of Bed (Right Hand Rule)	Sample strike (right hand rule)	Sample dip (right hand rule)	Bed Curvature/faulting	Rock Description			
94	90	7.00	2.1336	100	5	NA	NA	none	Triassic SS			
Start Ft	End ft	Trend Scanline	Plunge Scanline	scanline length (M)	Scanline Vector x = North	Scanline Vector y = East	Scanline Vector z = down					
0	31.4	94	0	9.57072	-0.07	1.00	0.00					
Fracture Distance (Ft)	Fracture Distance (M)	Fracture Length (Ft)	Fracture Length Weighting	Fracture Strike	Fracture Dip	Fracture Vector x coord	Fracture Vector y coord	Fracture Vector z coord	Weighting factor for fracture density		New Weighting factor for fracture density	COS of angle between Scanline & Fracture Vector
0	0	7.00	1.00	165	84	0.26	0.96	0.10	1.06		0.098251639	0.94
2.7	0.82296	2	0.29	158	84	0.37	0.92	0.10	0.32		0.026684673	0.89
6	1.8288	7	1.00	165	90	0.26	0.97	0.00	1.06		0.098792836	0.95
7	2.1336	7	1.00	91	66	0.91	0.02	0.41	20.92		0.004995578	-0.05
12.5	3.81	7	1.00	164	87	0.28	0.96	0.05	1.07		0.098049552	0.94
13.8	4.20624	4	0.57	178	86	0.03	1.00	0.07	0.58		0.059234193	0.99
18.6	5.66928	7	1.00	169	89	0.19	0.98	0.02	1.04		0.100909724	0.97
23	7.0104	7	1.00	166	82	0.24	0.96	0.14	1.06		0.098404394	0.94
26	7.9248	3	0.43	164	75	0.27	0.93	0.26	0.47		0.0406451	0.91
28.7	8.74776	7	1.00	170	90	0.17	0.98	0.00	1.03		0.101381686	0.97
									Line 1 Fractures	0.87		
Start Ft	End ft	Trend Scanline	Plunge Scanline	scanline length (M)	Scanline Vector x = North	Scanline Vector y = East	Scanline Vector z = down					
31.4	33.6	158	0	0.67056	-0.93	0.37	0.00					
Fracture Distance (Ft)	Fracture Distance (M)	Fracture Length (Ft)	Fracture Length Weighting	Fracture Strike	Fracture Dip	Fracture Vector x coord	Fracture Vector y coord	Fracture Vector z coord	Weighting factor for fracture density			COS of angle between Scanline & Fracture Vector
31.4	9.57072	7	1	84	77	0.97	-0.10	0.22	1.07		1.396779738	-0.94
31.7	9.66216	5	0.7142857	261	77	-0.96	0.15	0.22	0.75		1.011305075	0.95
33.7	10.27176	7	1	105	73	0.92	0.25	0.29	1.31		1.138956897	-0.76
									Line 2 Fractures	4.05		
Start Ft	End ft	Trend Scanline	Plunge Scanline	scanline length (M)	Scanline Vector x = North	Scanline Vector y = East	Scanline Vector z = down					
33.7	39.3	100	0	1.70688	-0.17	0.98	0.00					
Fracture Distance (Ft)	Fracture Distance (M)	Fracture Length (Ft)	Fracture Length Weighting	Fracture Strike	Fracture Dip	Fracture Vector x coord	Fracture Vector y coord	Fracture Vector z coord	Weighting factor for fracture density			COS of angle between Scanline & Fracture Vector
33.7	10.27176	7	1	160	90	0.34	0.94	0.00	1.15		0.507373338	0.87
35.2	10.72896	4.5	0.6428571	186	90	-0.10	0.99	0.00	0.64		0.375709584	1.00
37.7	11.49096	3	0.4285714	171	90	0.16	0.99	0.00	0.45		0.237405235	0.95
39.3	11.97864	7	1	164	89	0.28	0.96	0.02	1.11		0.526491116	0.90
									Line 3 Fractures	1.80		
Start Ft	End ft	Trend Scanline	Plunge Scanline	scanline length (M)	Scanline Vector x = North	Scanline Vector y = East	Scanline Vector z = down					
39.3	41.1	164	0	0.54864	-0.96	0.28	0.00					
Fracture Distance (Ft)	Fracture Distance (M)	Fracture Length (Ft)	Fracture Length Weighting	Fracture Strike	Fracture Dip	Fracture Vector x coord	Fracture Vector y coord	Fracture Vector z coord	Weighting factor for fracture density			COS of angle between Scanline & Fracture Vector
41.1	12.52728	7	1	66	82	0.90	-0.40	0.14	1.02		1.787384893	-0.98
									Line 4 Fractures	1.82		
									Outcrop Fracture Density without COS weighting factor (2)	1.206023028		

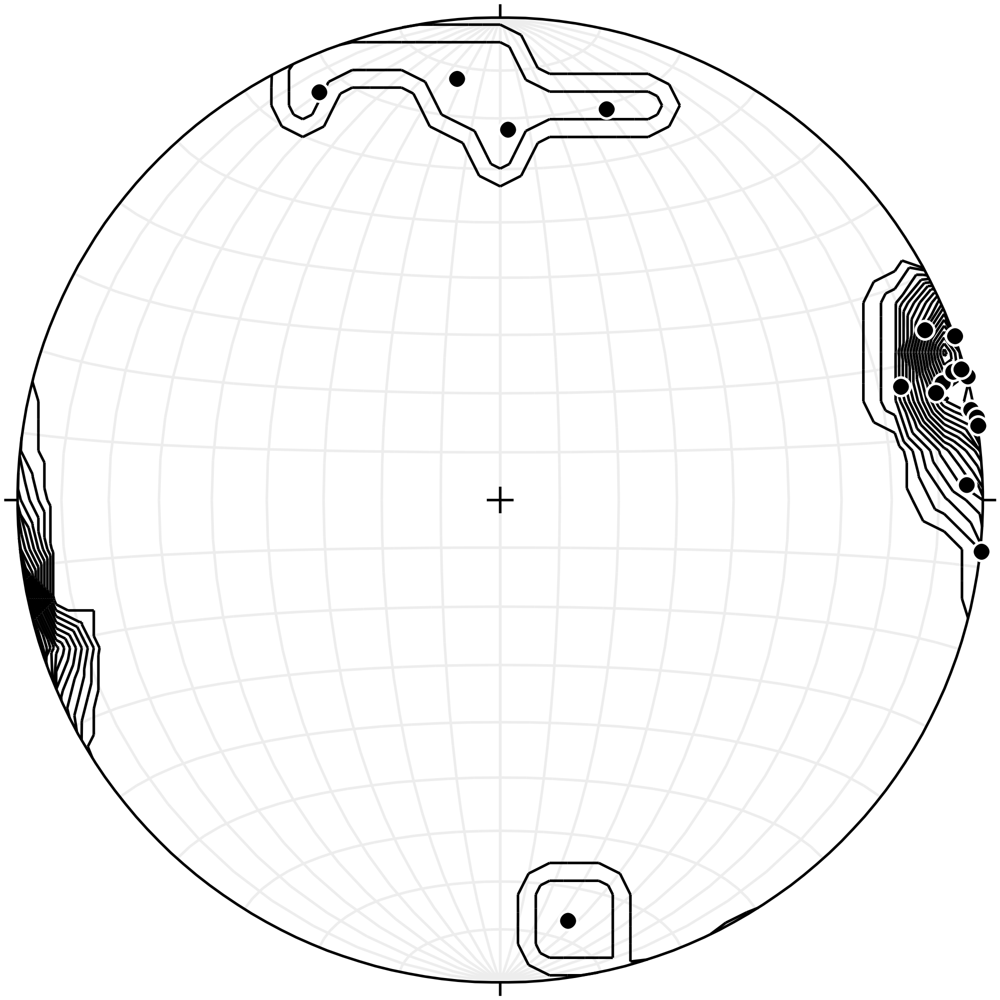

Figure 23 - Stereonet of poles to joints; Station 5-24-17C.

Figure 24 - Santa Rosa Sandstone. Bed measured outlined in red box; Station 5-24-17D.

Table 15 - Fracture Density measurements from the Santa Rosa Sandstone;

Station 5-24-17D. Part 1.

Station	UTM Coordinates	Strike of Outcrop (Right Hand Rule)	Dip of Outcrop (Right Hand Rule)	Thickness of Bed (Ft)	Thickness of Bed (M)	Strike of Bed (Right Hand Rule)	Dip of Bed (Right Hand Rule)	Sample strike (right hand rule)	Sample dip (right hand rule)	Bed Curvature/faulting	Rock Description			
5-24-17D	530218; 3930099	84	90	5.00	1.524	85	7	NA	NA	None	Triassic SS			
	Scanline #	Start Ft	End ft	Trend Scanline	Plunge Scanline	scanline length (M)	Scanline Vector x = North	Scanline Vector y = East	Scanline Vector z = down					
	1	0	9.8	84	0	2.98704	0.10	0.99	0.00					
		Fracture Distance (Ft)	Fracture Distance (M)	Fracture Length (Ft)	Fracture Length Weighting	Fracture Strike	Fracture Dip	Fracture Vector x coord	Fracture Vector y coord	Fracture Vector z coord	Weighting factor for fracture density		New Weighting factor for fracture density	COS of angle between Scanline & Fracture Vector
	1	0	0	5.00	1.00	154	80	0.43	0.89	0.17	1.08		0.309810574	0.93
	1	3.8	1.15824	5.00	1.00	165	86	0.26	0.96	0.07	1.01		0.329852423	0.99
	1	5.2	1.58496	5	1.00	169	80	0.19	0.97	0.17	1.02		0.328438944	0.98
	1	7.8	2.37744	5	1.00	198	87	-0.31	0.95	0.05	1.10		0.305417228	0.91
	1	8.7	2.65176	5	1.00	193	87	-0.22	0.97	0.05	1.06		0.316106505	0.94
	1	9.8	2.98704	5	1.00	145	66	0.52	0.75	0.41	1.25		0.267490513	0.80
											Line 1 Fractures	2.01		
	Scanline #	Start Ft	End ft	Trend Scanline	Plunge Scanline	scanline length (M)	Scanline Vector x = North	Scanline Vector y = East	Scanline Vector z = down					
	2	9.8	15.7	160	0	1.79832	-0.94	0.34	0.00					
		Fracture Distance (Ft)	Fracture Distance (M)	Fracture Length (Ft)	Fracture Length Weighting	Fracture Strike	Fracture Dip	Fracture Vector x coord	Fracture Vector y coord	Fracture Vector z coord	Weighting factor for fracture density			COS of angle between Scanline & Fracture Vector
	2	9.8	2.98704	5	1	79	85	0.98	-0.19	0.09	1.02		0.547138378	-0.98
	2	10.1	3.07848	5	1	79	73	0.94	-0.18	0.29	1.06		0.525229691	-0.94
	2	11.7	3.56616	5	1	195	37	-0.16	0.58	0.80	2.90		0.191949662	0.35
	2	14.1	4.29768	2	0.4	250	76	-0.91	0.33	0.24	0.41		0.215822707	0.97
	2	14.9	4.54152	1	0.2	245	50	-0.69	0.32	0.64	0.26		0.08487137	0.76
	2	15.7	4.78536	5	1	257	80	-0.96	0.22	0.17	1.02		0.543544611	0.98
											Line 2 Fractures	2.56		
	Scanline #	Start Ft	End ft	Trend Scanline	Plunge Scanline	scanline length (M)	Scanline Vector x = North	Scanline Vector y = East	Scanline Vector z = down					
	3	15.7	18.4	85	10	0.82296	0.09	0.98	0.17					
		Fracture Distance (Ft)	Fracture Distance (M)	Fracture Length (Ft)	Fracture Length Weighting	Fracture Strike	Fracture Dip	Fracture Vector x coord	Fracture Vector y coord	Fracture Vector z coord	Weighting factor for fracture density			COS of angle between Scanline & Fracture Vector
	3	18.1	5.51688	2.5	0.5	177	66	0.05	0.91	0.41	0.52		0.589182751	0.97
	3	18.4	5.60832	5	1	165	79	0.25	0.95	0.19	1.02		1.1970948	0.99
											Line 3 Fractures	1.82		
	Scanline #	Start Ft	End ft	Trend Scanline	Plunge Scanline	scanline length (M)	Scanline Vector x = North	Scanline Vector y = East	Scanline Vector z = down					
	4	18.4	19.5	165	5	0.33528	-0.96	0.26	0.09					
		Fracture Distance (Ft)	Fracture Distance (M)	Fracture Length (Ft)	Fracture Length Weighting	Fracture Strike	Fracture Dip	Fracture Vector x coord	Fracture Vector y coord	Fracture Vector z coord	Weighting factor for fracture density			COS of angle between Scanline & Fracture Vector
	4	19.5	5.9436	1.5	0.3	105	66	0.88	0.24	0.41	0.40		0.673491018	-0.75
											Line 4 Fractures	0.89		

Table 16 - Fracture Density measurements from the Santa Rosa Sandstone;

Station 5-24-17D. Part 2.

	Scanline #	Start Ft	End ft	Trend Scanline	Plunge Scanline	scanline length (M)	Scanline Vector x = North	Scanline Vector y = East	Scanline Vector z = down					
	5	19.5	25.4	100	0	1.79832	-0.17	0.98	0.00					
		Fracture Distance (Ft)	Fracture Distance (M)	Fracture Length (Ft)	Fracture Length Weighting	Fracture Strike	Fracture Dip	Fracture Vector x coord	Fracture Vector y coord	Fracture Vector z coord	Weighting factor for fracture density			COS of angle between Scanline & Fracture Vector
	5	20.2	6.15696	5	1	173	88	0.12	0.99	0.03	1.05		0.531452801	0.96
	5	20.5	6.2484	1	0.2	172	83	0.14	0.98	0.12	0.21		0.104983261	0.94
	5	22	6.7056	1.5	0.3	151	77	0.47	0.85	0.22	0.40		0.126322528	0.76
	5	25	7.62	4	0.8	167	70	0.21	0.92	0.34	0.92		0.384799866	0.86
		25.4	7.74192	5	1	140	81	0.634873828	0.756613165	0.156434465	1.58		0.353037183	0.634873828
											Line 5 Fracturee	1.28		
	Scanline #	Start Ft	End ft	Trend Scanline	Plunge Scanline	scanline length (M)	Scanline Vector x = North	Scanline Vector y = East	Scanline Vector z = down					
	6	25.4	26.4	129	0	0.3048	-0.63	0.78	0.00					
		Fracture Distance (Ft)	Fracture Distance (M)	Fracture Length (Ft)	Fracture Length Weighting	Fracture Strike	Fracture Dip	Fracture Vector x coord	Fracture Vector y coord	Fracture Vector z coord	Weighting factor for fracture density			COS of angle between Scanline & Fracture Vector
	6	26.5	8.0772	5	1	194	88	-0.24	0.97	0.03	1.00		3.270854203	1.00
											Line 6 Fracturee	3.28		
	Scanline #	Start Ft	End ft	Trend Scanline	Plunge Scanline	scanline length (M)	Scanline Vector x = North	Scanline Vector y = East	Scanline Vector z = down					
	7	26.4	27.2	10	0	0.24384	0.98	0.17	0.00					
		Fracture Distance (Ft)	Fracture Distance (M)	Fracture Length (Ft)	Fracture Length Weighting	Fracture Strike	Fracture Dip	Fracture Vector x coord	Fracture Vector y coord	Fracture Vector z coord	Weighting factor for fracture density			COS of angle between Scanline & Fracture Vector
	7	26.2	7.98576	5	1	90	80	0.98	0.00	0.17			0.701320832	-0.17
											Line 7 Fracturee	4.10		
											Outcrop Fracture Density without COS weighting factor (2)	2.134958314		

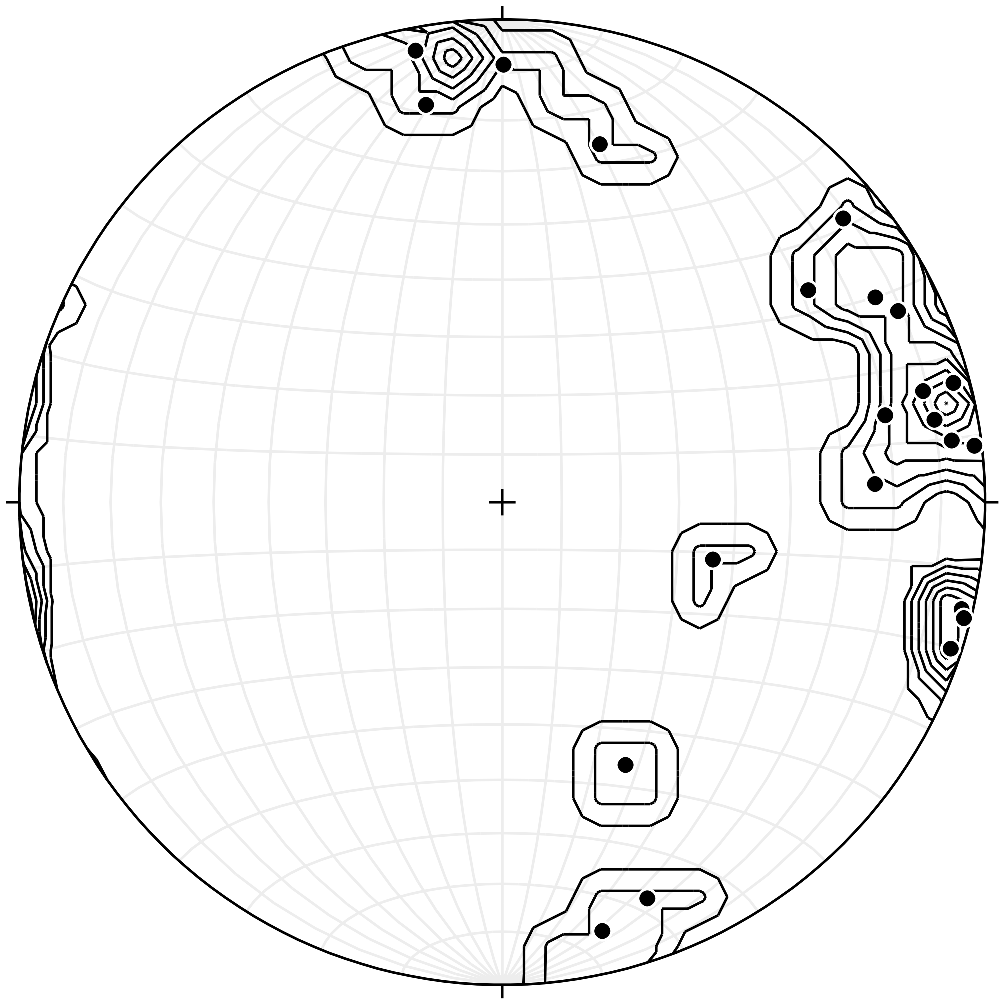

Figure 25 - Stereonet of poles to joints; Station 5-24-17D.

Table 17 - Summary of all outcrop stations and their measured fracture density.

Outcrop Specimen	Fracture Density M^{-1}
5-21-17A	0.447994561
5-21-17B	1.440999311
5-21-17C	1.177386573
5-22-17A	3.850344179
5-22-17B	2.333296625
5-22-17C	1.01
5-23-17A	0.553901292
5-24-17A	7.665513773
5-24-17B	1.552930884
5-24-17C	1.206023028
5-24-17D	2.134958314

5.2 Fracture Toughness

Previous researchers that investigated this topic used a statistical correlation, which relates the fracture toughness of a rock to its Young's Modulus (Smith, 2014; Kimiagar, 2014; Martin, 2015; Zastoupil, 2015; Bammel, 2016):

$$K_{IC} = 0.336 + 0.026E \text{……Equation 20}$$

This equation and method is described by Whittaker et al., (1993). In this study, rock fracture toughness was directly measured using the Cracked Chevron Notched Brazilian Disc Test, which is a method that is recommended by the International Society of Rock Mechanics to measure rock fracture toughness for Mode I fractures (KI_c) (See Figure 26 for Specimen Setup/Geometry). The measured values were then compared to values obtained by Equation 20. Preliminary work was done in Dr. Ashley Griffith's Rock Fracture Mechanics class on Berea Sandstone samples in order to verify this method. The reason for using Berea Sandstone is because there have been past studies performed on it and there are many sources for values of KI_c (Doolin,1994; Nara, et al., 2012; Park, 2006; Thiercelin, 1989; Thiercelin and Roegiers, 1986; Zoback, 1978). To perform this test, rocks need to be cut using rock saws with a diamond blade and mineral spirits, cored in a drill press with a diamond-bit core bit, have a notch cut into the middle of the disc with a dremel tool, and then broken in Dr. Griffith's rock mechanics lab using a Forney F-325 Compression Testing Machine (Figure

27). Specimens were compressed at a load rate of 0.2 kN/second. When the maximum load is recorded for the CCNBD, the values for fracture toughness are calculated according to Equation 21:

$$K_{CCNBD} = \frac{P_{max}}{B*\sqrt{D}} * Y_{min} \text{......Equation 21}$$

Where P_{max} is the maximum failure load in kN, B is the thickness of the specimen in millimeters, D is the diameter of the specimen in millimeters, and Y_{min} is the critical dimensionless stress intensity factor, which is determined by the specimen geometry. K_{CCNBD} denotes Mode I fracture toughness in units $MPa * m^{1/2}$. More specifically, this equation calculates the critical moment at the maximum load in conjunction with the minimum value of Y_{min}, (Wang, 2013). This equation was proposed by R.J. Fowell (1995). Y_{min} is determined by the specimen geometry dimensions α_0, α_1, and α_B and is calculated using the following formula:

$$Y_{min} = ue^{v\alpha_1} \text{......Equation 22}$$

Where u and v are constants determined by linear interpolation of the calibrated values corresponding to α_0 and α_B in Tables 4 and 5 in Wang, (2007) (See Tables 17 and 18 for Wang's values). Since two specimens were used for testing this method in order to validate the values obtained, the higher K_{IC} was used for calculations. Table 20 shows a comparison of the values obtained from the Whittaker et al., (1993) statistical correlation to Young's Modulus and the CCNBD method of measuring fracture touhgness. Figure 28 shows the correlation between the two methods. An R values of ~90% shows a good correlation between the two methods. The values obtained from the Young's Modulus correlation were used with the fracture density data (along with the CCNBD values) to see the effect the different values have on the final results. See Appendix A for measurements of P_{max} in Equation 21.

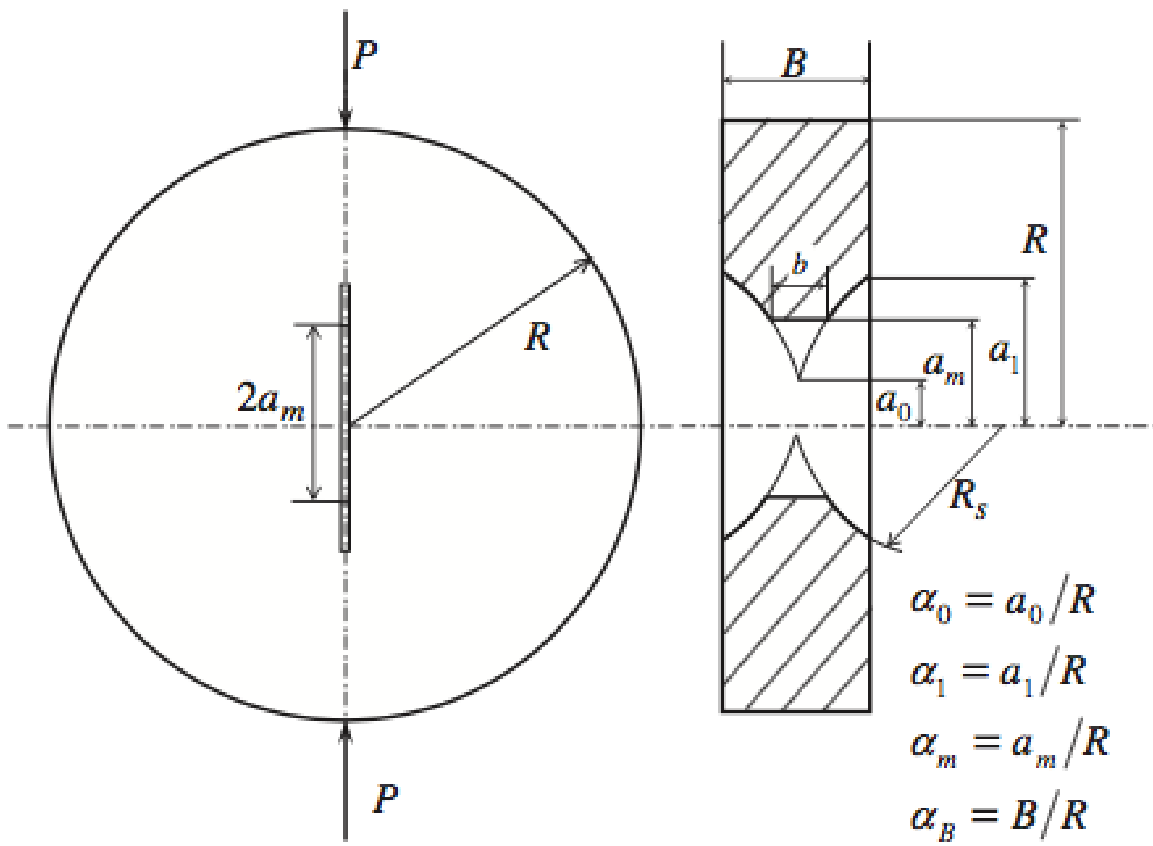

Figure 26 - Cracked Chevron Notched Specimen Geometry. Figure from Wang, (2010).

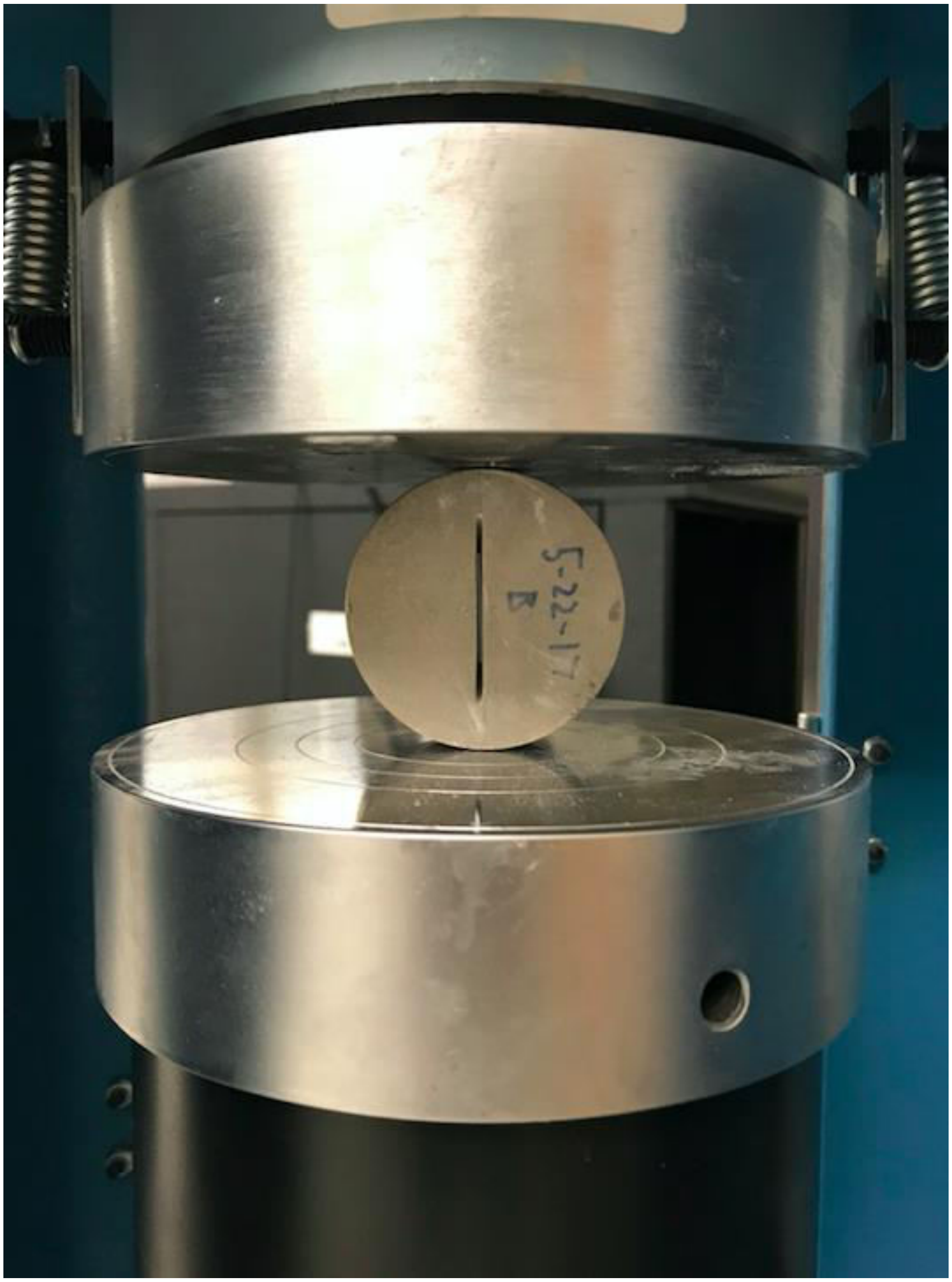

Figure 27 - Example of final specimen geometry and how testing is done in Forney F-325 Compression Testing Machine.

Table 18 - Values of u in Equation 21 for different values of α_o across the top and α_B in the left column. Table from Wang (2010).

α_o	0.100	0.150	0.175	0.200	0.225	0.250	0.275	0.300	0.325	0.350	0.375	0.400	0.425	0.450
α_B														
0.440	0.2723	0.2765	0.2788	0.2814	0.2843	0.2873	0.2906	0.2941	0.2977	0.3016	0.3055	0.3095	0.3136	0.3176
0.480	0.2754	0.2798	0.2823	0.2850	0.2879	0.2911	0.2944	0.2980	0.3017	0.3056	0.3095	0.3136	0.3176	0.3215
0.520	0.2787	0.2832	0.2858	0.2886	0.2916	0.2948	0.2983	0.3019	0.3056	0.3095	0.3135	0.3175	0.3215	0.3253
0.560	0.2821	0.2868	0.2894	0.2923	0.2954	0.2986	0.3021	0.3058	0.3095	0.3134	0.3174	0.3213	0.3252	0.3290
0.600	0.2857	0.2904	0.2931	0.2960	0.2991	0.3025	0.3060	0.3096	0.3134	0.3173	0.3212	0.3250	0.3289	0.3325
0.640	0.2894	0.2941	0.2969	0.2998	0.3029	0.3063	0.3098	0.3134	0.3172	0.3210	0.3248	0.3286	0.3323	0.3358
0.680	0.2931	0.2979	0.3006	0.3036	0.3067	0.3100	0.3135	0.3171	0.3208	0.3246	0.3284	0.3321	0.3357	0.3391
0.720	0.2969	0.3017	0.3044	0.3073	0.3104	0.3137	0.3172	0.3208	0.3244	0.3281	0.3318	0.3354	0.3389	0.3421
0.760	0.3008	0.3055	0.3082	0.3111	0.3141	0.3174	0.3208	0.3243	0.3279	0.3315	0.3351	0.3386	0.3420	0.3451
0.800	0.3047	0.3093	0.3119	0.3148	0.3178	0.3210	0.3244	0.3278	0.3313	0.3349	0.3384	0.3418	0.3450	0.3480
0.840	0.3086	0.3130	0.3156	0.3184	0.3214	0.3246	0.3278	0.3312	0.3347	0.3381	0.3415	0.3448	0.3480	0.3508
0.880	0.3125	0.3168	0.3193	0.3220	0.3250	0.3280	0.3313	0.3346	0.3380	0.3413	0.3446	0.3479	0.3509	0.3536
0.920	0.3164	0.3205	0.3230	0.3256	0.3285	0.3315	0.3347	0.3379	0.3412	0.3445	0.3477	0.3509	0.3538	0.3565
0.960	0.3203	0.3242	0.3266	0.3292	0.3320	0.3349	0.3380	0.3412	0.3445	0.3477	0.3509	0.3539	0.3568	0.3594
1.000	0.3241	0.3279	0.3302	0.3328	0.3355	0.3384	0.3414	0.3445	0.3477	0.3509	0.3540	0.3570	0.3598	0.3624
1.040	0.3281	0.3317	0.3339	0.3363	0.3390	0.3418	0.3448	0.3479	0.3511	0.3542	0.3573	0.3603	0.3631	0.3655

Table 19 - Values of v in Equation 21 for different values of α_o across the top and α_B in the left column. Table from Wang (2010).

α_o	0.100	0.150	0.175	0.200	0.225	0.250	0.275	0.300	0.325	0.350	0.375	0.400	0.425	0.450
α_B														
0.440	1.8688	1.8747	1.8752	1.8743	1.8720	1.8684	1.8638	1.8582	1.8518	1.8446	1.8369	1.8286	1.8199	1.8111
0.480	1.8341	1.8406	1.8416	1.8411	1.8395	1.8367	1.8329	1.8281	1.8227	1.8165	1.8099	1.8028	1.7955	1.7880
0.520	1.8017	1.8088	1.8102	1.8103	1.8092	1.8071	1.8040	1.8002	1.7956	1.7905	1.7850	1.7791	1.7730	1.7668
0.560	1.7717	1.7793	1.7811	1.7816	1.7811	1.7796	1.7773	1.7742	1.7706	1.7664	1.7619	1.7572	1.7523	1.7475
0.600	1.7438	1.7519	1.7540	1.7550	1.7550	1.7541	1.7525	1.7502	1.7474	1.7442	1.7407	1.7370	1.7334	1.7298
0.640	1.7180	1.7265	1.7289	1.7303	1.7308	1.7305	1.7295	1.7279	1.7259	1.7236	1.7211	1.7185	1.7160	1.7136
0.680	1.6942	1.7030	1.7057	1.7074	1.7084	1.7086	1.7082	1.7073	1.7061	1.7046	1.7030	1.7015	1.7001	1.6989
0.720	1.6723	1.6812	1.6842	1.6863	1.6876	1.6883	1.6884	1.6882	1.6877	1.6871	1.6864	1.6859	1.6855	1.6855
0.760	1.6520	1.6611	1.6643	1.6666	1.6683	1.6694	1.6702	1.6706	1.6708	1.6709	1.6711	1.6715	1.6722	1.6733
0.800	1.6334	1.6426	1.6459	1.6485	1.6505	1.6520	1.6532	1.6542	1.6551	1.6560	1.6570	1.6583	1.6600	1.6622
0.840	1.6162	1.6254	1.6288	1.6316	1.6339	1.6359	1.6375	1.6391	1.6406	1.6422	1.6440	1.6462	1.6488	1.6521
0.880	1.6004	1.6096	1.6131	1.6160	1.6186	1.6209	1.6229	1.6250	1.6271	1.6293	1.6319	1.6350	1.6385	1.6428
0.920	1.5859	1.5949	1.5984	1.6015	1.6043	1.6069	1.6093	1.6118	1.6145	1.6174	1.6207	1.6245	1.6290	1.6342
0.960	1.5725	1.5812	1.5848	1.5880	1.5910	1.5938	1.5966	1.5995	1.6027	1.6062	1.6102	1.6148	1.6201	1.6263
1.000	1.5601	1.5686	1.5721	1.5754	1.5785	1.5815	1.5846	1.5879	1.5916	1.5957	1.6003	1.6056	1.6117	1.6188
1.040	1.5486	1.5567	1.5602	1.5635	1.5667	1.5699	1.5733	1.5770	1.5810	1.5856	1.5909	1.5969	1.6038	1.6117

Table 20 - Values for KIC as calculated by the Cracked Chevron Notched Brazilian Disc test method using Equation 20 and comparison to statistical correlation equation from Whittaker et al, (1993).

Sample ID	Young's Modulus Correlation (MPa)	Sample ID2	CCNBD (MPa)
5-24-17D	0.297731832	5-23-17A	0.189477818
5-24-17B	0.358337831	5-24-17D	0.433052842
5-24-17C	0.452494967	5-24-17B	0.439722283
5-22-17C	0.473389684	5-24-17C	0.580664474
5-23-17A	0.500652849	5-21-17A	0.628404708
5-22-17A	0.823214837	5-22-17C	0.641662253
5-21-17A	0.907960522	5-21-17B	0.668192214
5-22-17B	0.920883964	5-21-17C	0.704619923
5-21-17C	0.969549943	5-22-17B	0.790289957
5-21-17B	0.993562757	5-22-17A	0.908717869
5-24-17A	1.264082584	5-24-17A	1.357432284

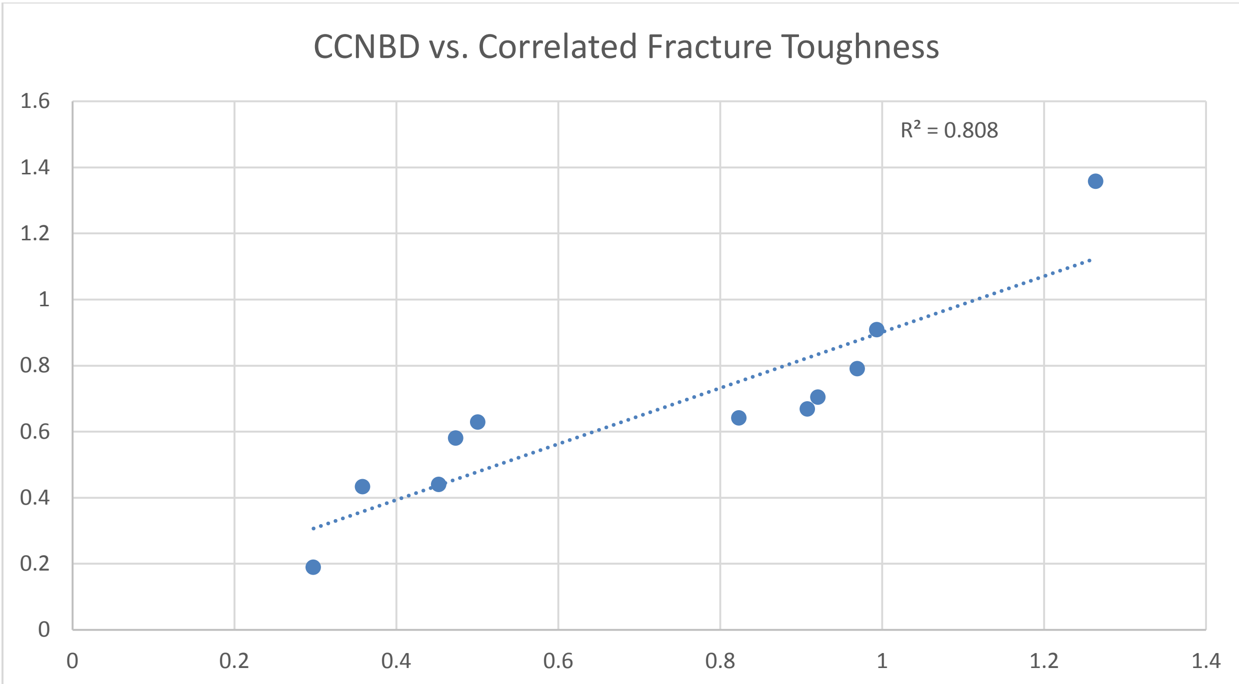

Figure 28 - Scatter plot of measured fracture toughness values vs. the fracture toughness values calculated by the Young's Modulus correlation equation. R value of ~90% shows very good correlation between the two methods.

5.3 Dynamic Elastic Properties

Acoustic properties, pressure waves and shear waves, of the rocks were measured on the samples in the Dr. Yu's Materials Characterization Lab in the Civil Engineering Department. P-wave (pressure wave) velocity is the measure of the amount of time in m/s that the pressure wave takes to pass through a sample parallel to the wave direction. The S-wave (shear wave) velocity is the amount of time in m/s that the shear wave passes through the material in the direction of travel, which is perpendicular to particle motion. Since S-waves travel slower than P-waves, they can be distinguished from one another. Travel time was estimated by picking peaks in wave forms and that travel time over the distance of the sample was used to calculate the velocity for P- and S-waves alike (See Figure 29 for example of waveform picking). Samples were cut with the same saws used to make the fracture toughness specimens so there are two smooth surfaces parallel to each other. Once P-wave and S-wave velocities are determined by performing wave form analysis, the Young's Modulus and Poisson's Ratio were calculated using the following equations:

$$E_d = \rho V_s^2 \left[\frac{3V_p^2 - 4V_s^2}{V_p^2 - V_s^2}\right] \text{......Equation 23}$$

$$\nu = \frac{\left(\frac{V_p}{V_s}\right)^2 - 2}{2\left(\left(\frac{V_p}{V_s}\right)^2 - 1\right)} \text{......Equation 24}$$

Where V_p = compressional wave velocity; V_s = shear wave velocity; and ρ = density (Zhixi et al., (1997); and Sheriff, (1991), respectively). See Appendix B for all waveform figures. Table 21 shows the results from the dynamic elastic properties measurements. Distance between the two receivers was measured with calipers in centimeters and then converted to meters. Travel time was measured in milliseconds and then converted to seconds and velocity was calculated in meters per second. Figure 29 explains how the travel time was picked. Table 22 shows the material properties calculated using Equations 23 and 24.

Table 21 - Results of Dynamic Elastic Properties Measurements.

Sample ID	Distance in Meters	Travel time in seconds	P-Wave Velocity (m/s)	S-Wave Velocity (m/s)
5-21-17A	0.11088	0.0000286	3876.923	2570.832367
5-21-17B	0.08565	0.00002007	4267.564	2641.887724
5-21-17C	0.10954	0.00002673	4098.017	2666.504382
5-22-17A	0.07207	0.0000195	3695.897	2402.333333
5-22-17B	0.13734	0.00003375	4069.333	2359.388421
5-22-17C	0.13464	0.00004689	2871.401	1806.278508
5-23-17A	0.15621	0.00005051	3092.655	2039.295039
5-24-17A	0.1264	0.00002441	5178.206	3416.216216
5-24-17B	0.08647	0.00003483	2482.630	1623.240098
5-24-17C	0.1031	0.00003633	2837.875034	1775.749225
5-24-17D	0.05008	0.00002147	2332.557056	1430.857143

Table 22 - Calculated Material Properties using Dynamic Elastic Properties and Equations 23 and 24.

Sample ID	Poisson's Ratio	Shear Modulus	Young's Modulus
5-21-17A	0.107594012	15764596606	34921545620
5-21-17B	0.189314332	16065533824	38213939273
5-21-17C	0.132867969	16458391663	37290369484
5-22-17A	0.134199134	13957908824	31662096206
5-22-17B	0.246800908	14203791813	35418601068
5-22-17C	0.172576883	7763790540	18207282618
5-23-17A	0.115345388	8632243462	19255865874
5-24-17A	0.114662979	19048642167	68521973755
5-24-17B	0.126629391	6116568344	13782211337
5-24-17C	0.178252569	7385360371	17403639664
5-24-17D	0.198339457	4789390146	11478630372

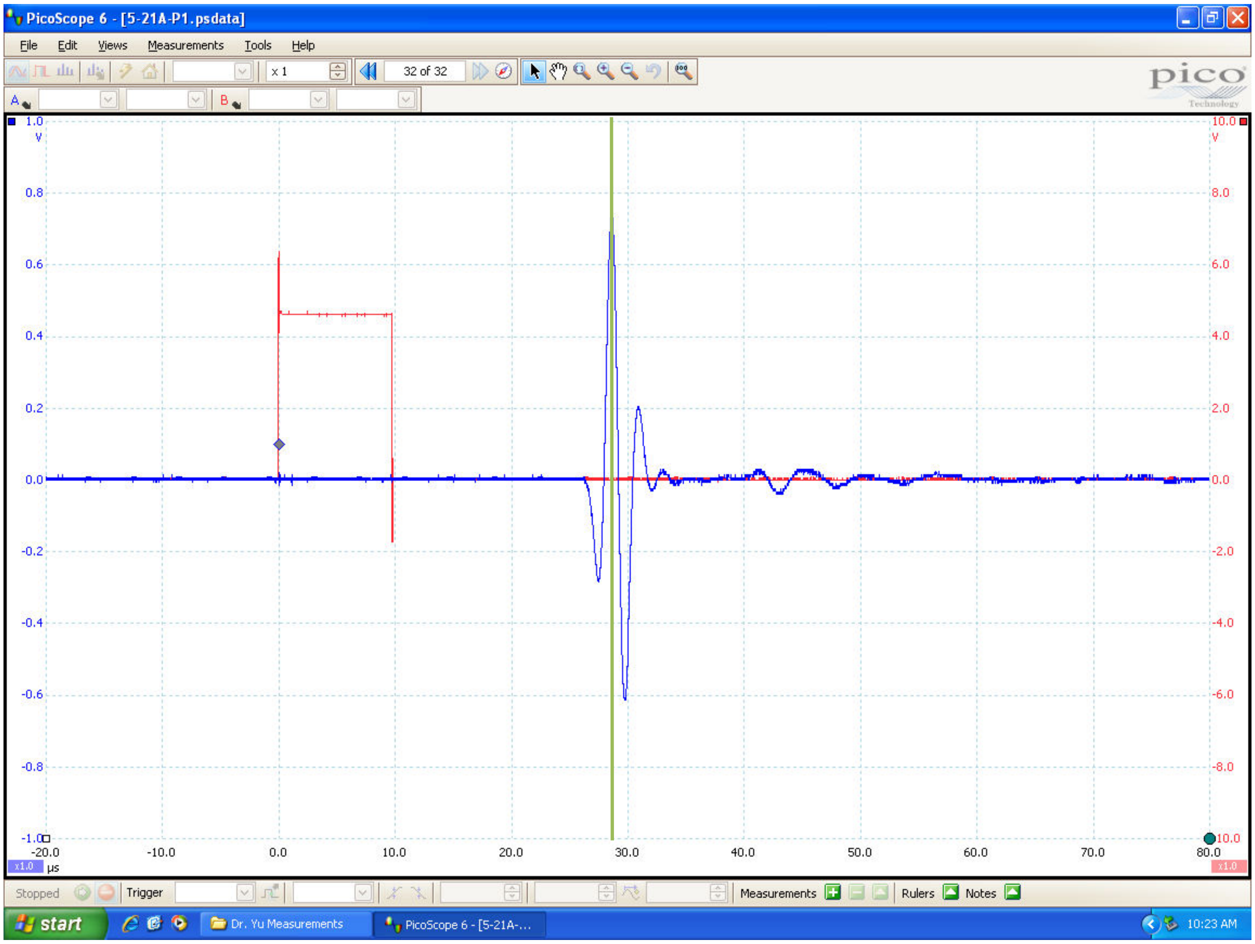

Figure 29 - Example of wave form used to pick travel time and calculate P-wave Velocity, 5-21-17A. Orange line indicates where travel-time was picked for calculations. X-axis is wave travel time measured in milliseconds and the y-axis is the amplitude of the wave measured in volts. The signal travels through the samples and being emitted from a source receiver and then being detected by another receiver on the other end of the sample.

5.4 Density

Density was measured in Dr. Hu's lab in the Geoscience Building at UTA with Qiming Wang, one of Dr. Hu's Master's Students. Samples were measured for bulk density using a Vacuum Saturation method, which is commonly used to investigate pore structure and properties of geologic and man-made materials. The setup consists of a sample chamber (a steel cylinder), a vacuum pump, a CO_2 cylinder, and a fluid reservoir. The goal is to evacuate the samples with the vacuum and then introduce CO_2 into the chamber. While still under vacuum the samples are immersed in a saturating fluid that occupies the evacuated pore space. This is done while still under vacuum in order for the saturating fluid to occupy more pore space since CO_2 is a water-wetting gas. In this case, about 500mL of DI (deionized) water was boiled for 10 minutes and then cooled to room temperature. By weighing the samples before and after saturation, the total mass of fluid saturated into the samples can be used to calculate the accessible pore volume as well as the density of the sample. Bulk volume in Table 23 does not include the pore space as it is saturated with fluid. Porosity is calculated by dividing the average fluid contained in the rock by the bulk volume of the rock and multiplying by 100

Table 23 - Results of vacuum saturation method. Air dry weight, bulk volume, and bulk density were all given from vacuum saturation method. Porosity was calculated using an Excel Spreadsheet.

Sample	# of samples	Air dry weight (g)	Bulk volume(cm3)	Bulk Density(g/cm^3)	Porosity (%)
1	5-21-17c	19.1349	8.267	2.314743055	11.707
2	5-24-17d	17.9433	7.670	2.339309393	10.655
3	5-21-17a	22.0242	9.233	2.385257906	8.771
4	5-24-17c	20.2295	8.637	2.342116125	11.728
5	5-21-17b	20.4117	8.868	2.301793966	10.795
6	5-22-17a	21.4470	8.868	2.418543051	7.582
7	5-22-17b	19.0472	7.465	2.551557799	2.935
8	5-24-17b	14.7818	6.368	2.321358993	12.669
9	5-22-17b	16.9648	7.129	2.379602305	9.784
10	5-24-17a	18.5124	7.029	2.633695681	0.958
11	5-23-17a	15.7549	7.590	2.075695076	18.982

Chapter 6

Results

6.1. Results using CCNBD method of calculating fracture toughness.

One goal of this study was to see if the outcrops in the study area were subjected to the same strain state by testing the dimensionless geomechanical equation (Equation 19, repeated below):

$$\frac{F_d K_{IC}^2}{4\mu^2(1+v)} = (A\frac{v}{1-2v} + B)$$

If the layers measured were subjected to the same strain state, Equation 19 should plot as a straight line with A as the slope and B as the intercept. A and B represent the strain state and are related to the strain invariants:

$$A = I_1^2 = \varepsilon_1^2 + \varepsilon_2^2 + \varepsilon_3^2(\varepsilon_1\varepsilon_2 + \varepsilon_2\varepsilon_3 + \varepsilon_3\varepsilon_1)$$

$$B = I_1^2 - 2I_2 = \varepsilon_1^2 + \varepsilon_2^2 + \varepsilon_3^2$$

If the data in Equation 19 does not plot on a straight line or is scattered, then the tensile strength of the rock was probably exceeded.

If the rock layers were subject to constant strain and are consistent with the simplifying assumptions of the dimensionless geomechanical equation (Equation 19), then the data should plot in a straight line with a positive slope. The results in Figure 30 show that the data plots as a line with a positive slope, with A equal to 94 and a y-intercept, B, equal to 4.6852. It has an r^2 value of 0.5296.

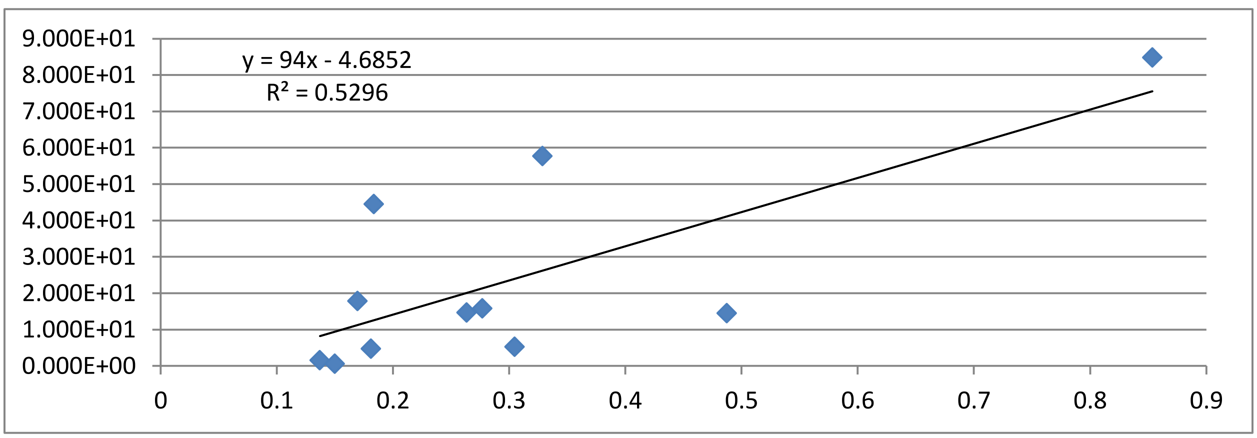

Figure 30 - Plot of all outcrop data using the dimensionless equation (Equation 19) and the measured fracture toughness from CCNBD.

This graph suggests that the layers were subjected to constant levels of strain and has a correlation coefficient of r $= 0.5^{1/2} = 0.728$, which says relationship has a probability of ~73%. Although this is a good correlation value, there are areas where error is present. Some of those sources of error include: waveform picking for the sonic velocities (Appendix B); picking the failure point from the CCNBD graphs (Appendix A); human error when creating the CCNBD specimens.

Geomechanical Equation 4, repeated below:

$$F_d = \frac{4\mu^2(1+v)}{K_{IC}^2}(A\frac{v}{1-2v}+B)$$

uses the mechanical properties and constant strain condition to predict fracture densities and therefore, brittleness of the rock. The predicted fracture densities can be plotted as a function of strain using Equation 4. The coefficients A and B were calculated from the invariants using increasing uniaxial extension. Figure 31 shows increasing uniaxial extension on the x-axis with the calculated fracture density on the y-axis.

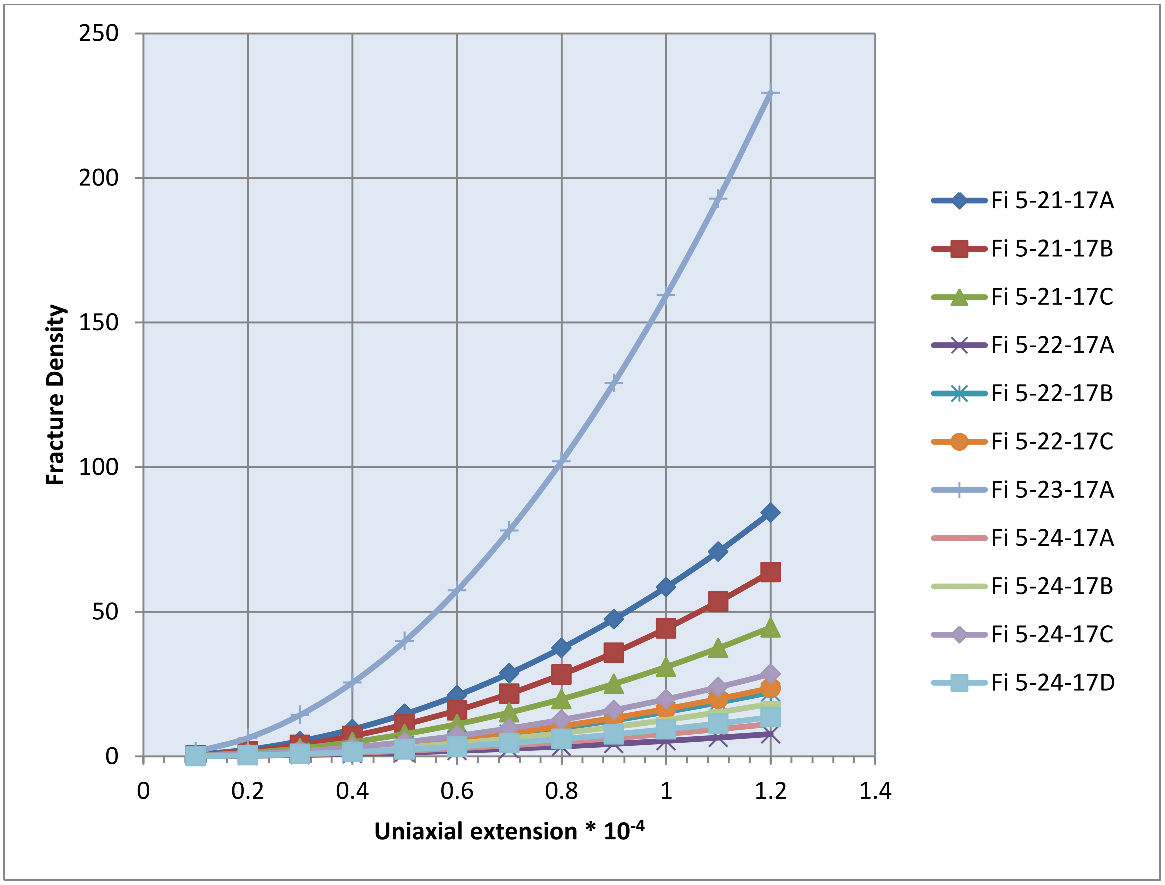

Figure 31 - Plot of Uniaxial Extension vs. Fracture Density with the measured fracture toughness from CCNBD.

The measured fracture densities of each rock sample collected are compared to each other to give a comparative brittleness based on the calculated fracture densities at the same strain state. In this case, the sample with the highest fracture density is the most brittle, while the sample with the lowest fracture density is the least brittle. Based off of this data in Figure 31, 5-23-17A is the most brittle and

5-22-17A is the least brittle.

Equation 1, Jin et al., (2014), which uses the normalized Young's Modulus and Poisson's Ratio shows 5-21-17A as the most brittle and 5-24-17D as the least brittle. Table 24 shows all brittleness results for Equation 1 from least to greatest and how they compare to the fracture density calculations from outcrop data and the fracture density brittleness shown in Figure 31.

Jin et al., (2014) defines brittleness in terms of normalized Young's Modulus and Poisson's Ratio values (see equations 1-3 repeated below):

$$B_{19} = \frac{E_n + \upsilon_n}{2} \text{......Equation 1}$$

$$E_n = \frac{E - E_{min}}{E_{max} - E_{min}} \text{......Equation 2}$$

$$\upsilon_n = \frac{\upsilon_{max} - \upsilon}{\upsilon_{max} - \upsilon_{min}} \text{......Equation 3}$$

The brittleness calculated by Equation 18 is compared to the normalized Young's Modulus and Poisson's Ratio brittleness from Jin et al., (2014), Equations 1-3 above. Table 24 shows a comparison of the results between the two methods for calculating brittleness. The column for "Geomechanical Equation 4" is the order in which brittleness was calculated using the fracture density field measurements in Figure 31 and is listed from the least brittle to the most brittle based off of

Figure 31. “Jin B19 Brittleness Equation 1” is listed in order from least brittle to most brittle and the “Sample ID” column was sorted along that parameter. The two methods show very little correlation with respect to the order of brittleness for each rock.

Table 24 - Comparison of brittleness calculations between Equation 1 (Jin et al., (2014) and the Geomechanical Equation 4. “Sample ID” is associated with Equation 1 and Geomechanical Equation 4 is associated with Figure 31. The least brittle is at top and the most brittle is at the bottom for all columns.

Sample ID	Jin B19 Brittleness Equation 1	Geomechanical Equation 4
5-24-17D	0.2815695	5-22-17A
5-24-17C	0.406606615	5-24-17A
5-22-17C	0.430669824	5-24-17D
5-22-17B	0.474771296	5-24-17B
5-24-17B	0.483995479	5-22-17B
5-24-17A	0.5	5-22-17C
5-23-17A	0.582001623	5-24-17C
5-21-17B	0.649325109	5-21-17C
5-22-17A	0.69719154	5-21-17B
5-21-17C	0.773241731	5-21-17A
5-21-17A	0.803418507	5-23-17A

6.2. Results using correlation method of calculating fracture toughness.

Past research (Smith, 2014; Kimiagar, 2014; Martin, 2015; Zastoupil, 2015; Bammel, 2016; Wickham et al., 2013) has used a statistical correlation relating mode I fracture toughness to a rock's Young's Modulus in order to calculate that rock's fracture toughness. Since this project directly measured rock fracture toughness using the Cracked Chevron Notched Brazilian Disc Test, a comparison was made between the two methods (See Figures 30, 31, 32, and 33).

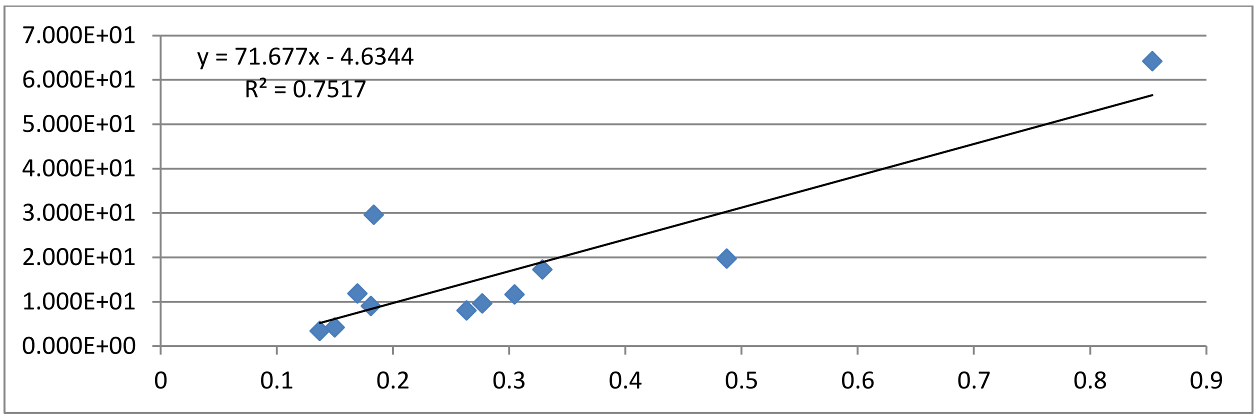

Figure 32 - Plot of all outcrop data using the dimensionless equation (Equation 19) and the statistical correlation of rock fracture toughness and Young's Modulus (Whittaker et al., 1993). The statistical correlation used was for Mode I Fractures: K_{IC}=0.336+0.026E where E is the Young's Modulus. The x-axis is $\frac{v}{(1-2v)}$ wherev, the Poisson's Ratio, is and the y-axis is $\frac{F_d K_{IC}^2}{4\mu^2(1+v)}$ where Fd is the fracture density, F_d is the fracture density, K_{IC} is mode I fracture toughness, μ is the Shear Modulus and v is Poisson's Ratio.

The results in Figure 32 show that the data plots as a line with a positive slope, with A equal to 71.677 and a y-intercept, B, equal to 4.6344 and an r value of ~87% probability. As with Figure 30, this graph suggests that the layers were subjected to constant levels of strain, but the sources for error are slightly different. The error in sonic velocities remain (see Appendix A), but this time the issue with fracture toughness is using a correlation equation (Whittaker et al., 1993) rather than a direct measurement of fracture toughness. Although it is not a direct measurement, it does provide less error as there is less room human error compared to using the CCNBD method.

The predicted fracture densities using the statistical correlation of K_{IC} were again plotted as a function of strain using Equation 4. Figure 33 shows increasing uniaxial extension on the x-axis with the calculated fracture density on the y-axis.

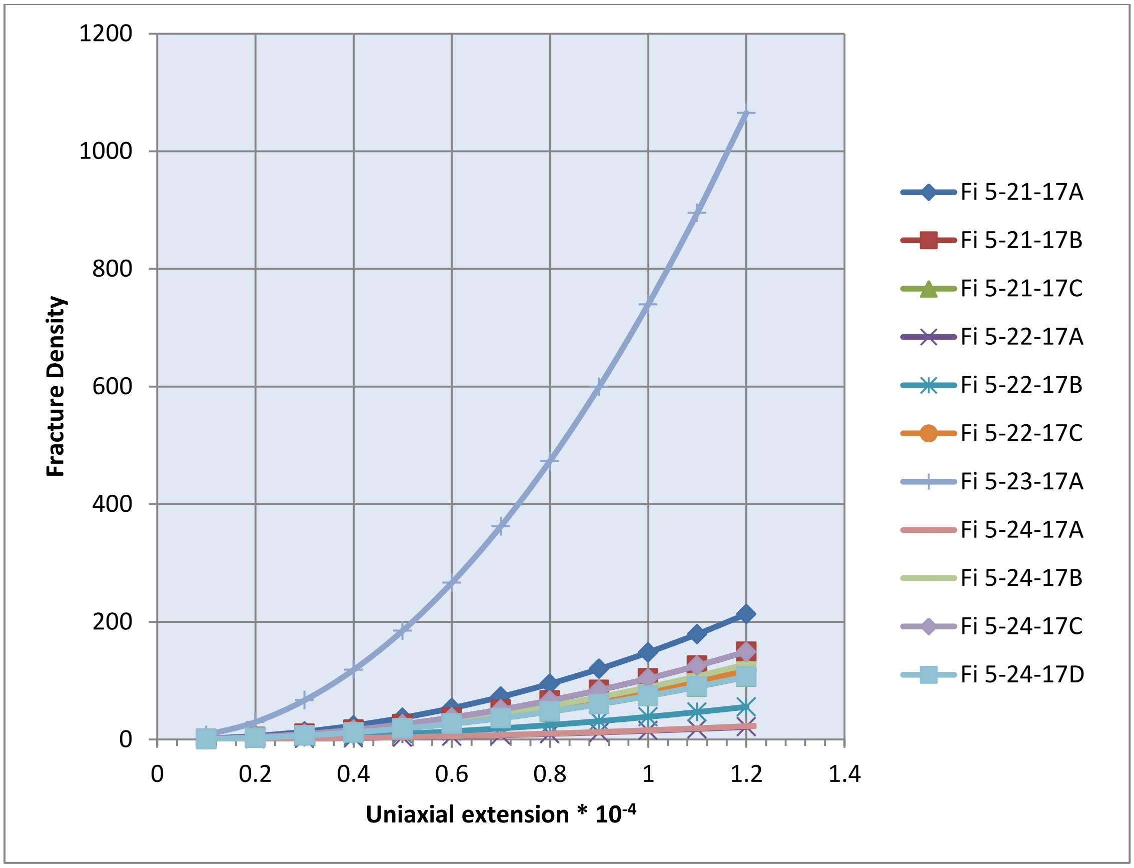

Figure 33 - Plot of Uniaxial Extension vs. Fracture Density using the statistical correlation of rock fracture toughness with Young's Modulus.

Overall fracture density increased likely due to higher fracture toughness values predicted by the correlation with Young's Modulus (See Table 19). However, the order of fracture toughness is not the same between the two methods and did have a slight effect on the order of relative brittleness using Equation 4. This could be due to a multitude of reasons including inaccuracy of the Young's Modulus correlation or imprecision when creating the CCNBD specimens (human error).

6.3 Comparison of fracture density brittleness to Equation 1 brittleness.

To compare the fracture density brittleness values more easily to the Jin et al., (2014) brittleness values (Equation 1), the calculated values were normalized using the following equation:

$$Fd\ Normalized = \frac{Fd - Fd_{min}}{Fd_{max} - Fd_{min}}$$

and put in order from least to greatest. The overall trend shows Jin et al., (2014) Equation 1 providing higher values of brittleness compared to the Fd brittlness. Table 25 and Figure 34 show the relationship between the two different methods of predicting brittleness. Table 25 shows the Sample ID listed in order according to normalized results of Equation 1, so 5-24-17C is the least brittle and 5-21-17A is the most brittle. Sample ID2 is listed in order according to normalized results of the fracture density brittleness.

Table 25 - Normalized values for Equation 1 brittleness and Equation 19 Fd brittleness. Sample ID is ordered according to the normalized Equation 1 brittleness and Sample ID2 is ordered according to normalized fracture density brittleness.

Sample ID	Normalized Jin B19 Brittleness Equation 1	Sample ID2	Normalized Fd Brittleness Equation 19
5-24-17C	0	Fd 5-24-17D	0
5-22-17C	0.05804832	Fd 5-22-17C	0.032912497
5-24-17B	0.124474496	Fd 5-24-17C	0.044559068
5-22-17B	0.322207388	Fd 5-22-17A	0.05492619
5-23-17A	0.382956755	Fd 5-24-17B	0.055068037
5-24-17A	0.521895951	Fd 5-24-17A	0.072126682
5-24-17D	0.521895951	Fd 5-22-17B	0.173913484
5-21-17B	0.712870865	Fd 5-21-17C	0.282386918
5-22-17A	0.74663526	Fd 5-21-17A	0.318315567
5-21-17C	0.961053297	Fd 5-21-17B	0.341127371
5-21-17A	1	Fd 5-23-17A	1

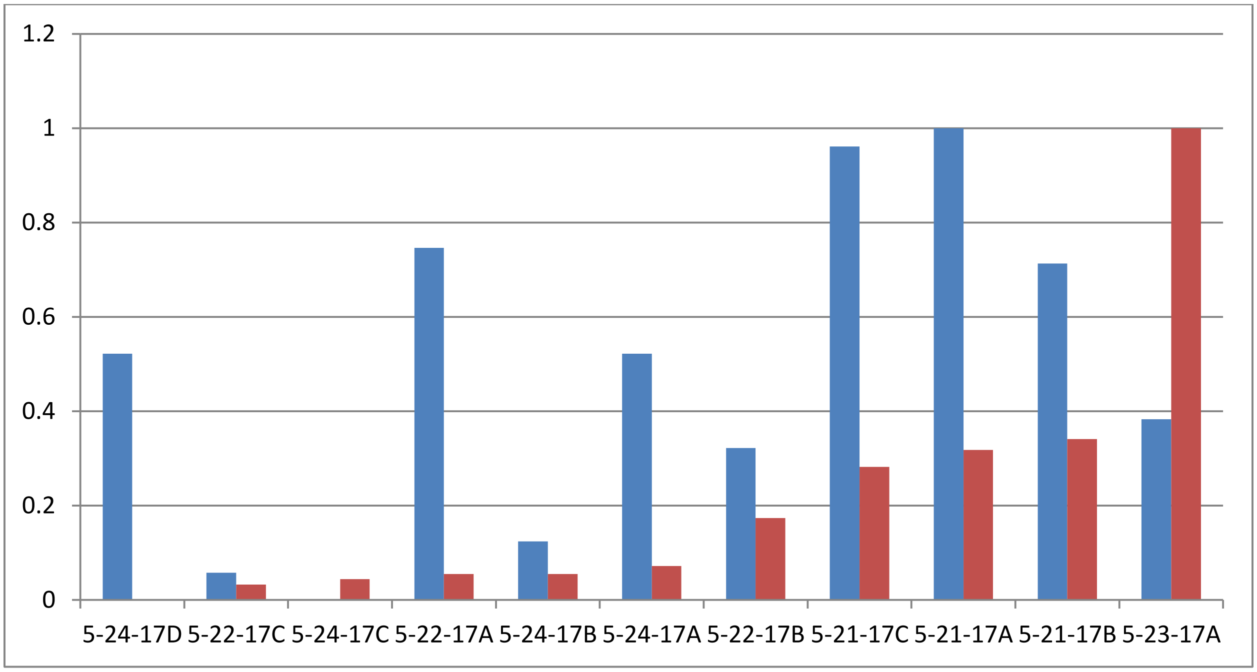

Figure 34 - Bar chart showing normalized fracture density brittleness equation (green) vs normalized Jin et al., (2014) brittleness equation (blue).

Chapter 7

Summary and Conclusions

7.1

This study had three goals. One goal was to use the dimensionless geomechanical equation (Equation 19):

$$\frac{F_d K_{IC}^2}{4\mu^2(1+\nu)} = A\frac{\upsilon}{1-2\upsilon} + B$$

to test whether strain conditions were constant in the sampled stratigraphic layers. This was done by measuring scanlines in the field and using a sample from the measured roadcut to calculate fracture toughness, Poisson's Ratio, and the Shear Modulus to then calculate fracture density. If strain conditions were constant, then the data will plot as a straight line with a positive slope where A is the slope of the line and B is the intercept.

This was done using two different methods. One by using a measured value of fracture toughness using a method recommended by the International Society of Rock Mechanics; the Cracked Chevron Notched Brazilian Disc Test (CCNBD). And also, by using a past method for estimating fracture toughness that correlates K_{IC} to the Young's Modulus of the rock.

As expected, both methods show that the measured stratigraphic layers were subject to constant strain conditions in Figures 30 and 32. Figure 30 shows fracture density for the measured stratigraphic layers calculated using the CCNBD and has a probability of about 73%. The sources for error here could be waveform picking for the sonic velocities, picking the failure point during the CCNBD tests, and imprecision when creating the CCNBD specimens since they were made by hand. Figure 32 shows fracture density for the measured stratigraphic layers using the Whittaker et al., (1993) equation that correlates fracture toughness to the Young's Modulus of the rock and it shows a probability of about 87%, which is a very good correlation. This method is subject to the same sources of error, but likely has a higher correlation coefficient because of the consistency with calculating fracture toughness.

7.2

A second goal of this study was to compare the relative brittleness predicted by Equation 4:

$$F_d = \frac{4\mu^2(1+v)}{K_{IC}^2}[A\frac{v}{1-2v}+B]$$

with brittleness values estimated by Equation 1:

$$B_{19} = \frac{E_n + v_n}{2}$$

And the measurements of fracture density measured along the roadcuts.

Brittleness estimated by Equation 4 was done so in the same way as described in section 7.1: using the measured fracture toughness and the fracture toughness correlated to Young’s Modulus. The predicted fracture densities calculated from Equation 19 can be plotted as a function of strain using Equation 4. The coefficients A and B were calculated from the invariants using increasing uniaxial extension. Figures 31 and 33 show increasing uniaxial extension on the x-axis and calculated fracture density on the y-axis. Much like in section 7.1, with the correlated fracture toughness values, there is less scatter (Figure 33) than with the calculated fracture toughness values (Figure 31), and although the order of relative brittleness is not the same, it is very similar. The brittleness values calculated using Equation 4 were compared to brittleness values calculated using Equation 1.

As expected, the order of brittleness calculated by the two methods didn’t come out the same. Table 24 shows that Equation 1 calculated 5-24-17D as the least brittle, while Equation 4 calculated 5-22-17A and the least brittle. Equation 1 calculated 5-21-17A as the most brittle, while Equation 4 calculated 5-23-17A as the most brittle. This is likely due to the amount and specificity of the mechanical properties taken into account in Equation 4.

Additionally, the fracture density values were normalized for a more direct comparison of brittleness to the values calculated by Equation 1. Table 25 shows that Equation 1 produces higher values of brittleness overall when compared to the normalized fracture density brittleness, but the fracture density brittleness takes into account more and more specific mechanical properties of the individual rock samples, and again, the order of brittleness is not the same, which was expected.

7.3

A third goal of this study was to measure K_{IC} using the Cracked Chevron Notched Brazilian Disc Test (CCNBD) and to compare those results to results given by an equation that correlates the Young's Modulus of the rock to fracture toughness. Table 20 shows the results of the two methods, each listed in order from the lowest fracture toughness to the highest fracture toughness. Although the resulting orders of fracture toughness is not the same, they are very similar. The scatter plot in Figure 28 shows a correlation value of about 90%, which is a good correlation.

Potential error could be due to waveform picking when calculating sonic velocities to then calculate the Young's Modulus. Or it could be because of imprecision when creating the CCNBD specimens since they were made by hand. Calculating fracture toughness is best done depending on the equipment that is at one's disposal.

Appendix A

Fracture Toughness Charts

Note on picking maximum load: The maximum load used in the calculations is where the specimen was observed to have broken (failure). After failure occurred a piece of the specimen may have gotten lodged in the press causing the compression to continue, which is the reason for some of the graphs appearing to have a higher failure point than what was used in the CCNBD calculations.

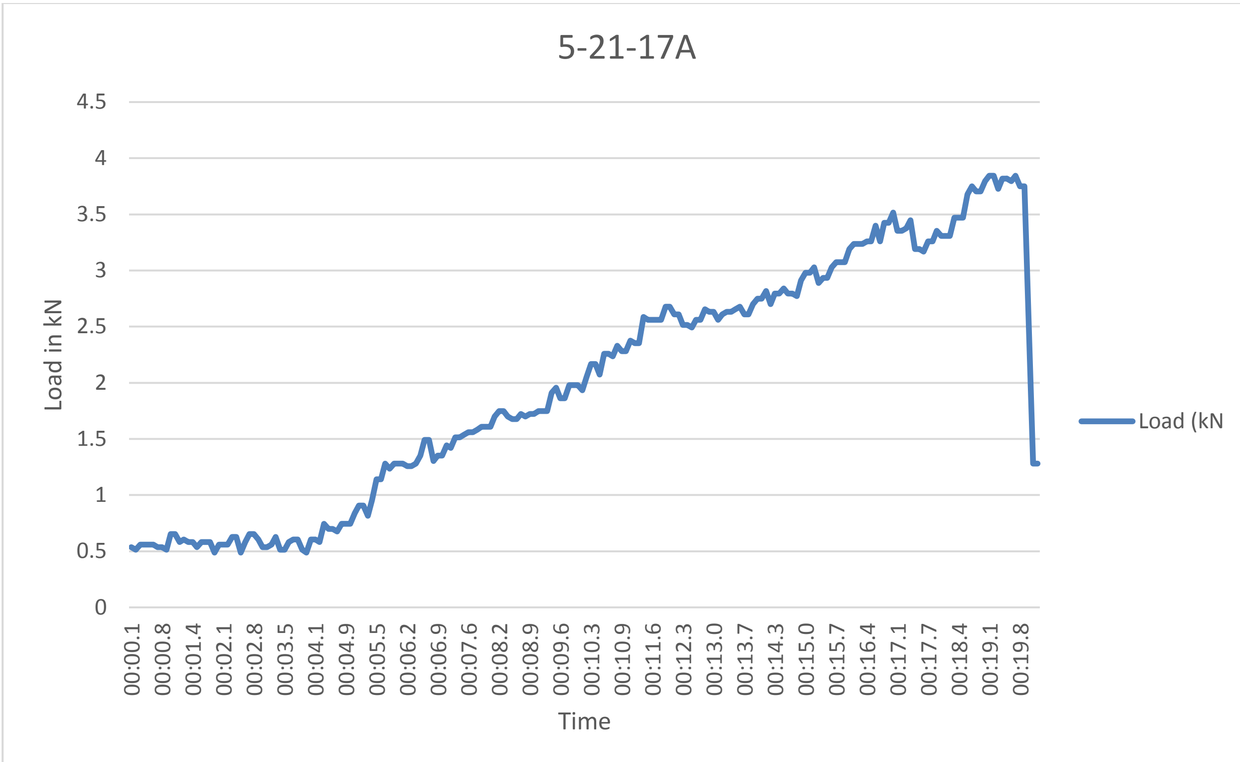

Figure A - 1 - Load vs. Time for Fracture Toughness, 5-21-17A. Load at failure: 3.84kN.

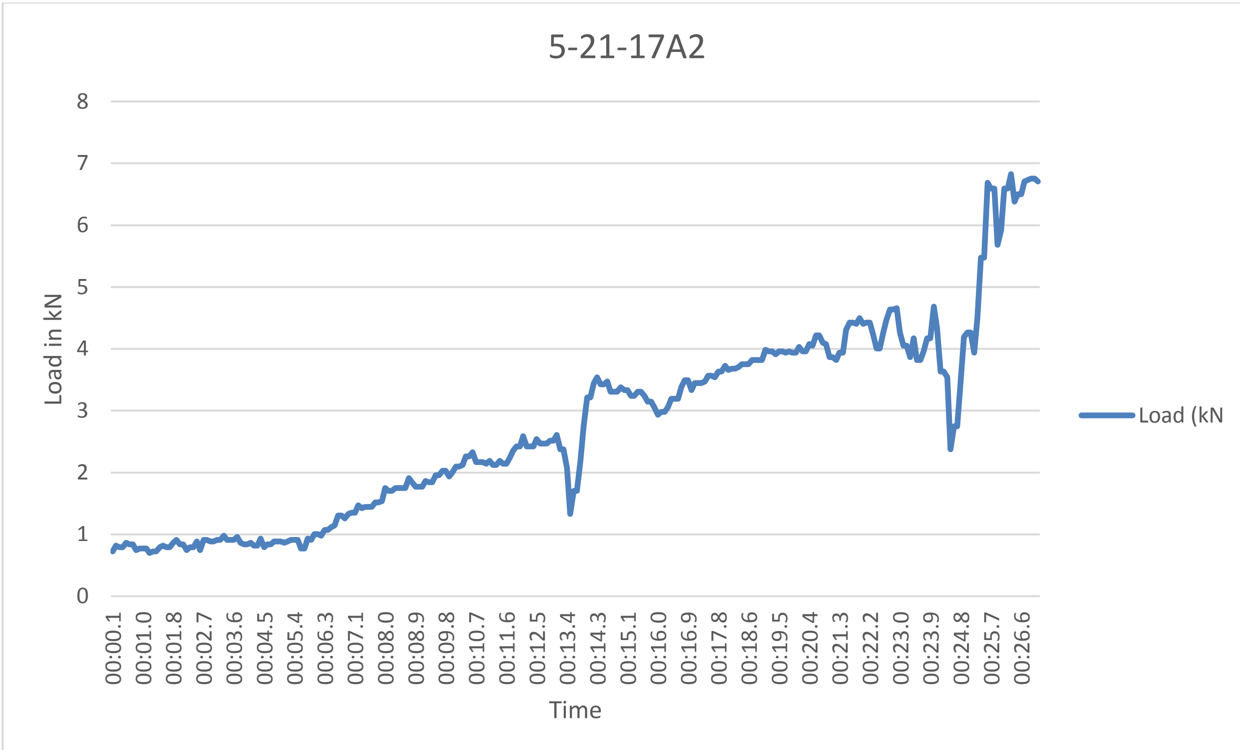

Figure A - 2 - Load vs. Time for Fracture Toughness, 5-21-17A2. Load at failure: 3.54kN.

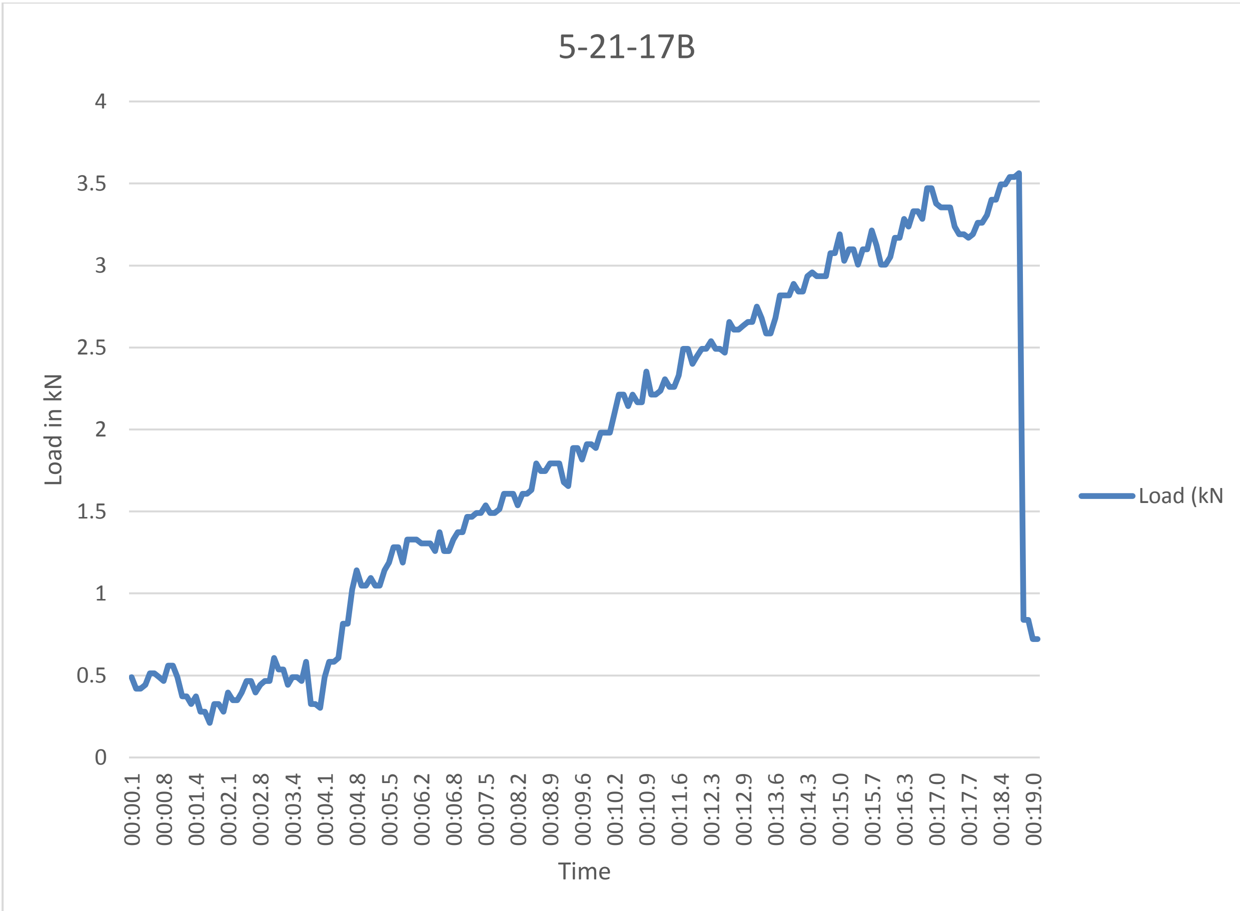

Figure A - 3 - Load vs. Time for Fracture Toughness, 5-21-17B. Load at failure: 3.56kN.

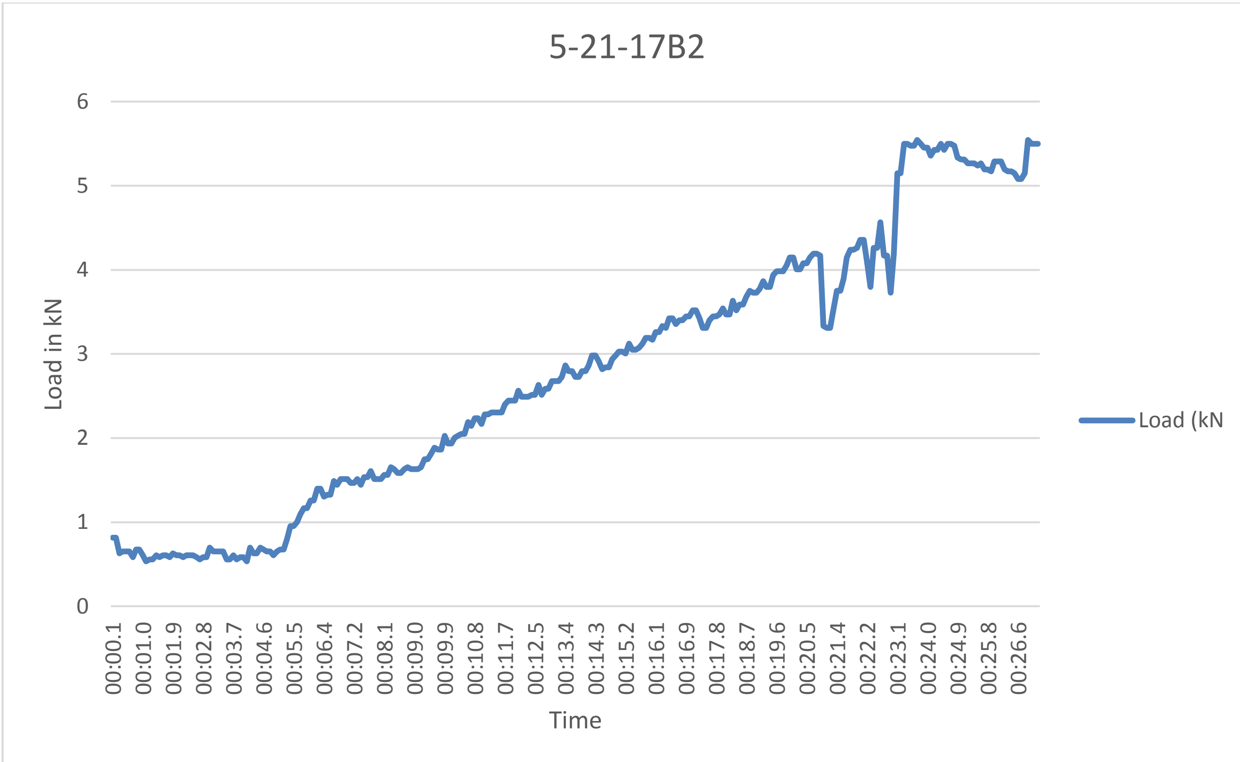

Figure A - 4 - Load vs. Time for Fracture Toughness, 5-21-17B2. Load at failure: 4.19kN.

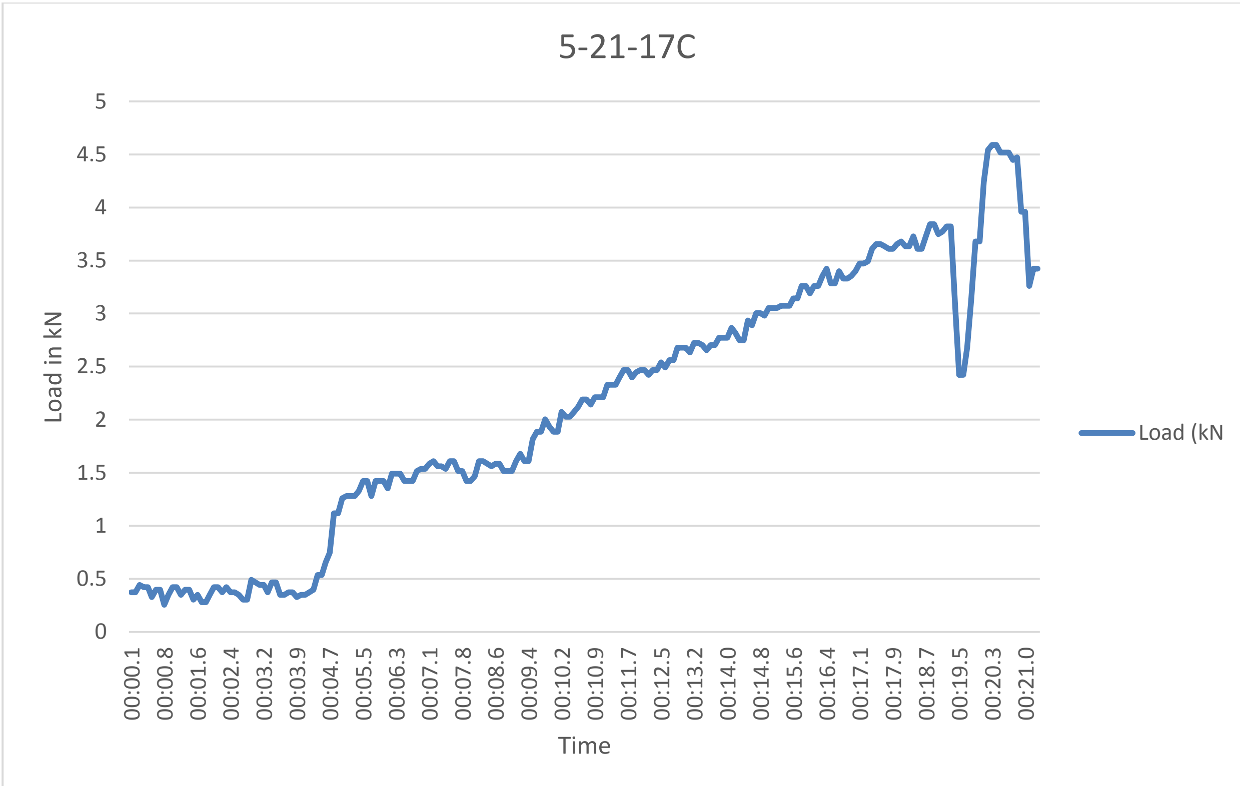

Figure A - 5 - Load vs. Time for Fracture Toughness, 5-21-17C. Load at failure: 3.84kN.

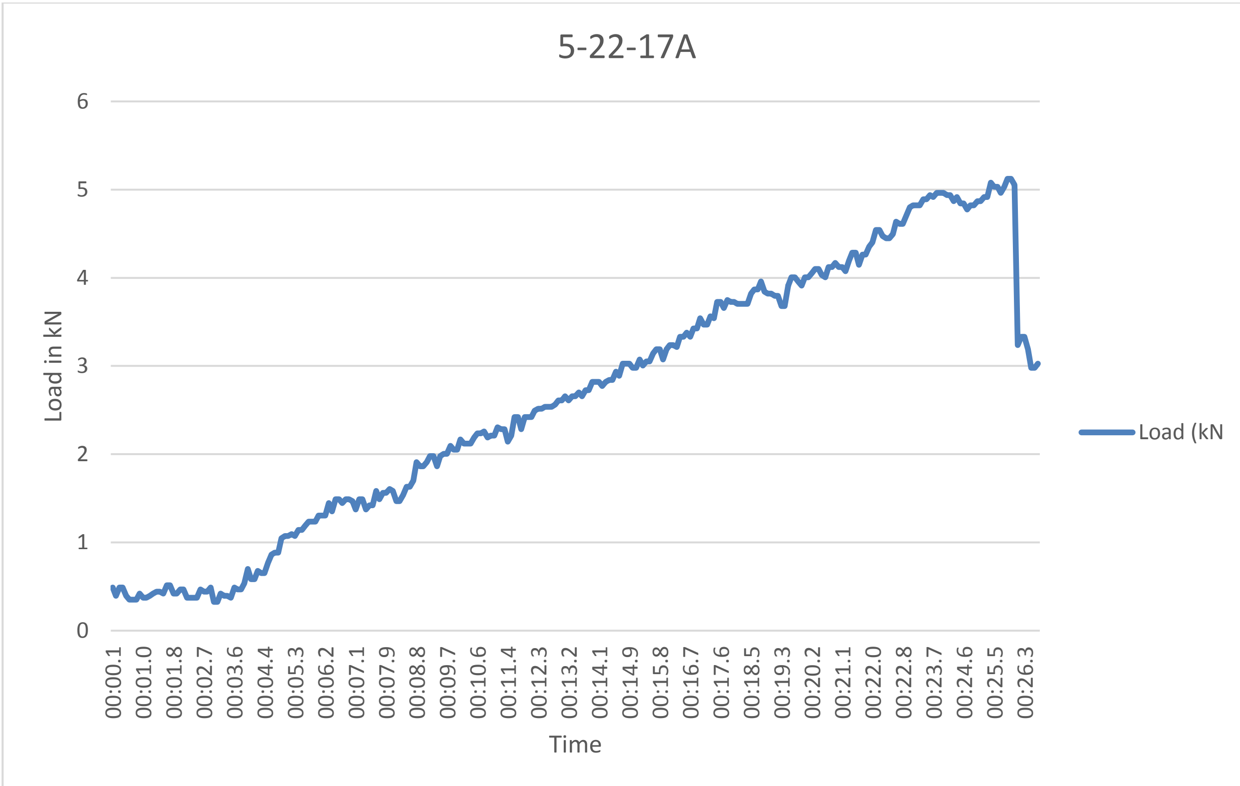

Figure A - 6 - Load vs. Time for Fracture Toughness, 5-22-17A. Load at failure: 5.07kN.

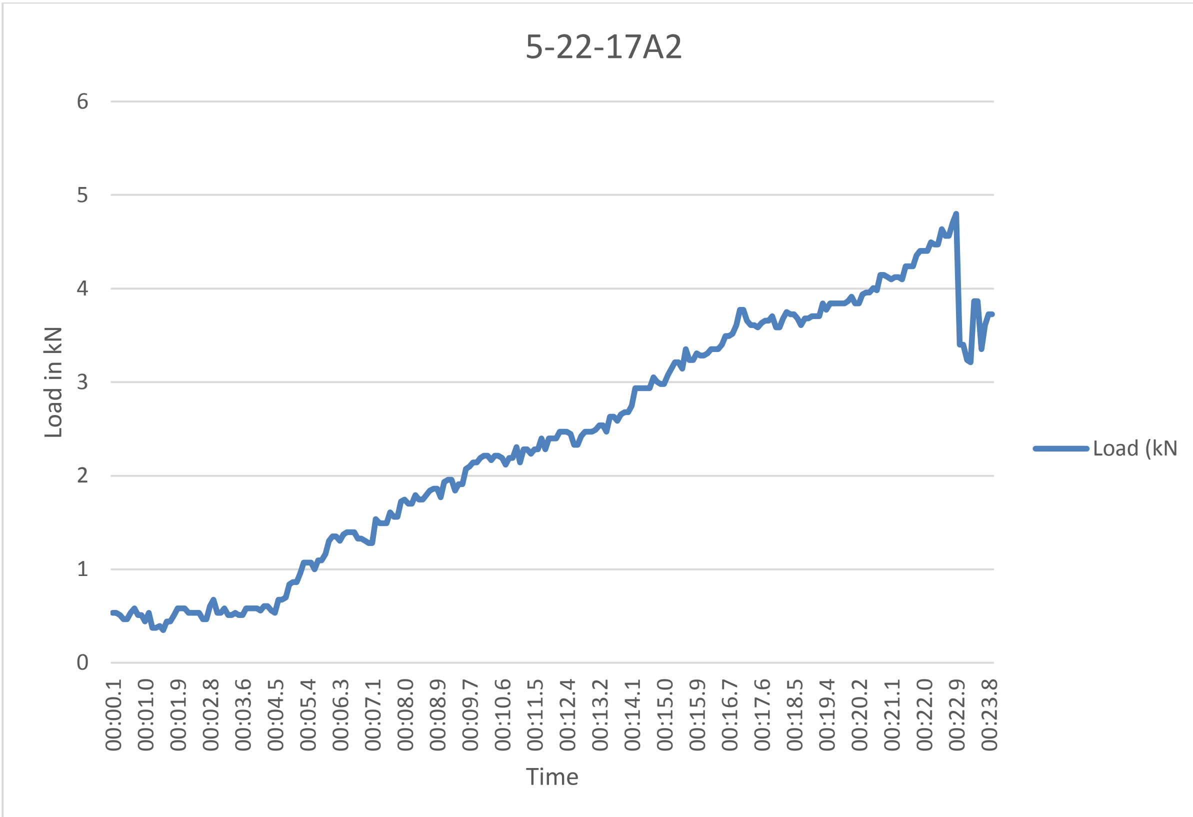

Figure A - 7 - Load vs. Time for Fracture Toughness, 5-22-17A2. Load at failure: 4.8kN.

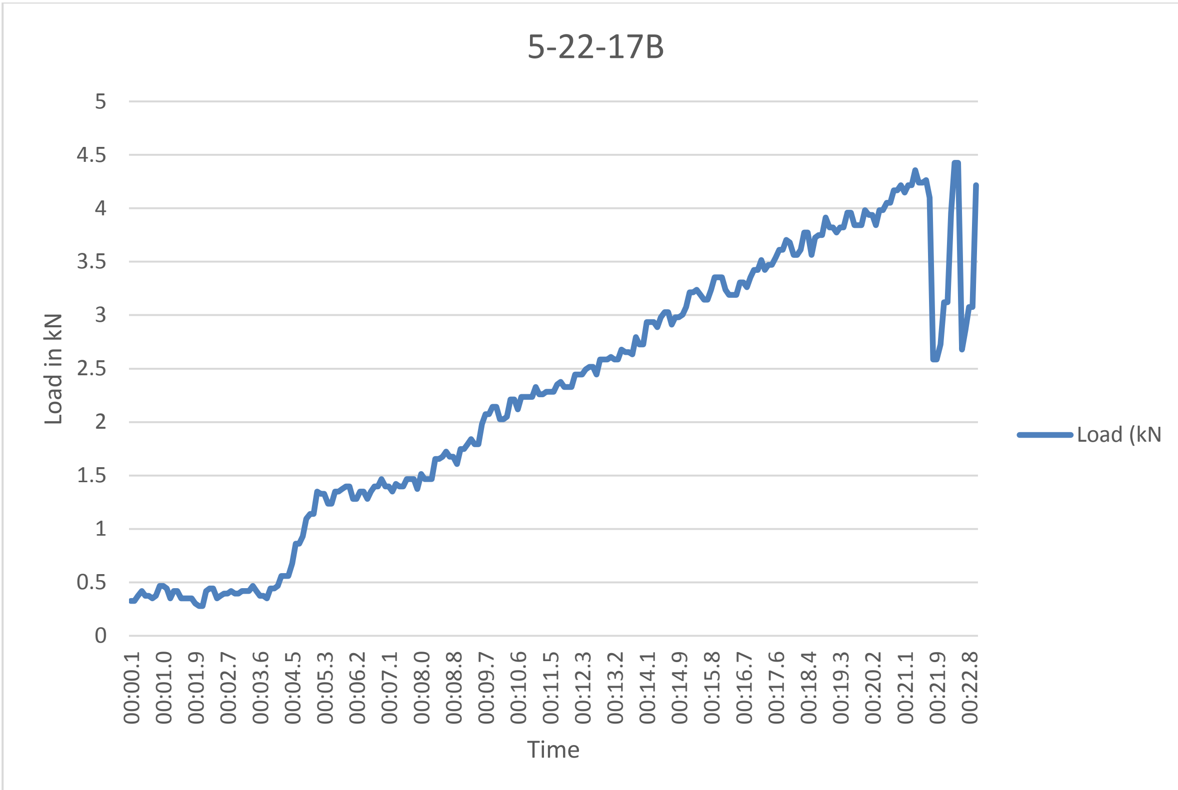

Figure A - 8 - Load vs. Time for Fracture Toughness, 5-22-17B. Load at failure: 4.35kN.

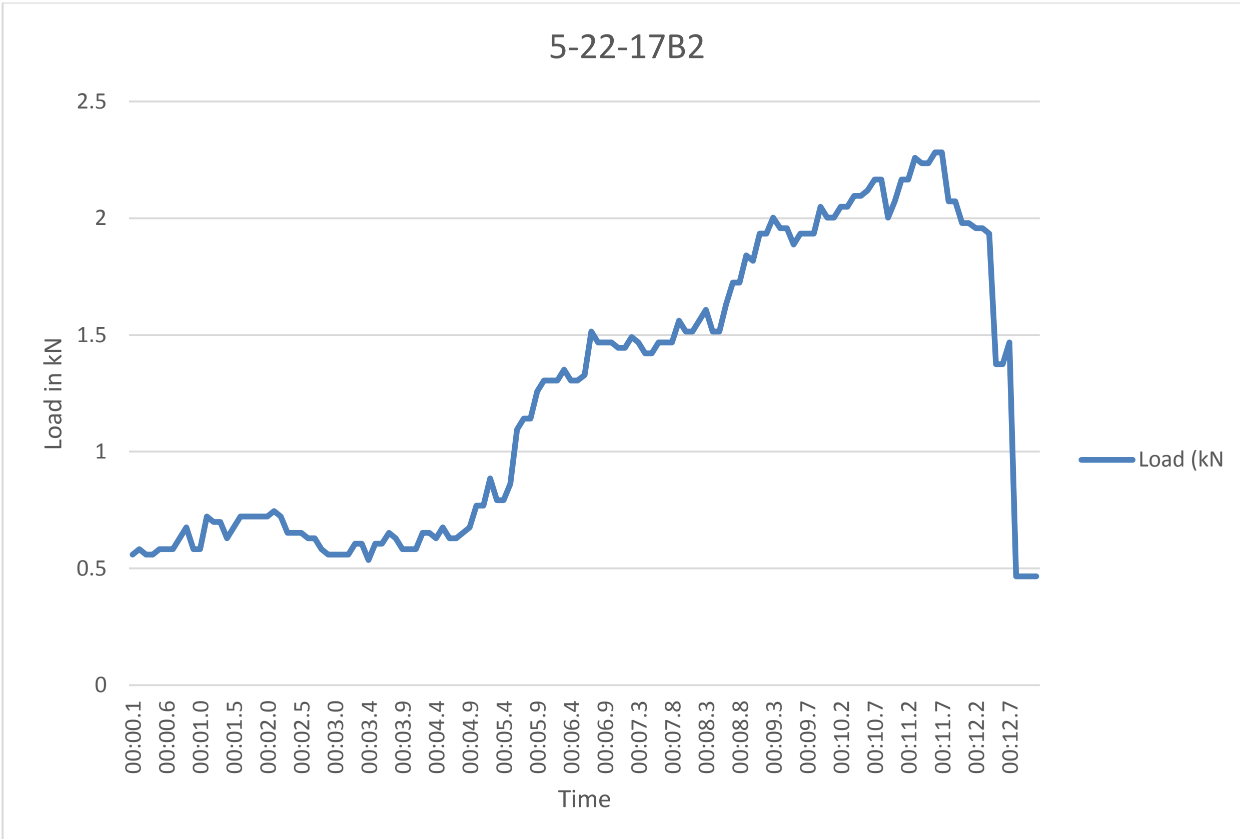

Figure A - 9 - Load vs. Time for Fracture Toughness, 5-22-17B2. Load at failue:

2.28kN.

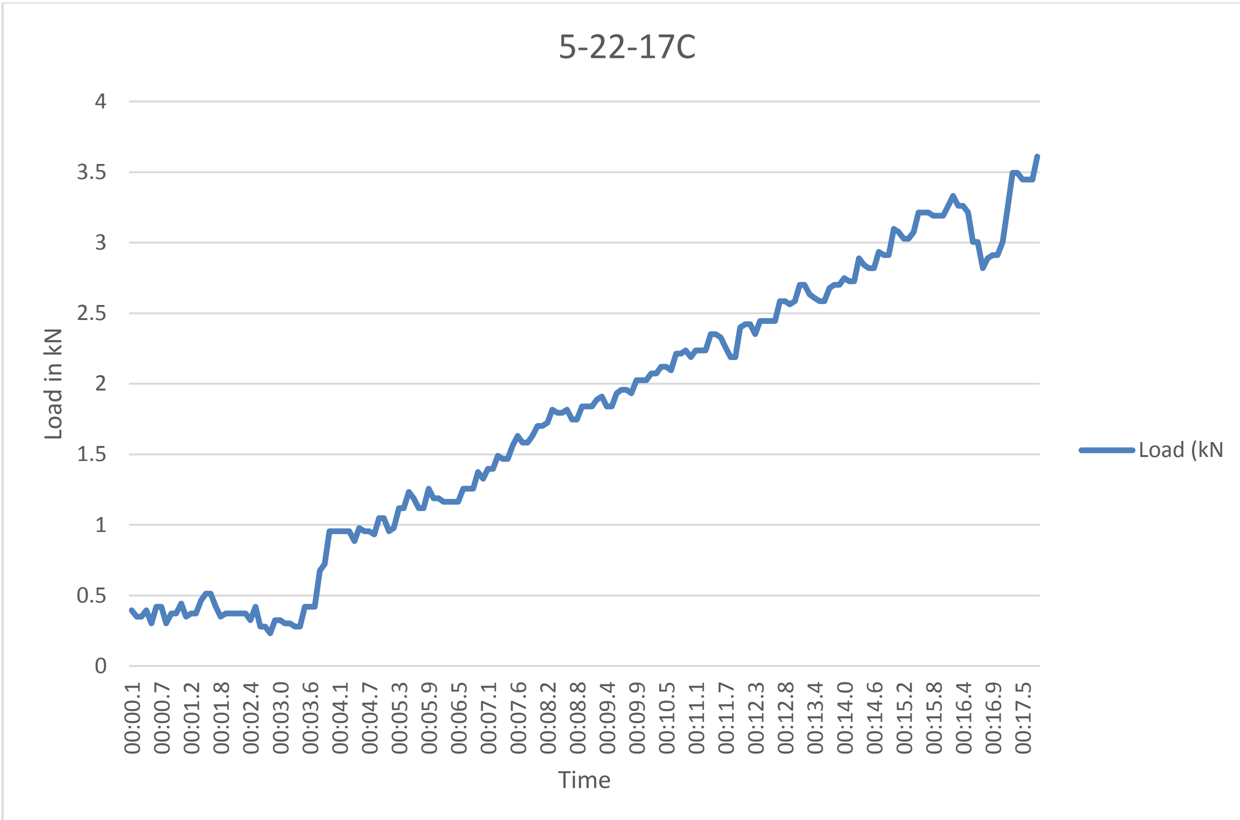

Figure A - 10 - Load vs. Time for Fracture Toughness, 5-22-17C. Load at failure: 3.33kN.

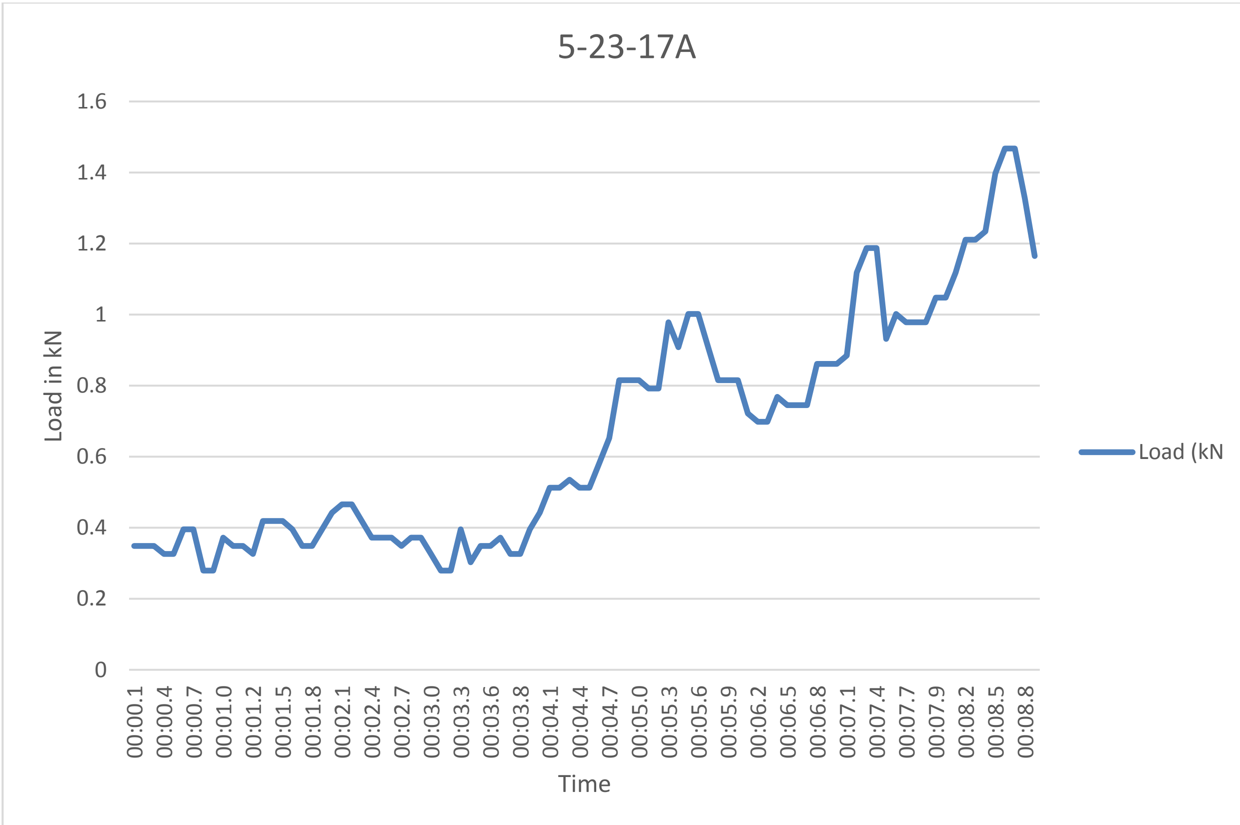

Figure A - 11 - Load vs. Time for Fracture Toughness, 5-23-17A. Load at failure: 1.0kN.

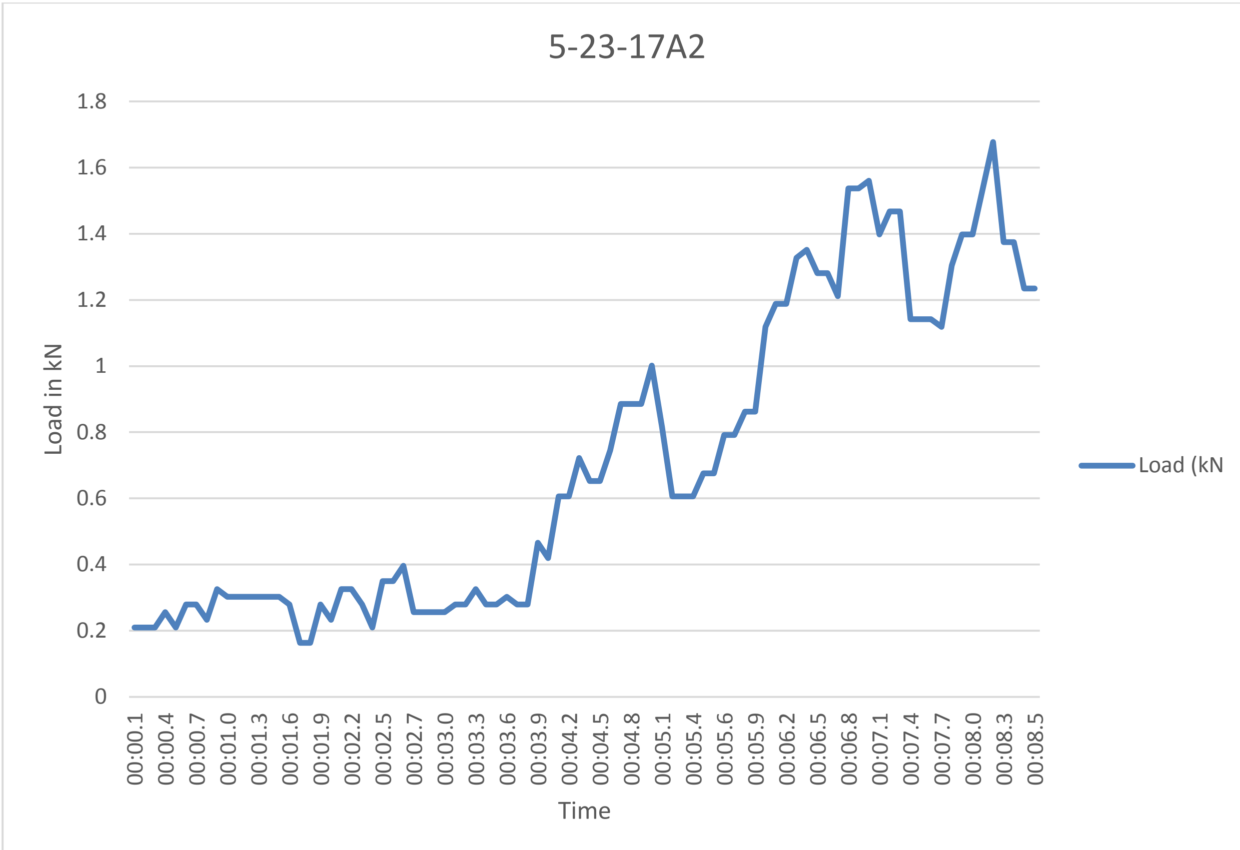

Figure A - 12 - Load vs. Time for Fracture Toughness, 5-23-17A2. Load at failure: 1.0kN.

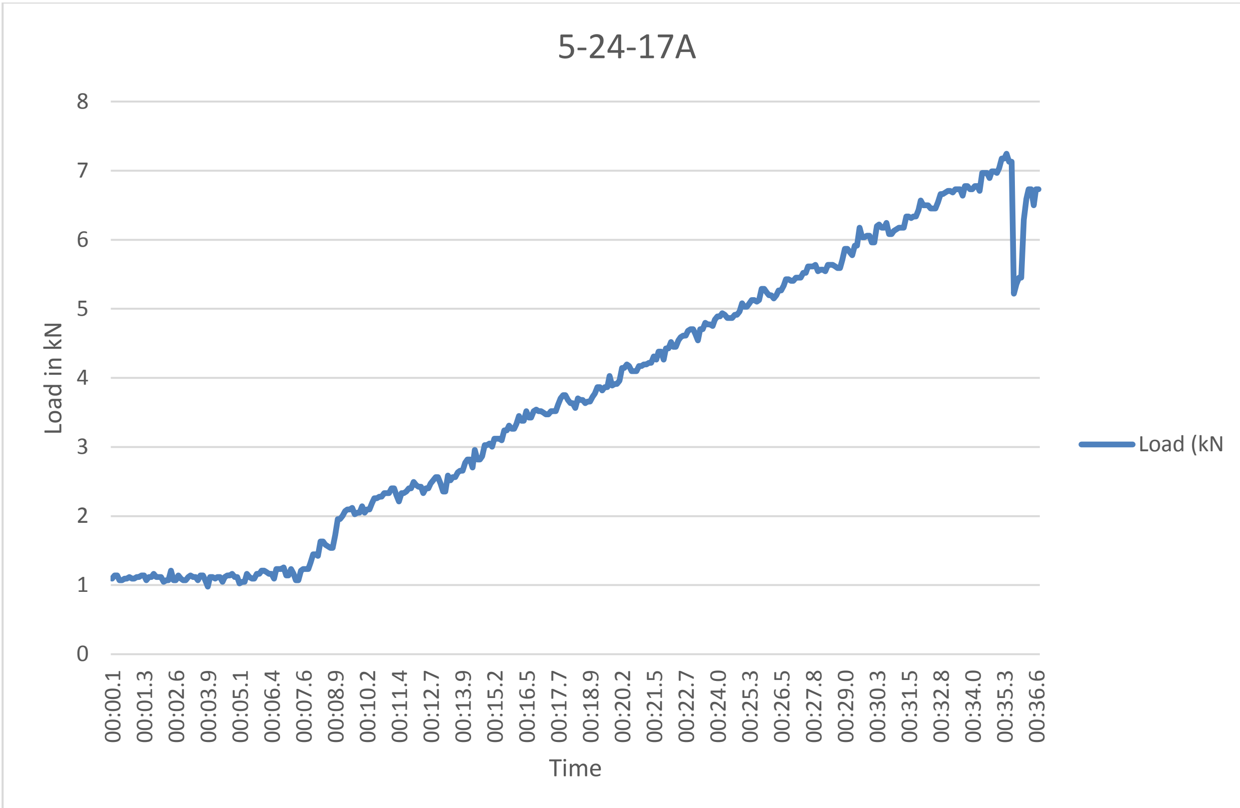

Figure A - 13 - Load vs. Time for Fracture Toughness, 5-24-17A. Load at failure: 7.24kN.

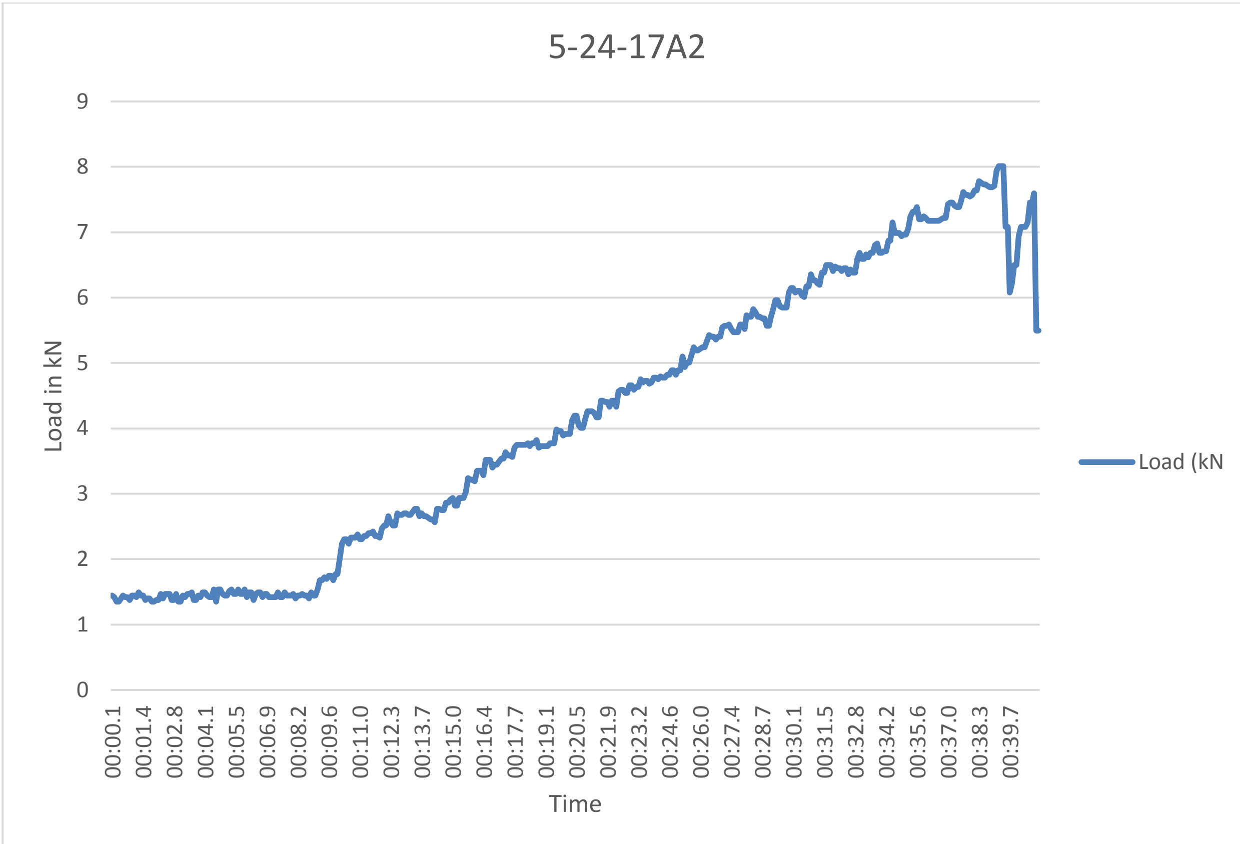

Figure A - 14 - Load vs. Time for Fracture Toughness, 5-24-17A2. Load at failure: 8.01kN.

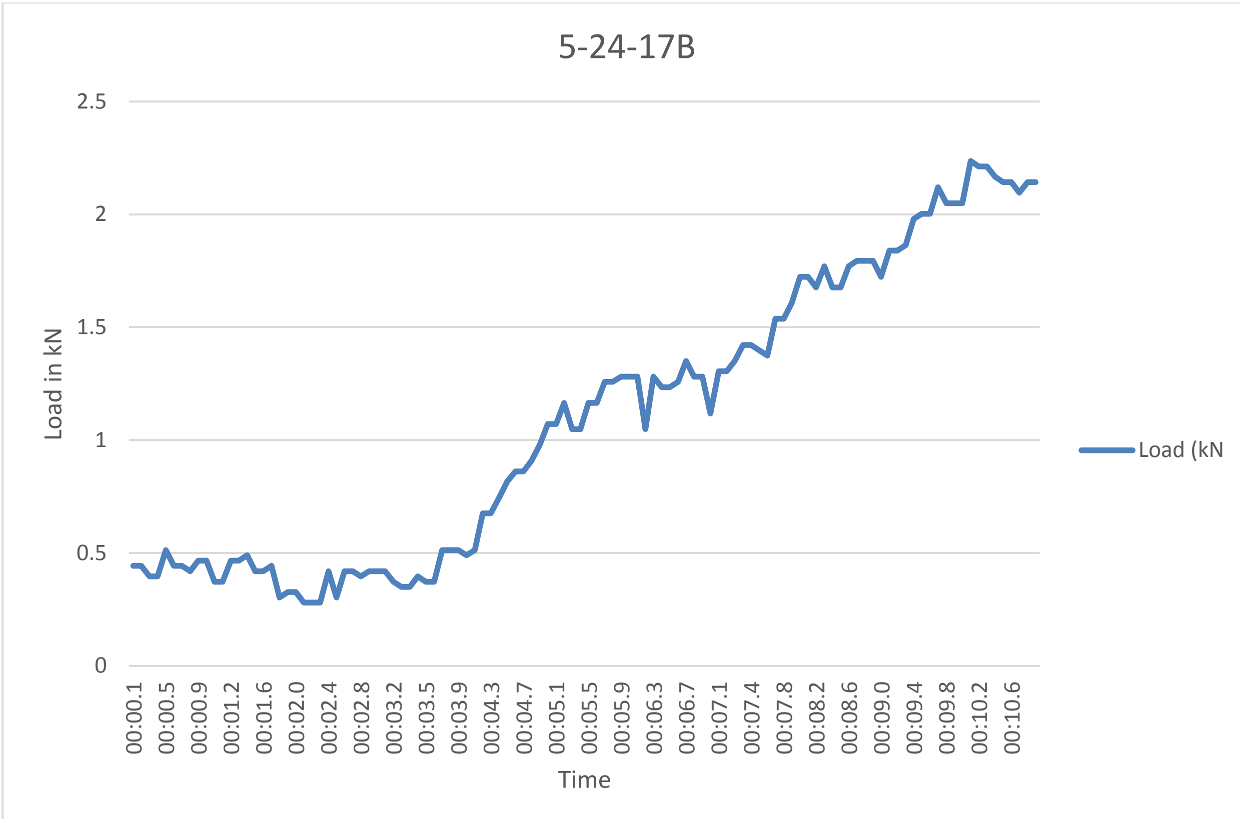

Figure A - 15 - Load vs. Time for Fracture Toughness, 5-24-17B. Load at failure: 2.24kN.

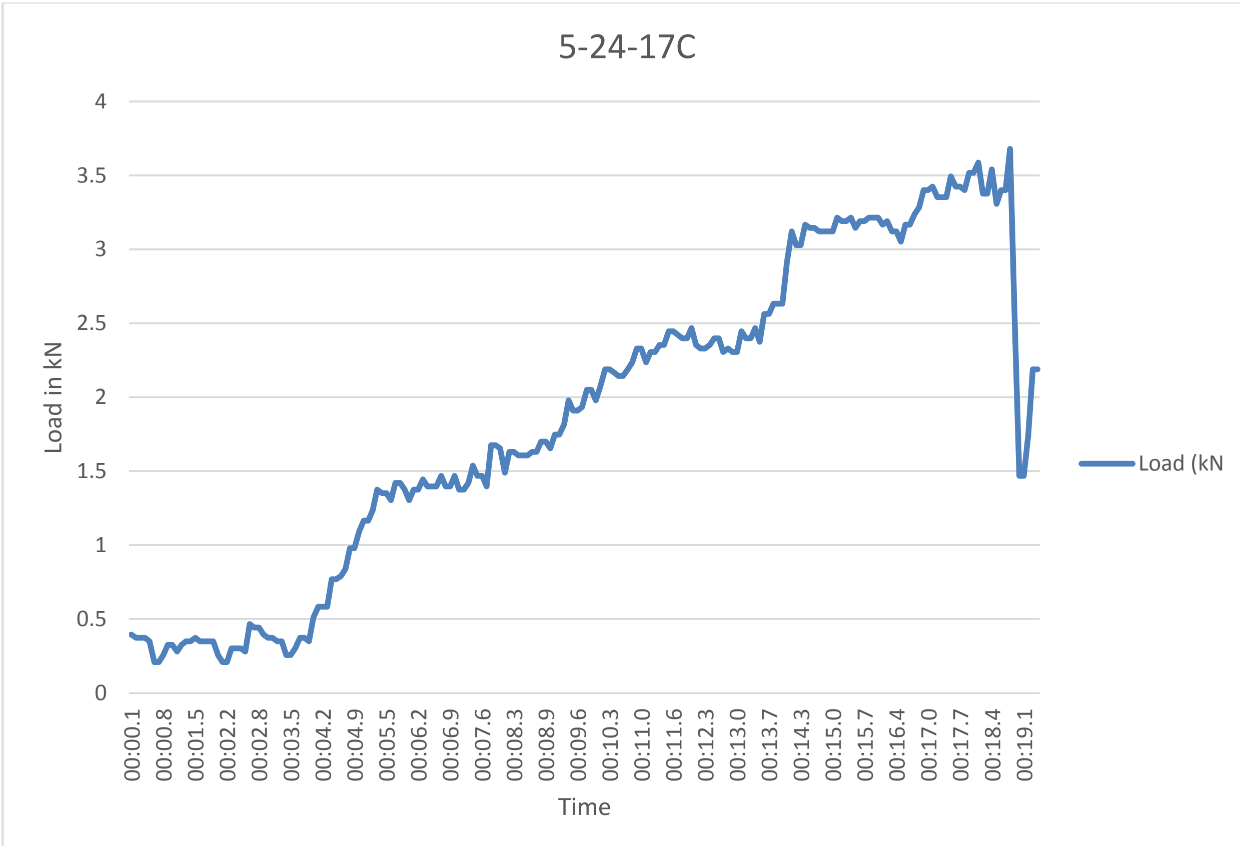

Figure A - 16 - Load vs. Time for Fracture Toughness, 5-24-17C. Load at failure: 3.58kN.

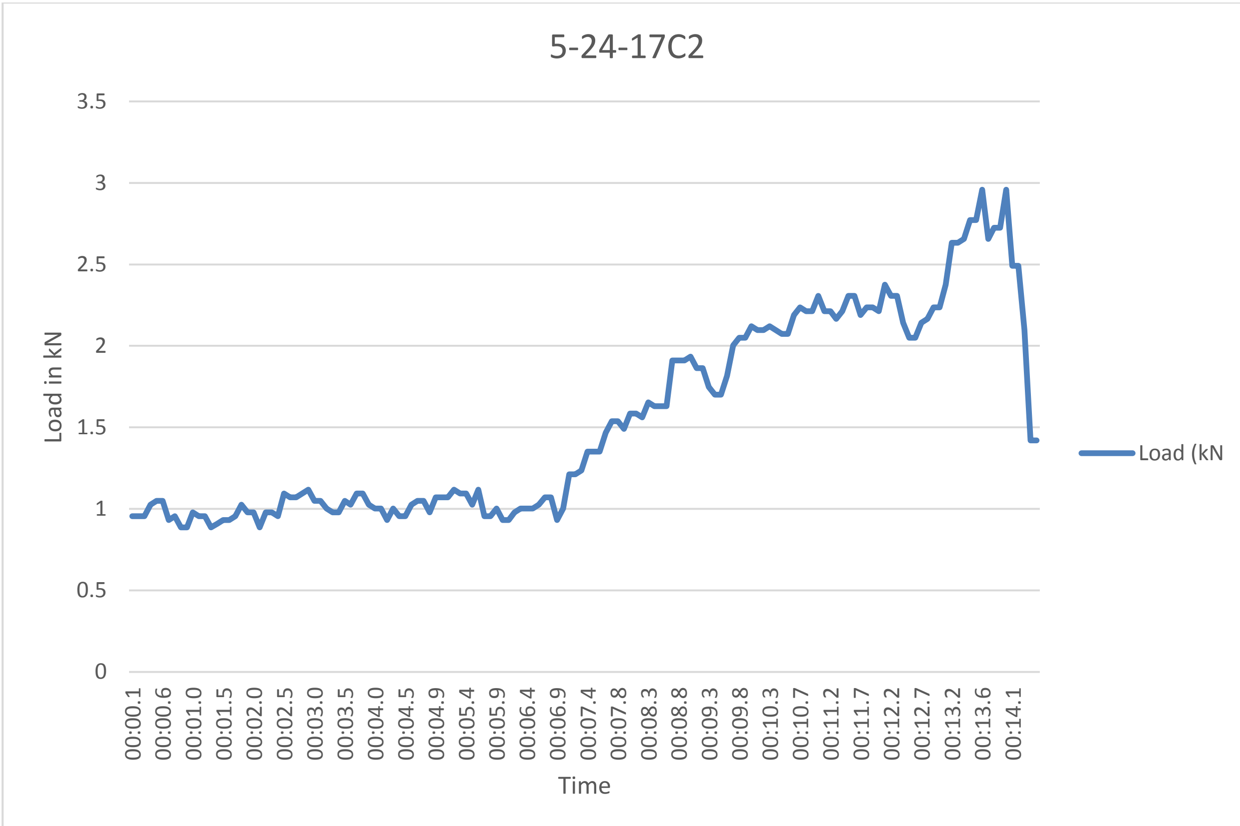

Figure A - 17 - Load vs. Time for Fracture Toughness, 5-24-17C2. Load at failure:

2.96kN.

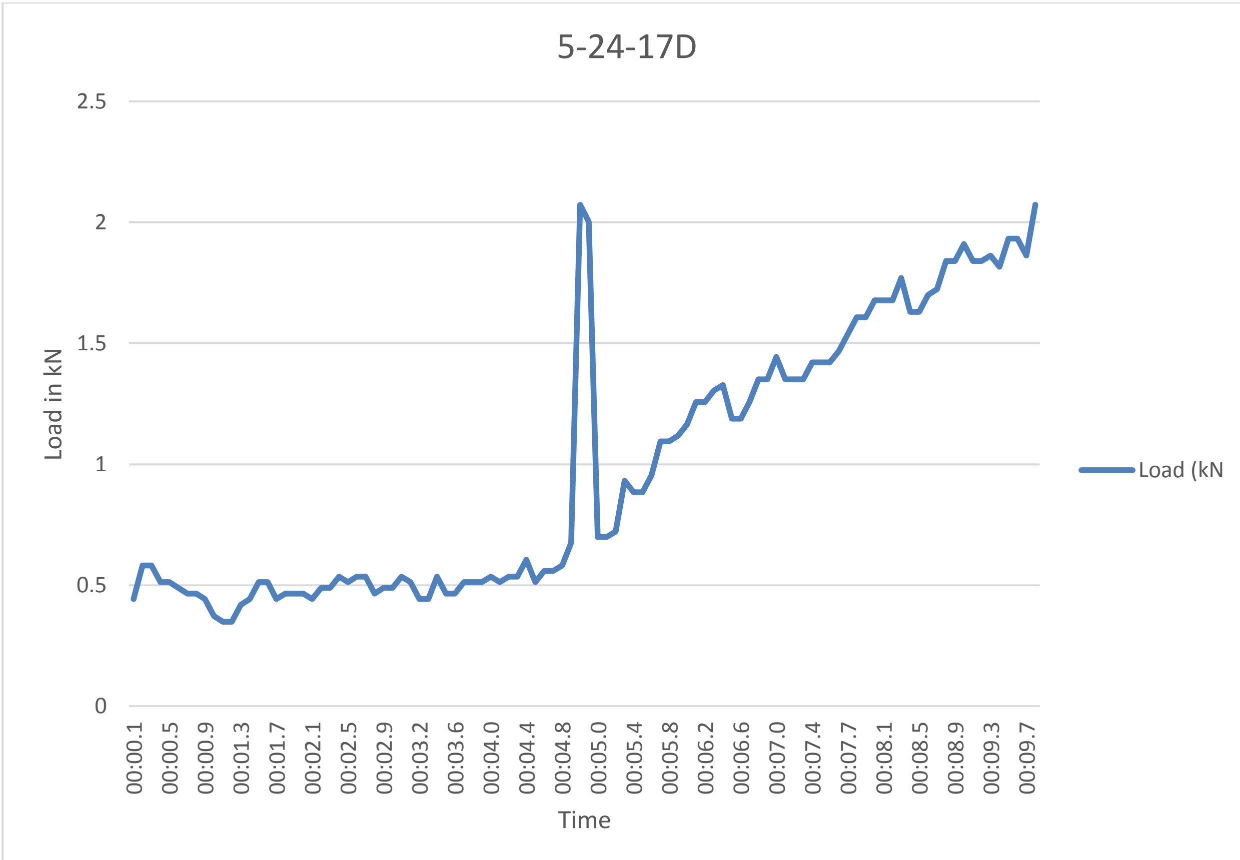

Figure A - 18 - Load vs. Time for Fracture Toughness, 5-24-17D. Load at failure: 2.07kN.

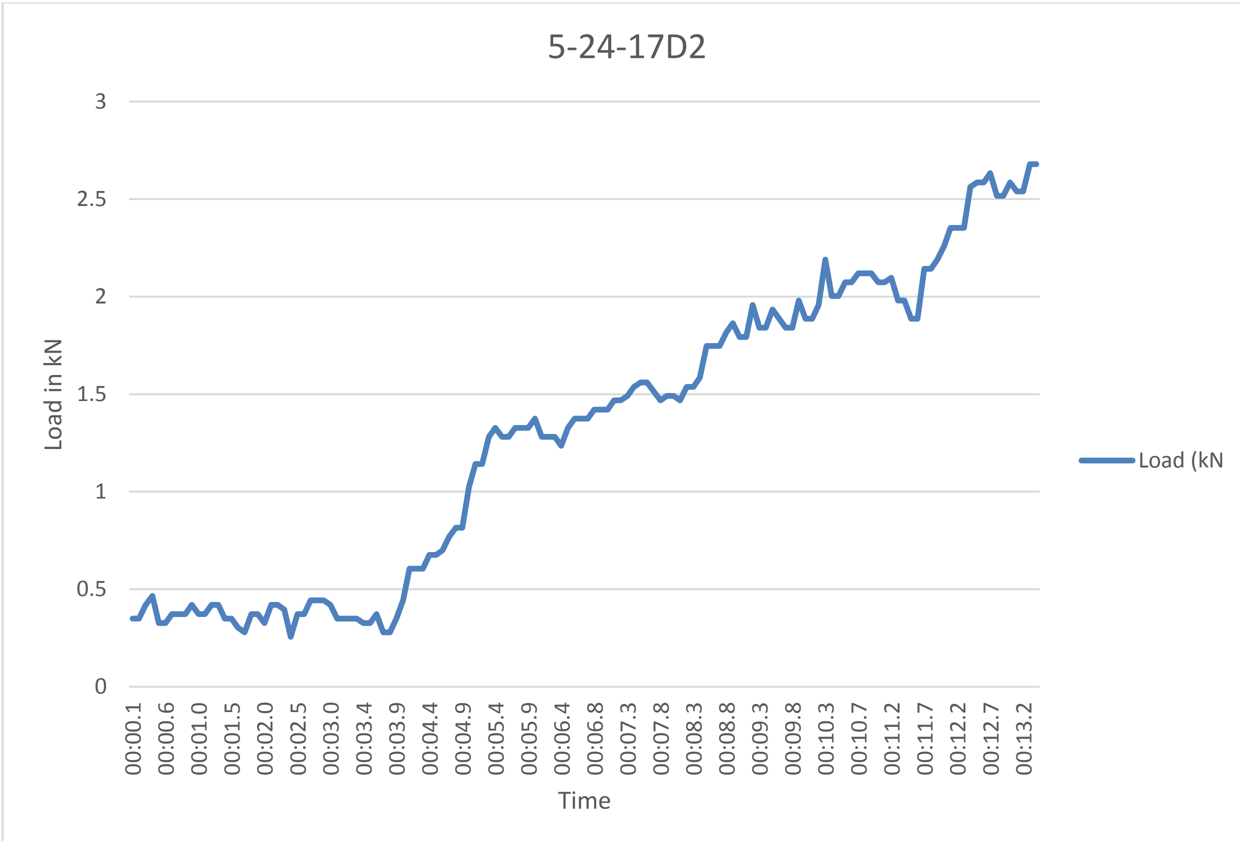

Figure A - 19 - Load vs. Time for Fracture Toughness, 5-24-17D2. Load at failure: 2.68kN.

Appendix B

Dynamic Elastic Properties Waveform Picking

Note on P-wave and S-wave picking: P-waves were picked on the first peak received by the transducers. The s-wave is shown by a change in frequency where there is an abrupt change in direction and then it is picked on the first peak after that change. X-axis is travel time in milliseconds and y-axis is amplitude in volts.

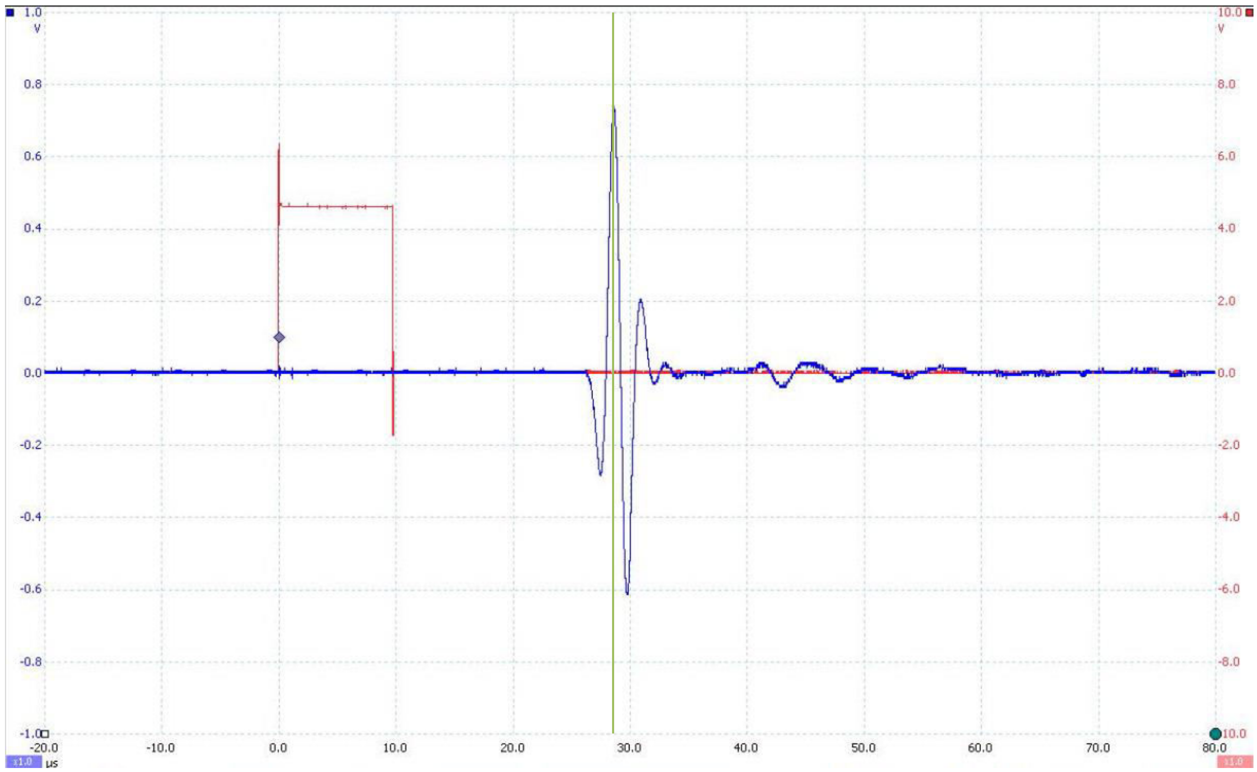

Figure B-1 – P-Wave waveform for sample 5-21-17A. Orange line indicates where travel-time was picked for calculations. Travel time: 28.6ms.

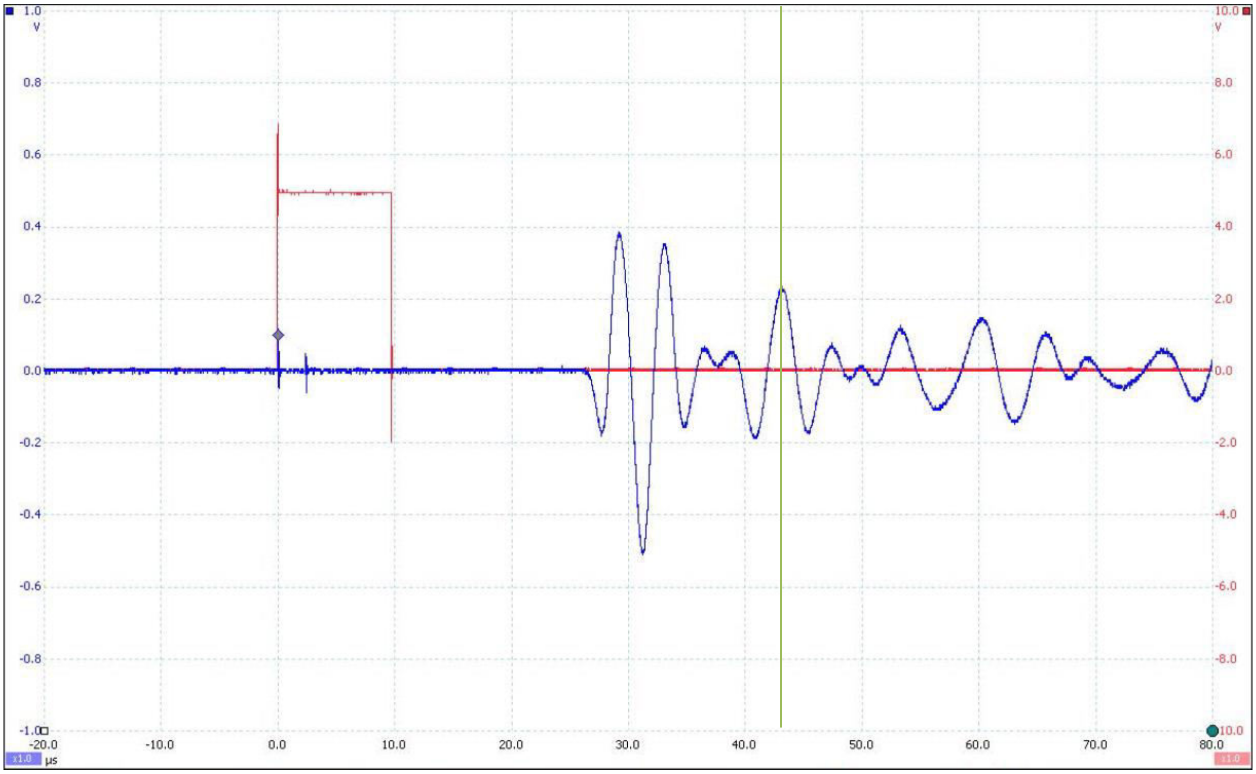

Figure B-2 – S-Wave waveform for sample 5-21-17A. Orange line indicates where travel-time was picked for calculations. Travel time: 43.13ms.

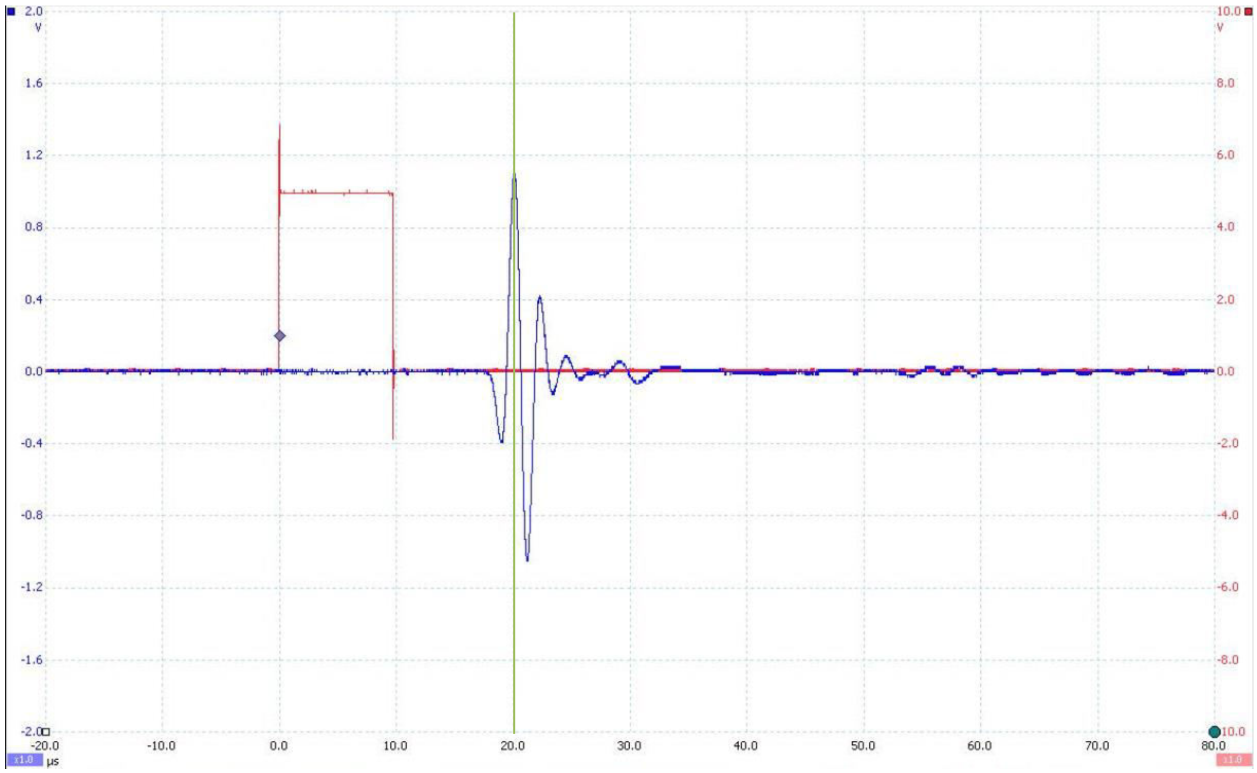

Figure B-3 – P-Wave waveform for sample 5-21-17B. Orange line indicates where travel-time was picked for calculations. Travel time: 20.07ms.

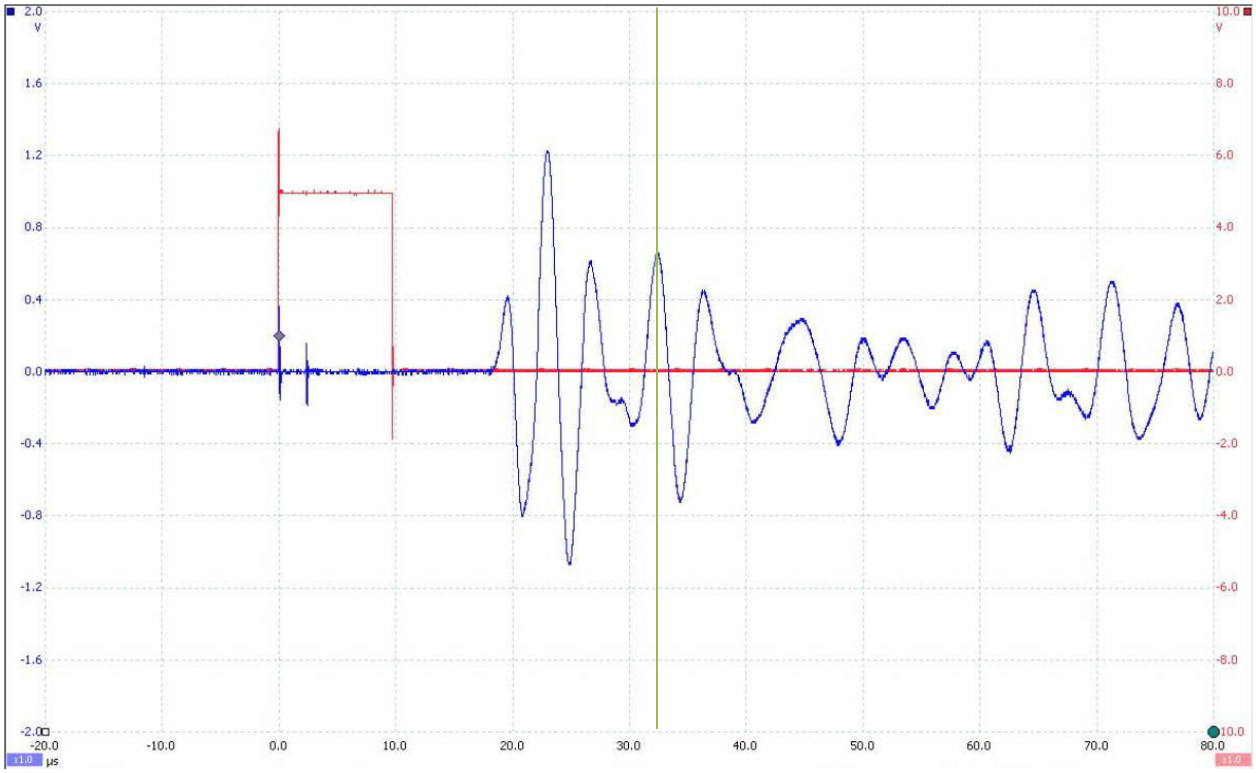

Figure B-4 – S-Wave waveform for sample 5-21-17B. Orange line indicates where travel-time was picked for calculations. Travel time: 32.42ms.

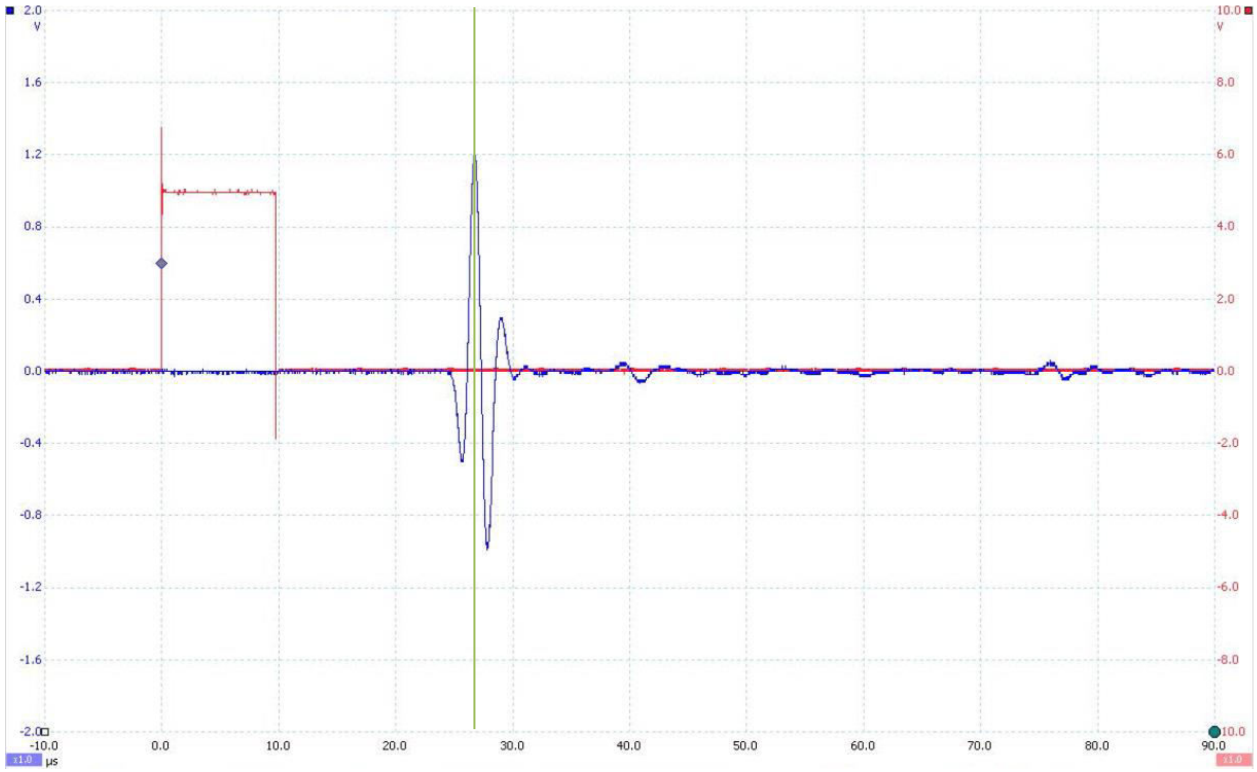

Figure B-5 – P-Wave waveform for sample 5-21-17C. Orange line indicates where travel-time was picked for calculations. Travel time: 26.73ms.

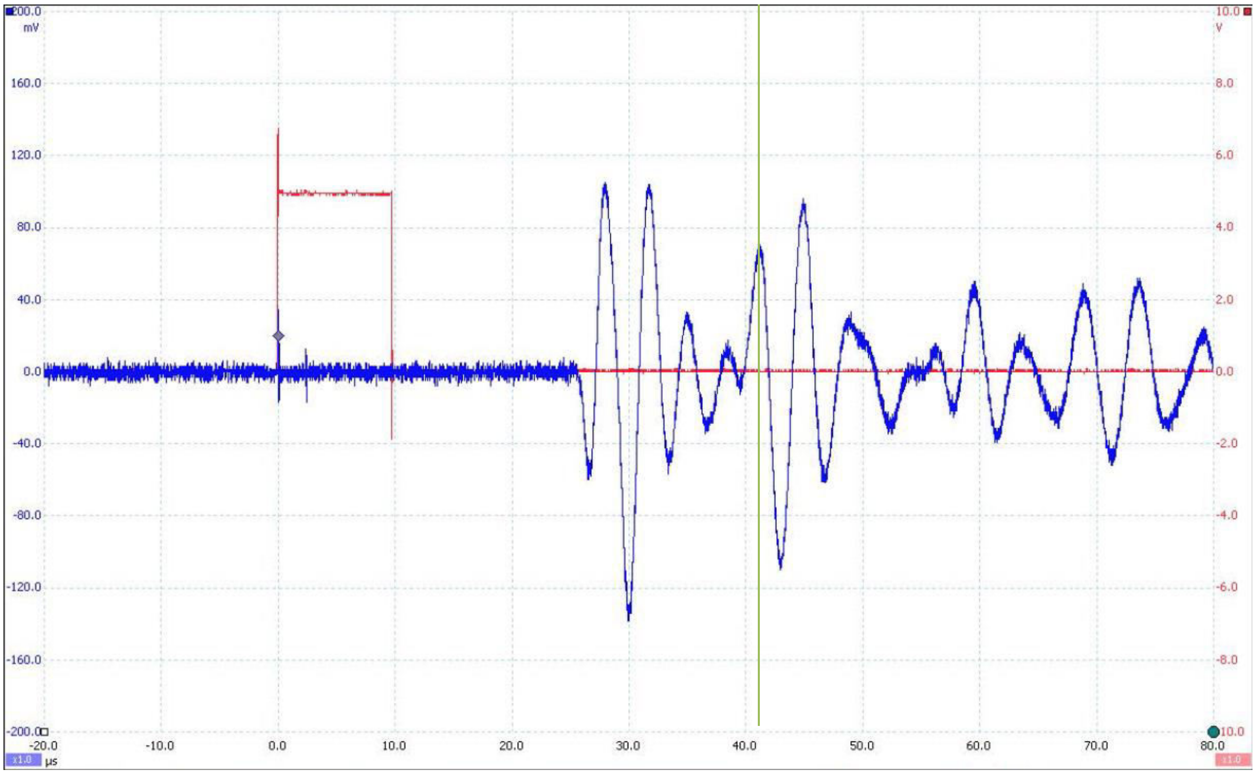

Figure B-6 – S-Wave waveform for sample 5-21-17C. Orange line indicates where travel-time was picked for calculations. Travel time: 41.08ms.

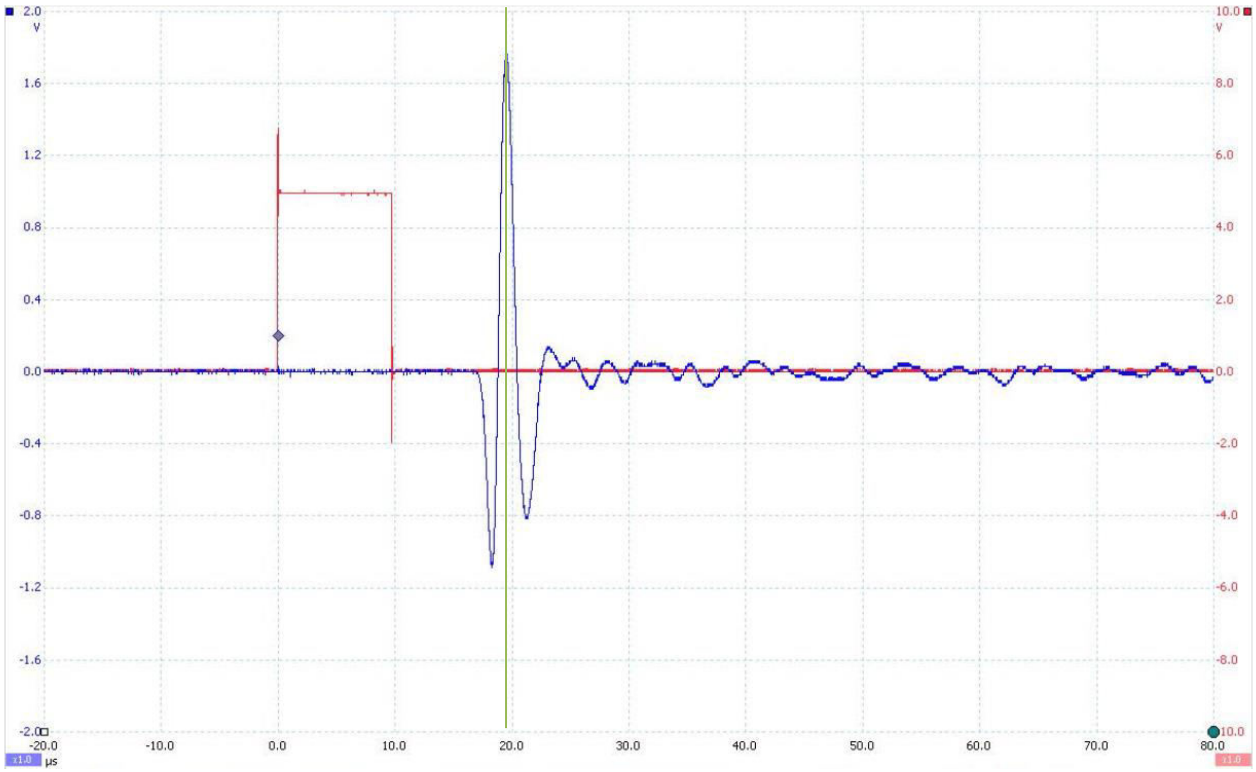

Figure B-7 – P-Wave waveform for sample 5-22-17A. Orange line indicates where travel-time was picked for calculations. Travel time: 19.5ms.

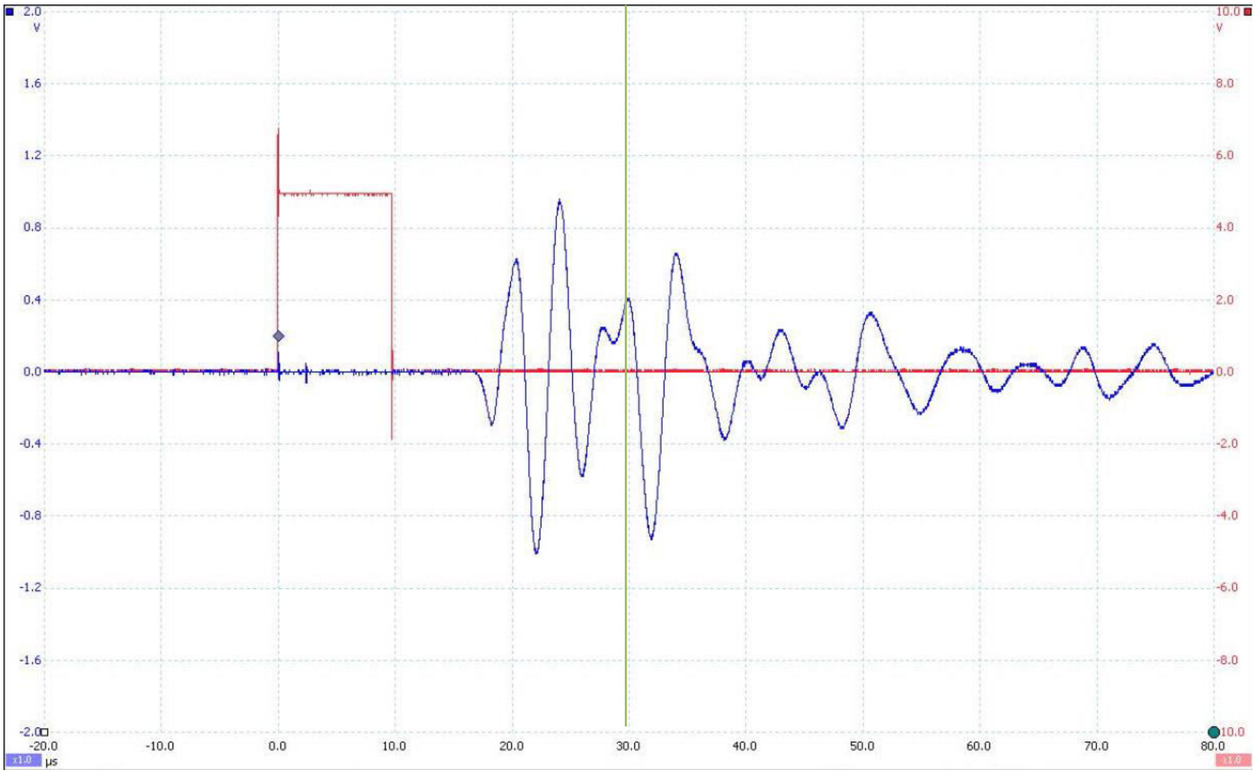

Figure B-8 – S-Wave waveform for sample 5-22-17A. Orange line indicates where travel-time was picked for calculations. Travel time: 30ms.

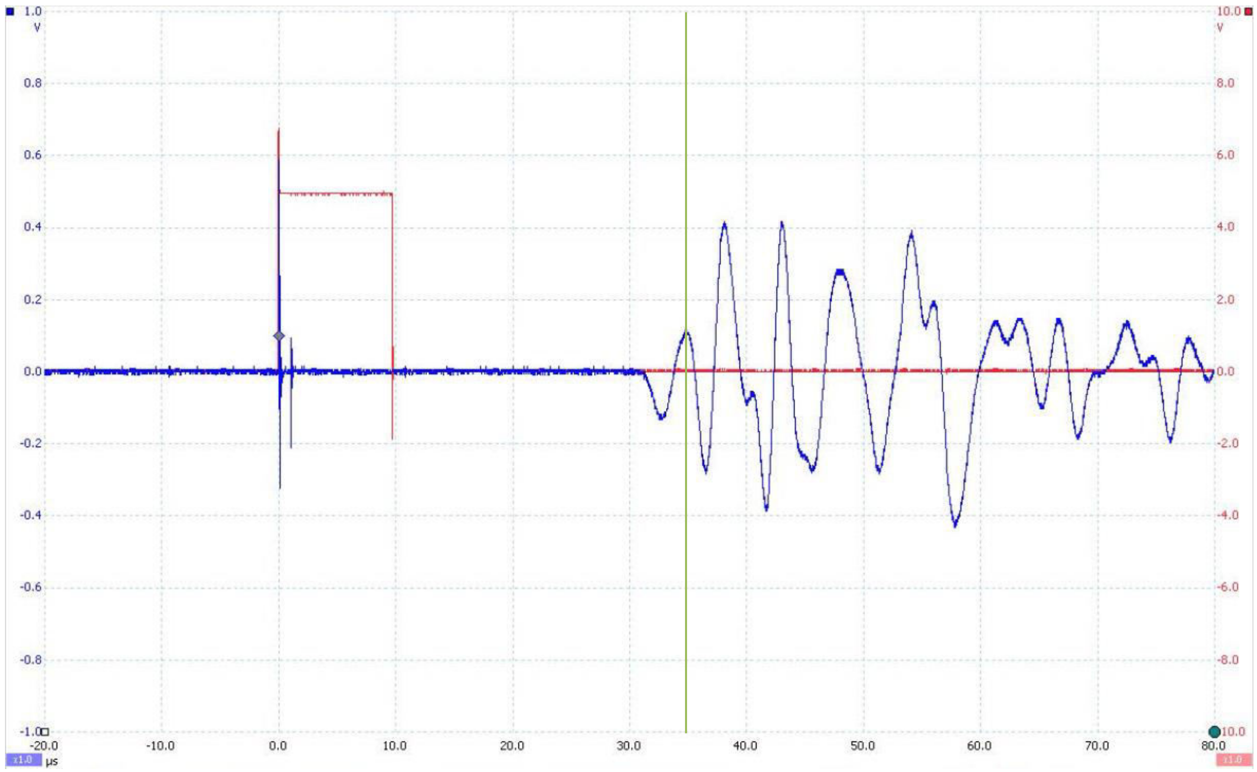

Figure B-9 – P-Wave waveform for sample 5-22-17B. Orange line indicates where travel-time was picked for calculations. Travel time: 34.75ms.

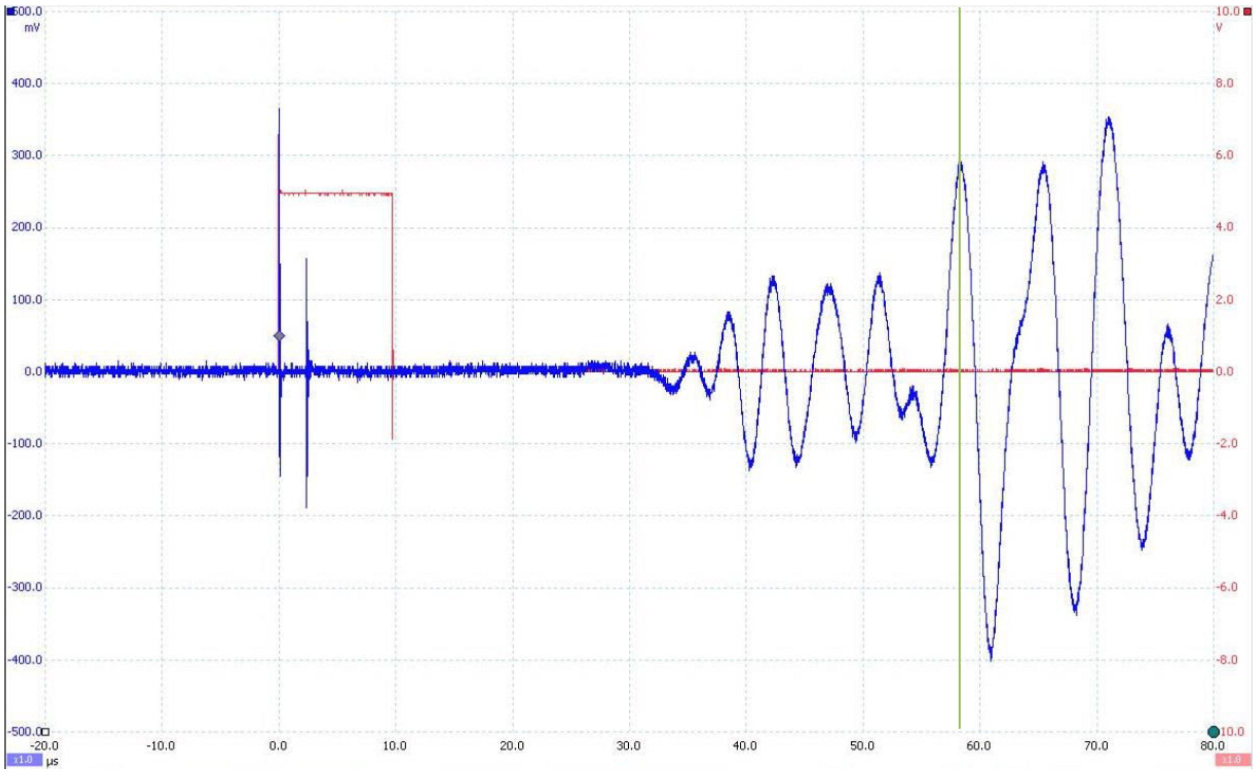

Figure B-10 – S-Wave waveform for sample 5-22-17B. Orange line indicates where travel-time was picked for calculations. Travel time: 58.21ms.

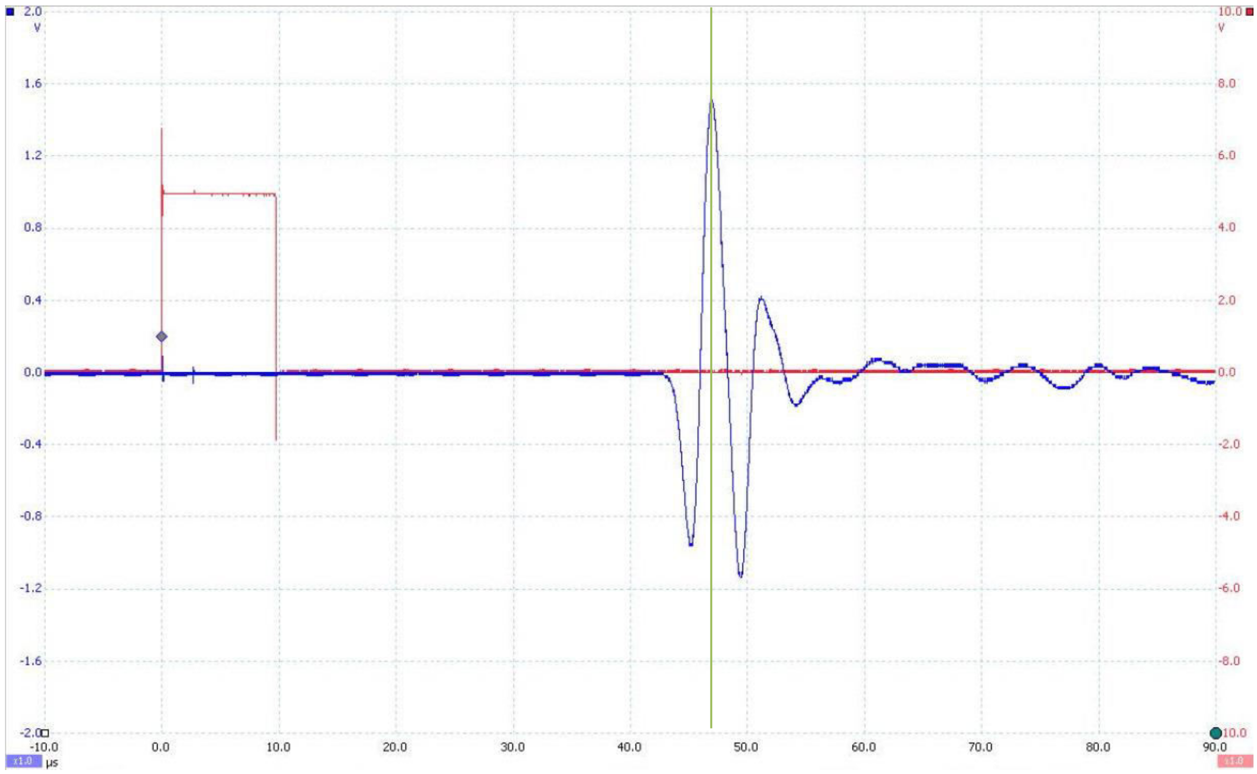

Figure B-11 – P-Wave waveform for sample 5-22-17C. Orange line indicates where travel-time was picked for calculations. Travel time: 46.89ms.

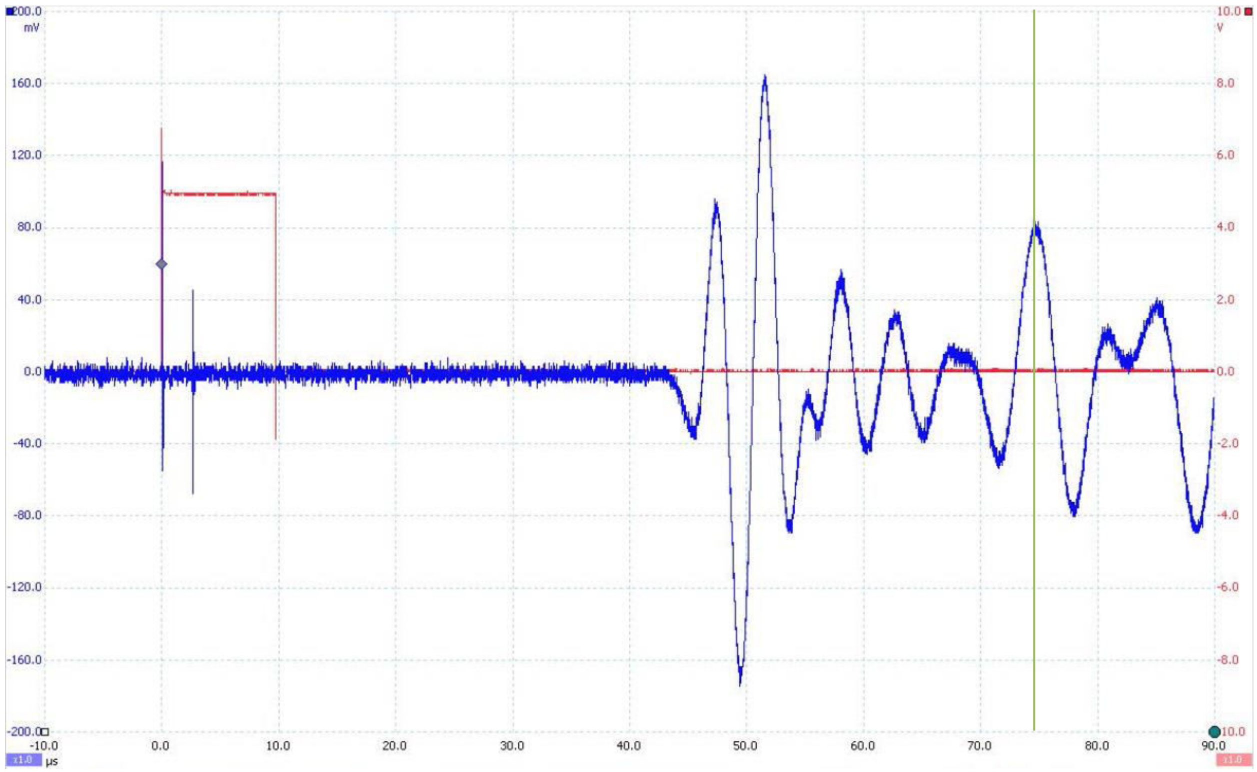

Figure B-12 – S-Wave waveform for sample 5-22-17C. Orange line indicates where travel-time was picked for calculations. Travel time: 74.54ms.

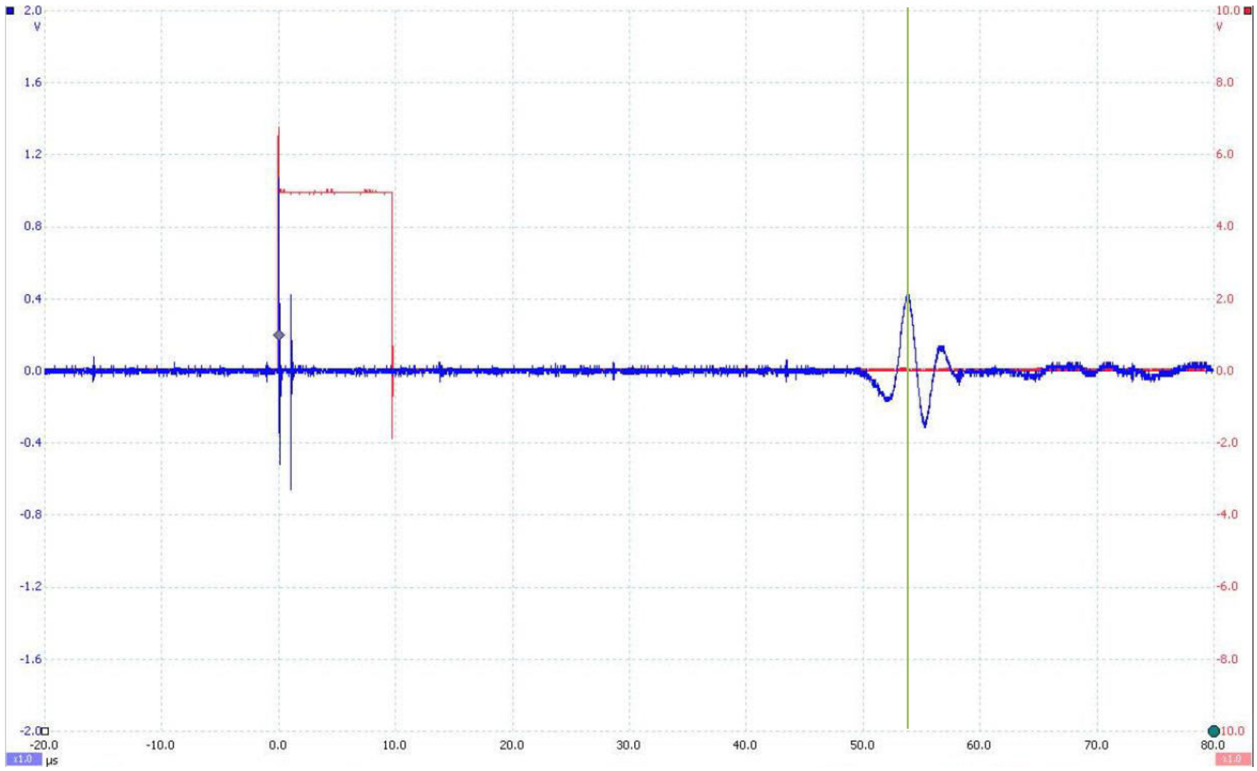

Figure B-13 – P-Wave waveform for sample 5-23-17A. Orange line indicates where travel-time was picked for calculations. Travel time: 53.77ms.

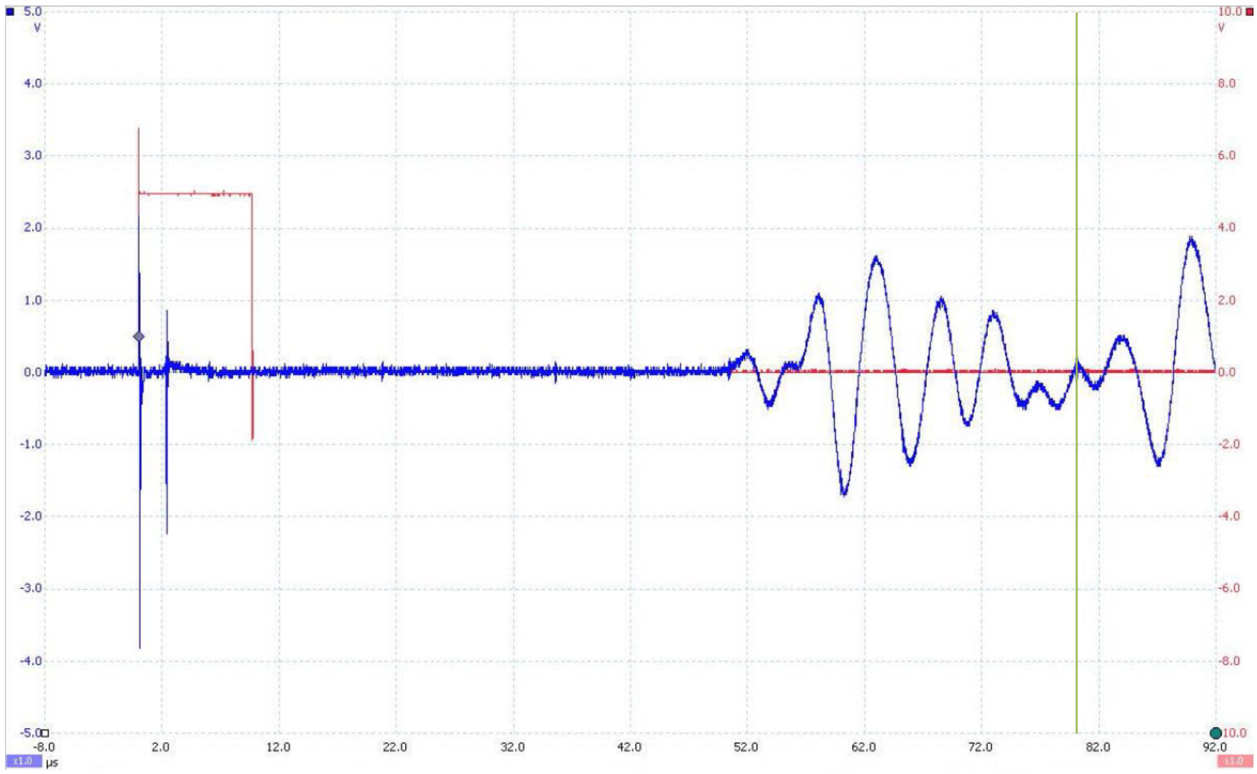

Figure B-14 – S-Wave waveform for sample 5-23-17A. Orange line indicates where travel-time was picked for calculations. Travel time: 76.6ms.

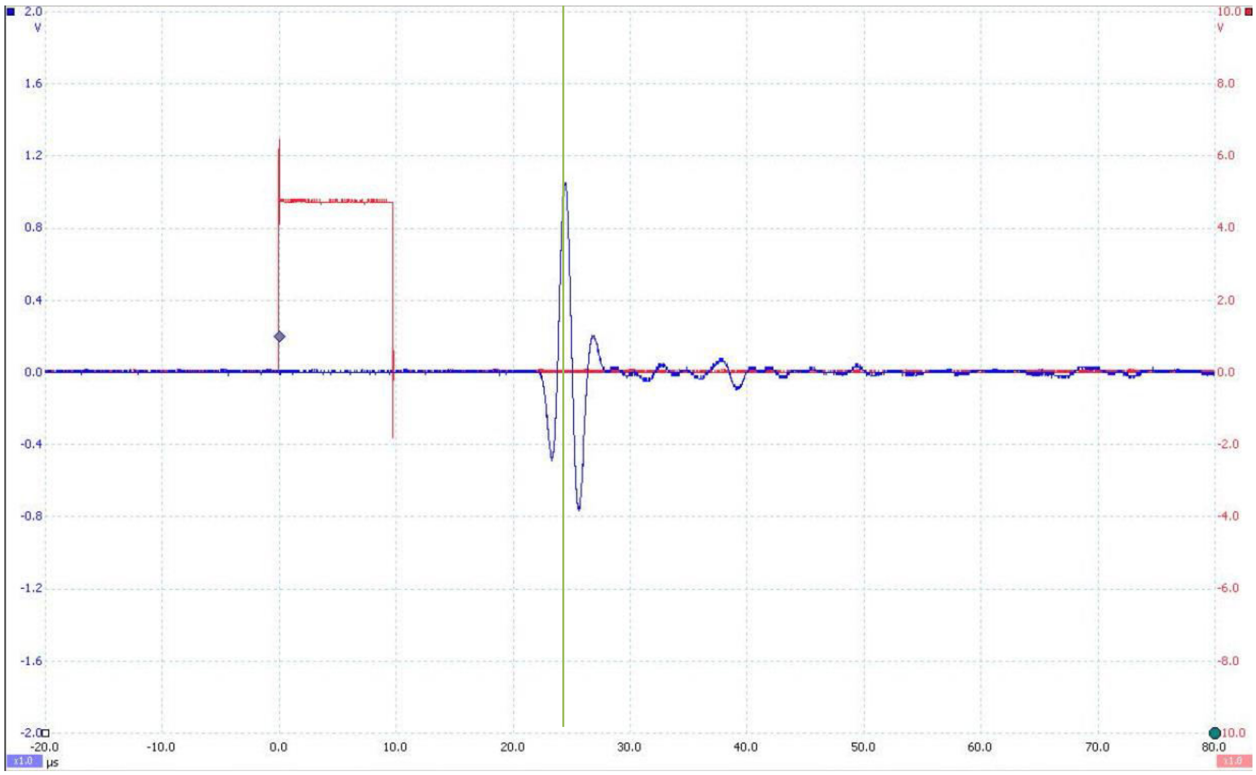

Figure B-15 – P-Wave waveform for sample 5-24-17A. Orange line indicates where travel-time was picked for calculations. Travel time: 24.41ms.

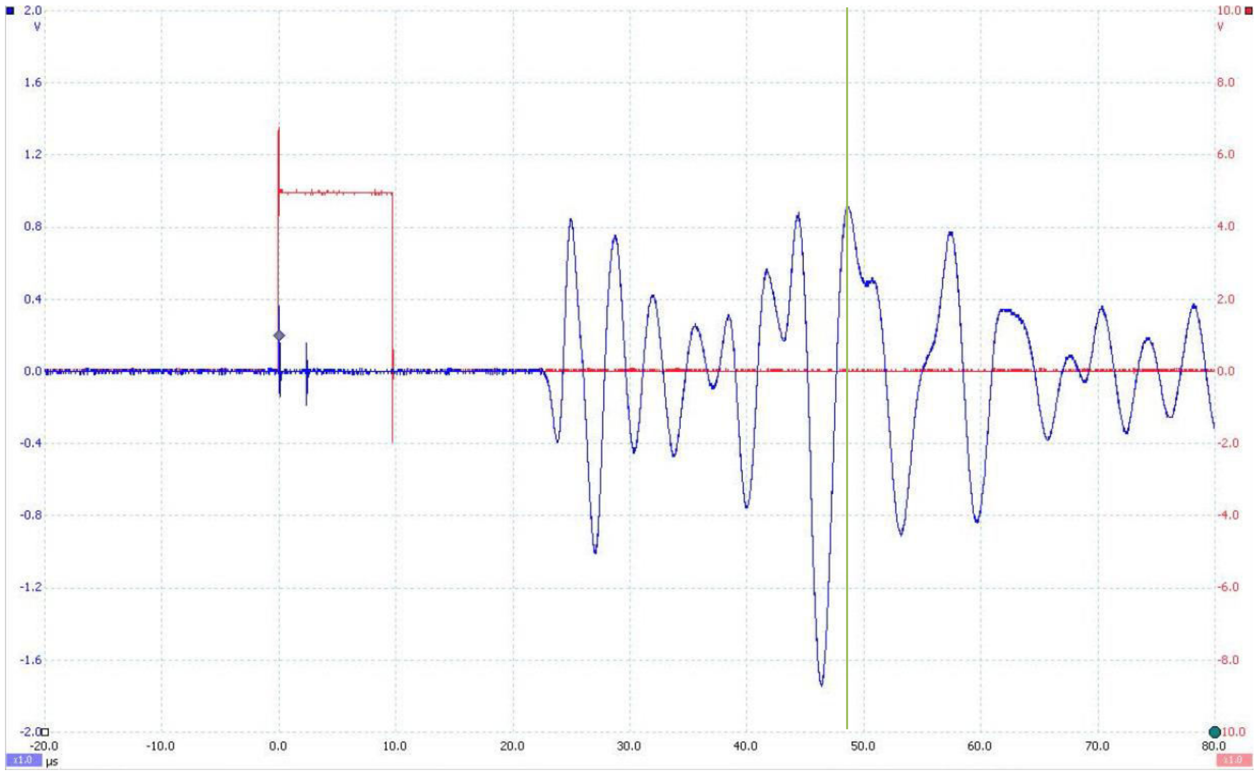

Figure B-16 – S-Wave waveform for sample 5-24-17A. Orange line indicates where travel-time was picked for calculations. Travel time: 44.ms.

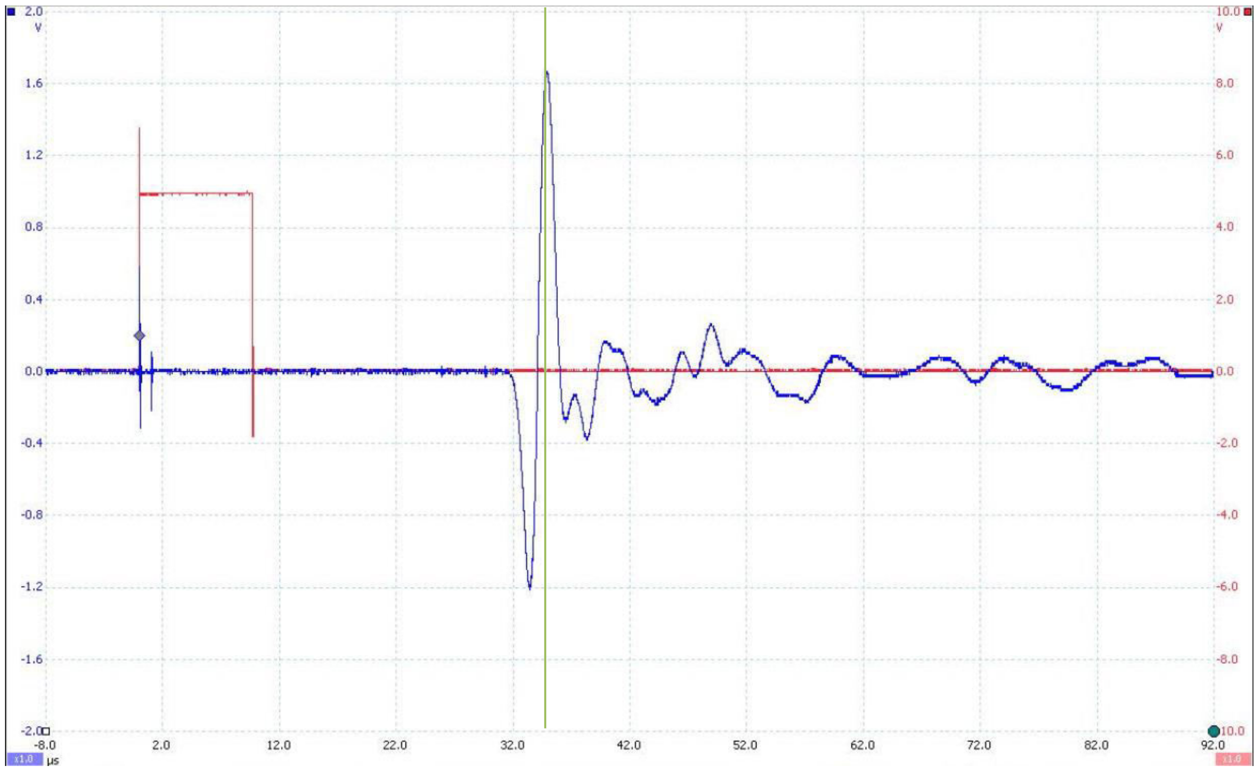

Figure B-17 – P-Wave waveform for sample 5-24-17B. Orange line indicates where travel-time was picked for calculations. Travel time: 34.83ms.

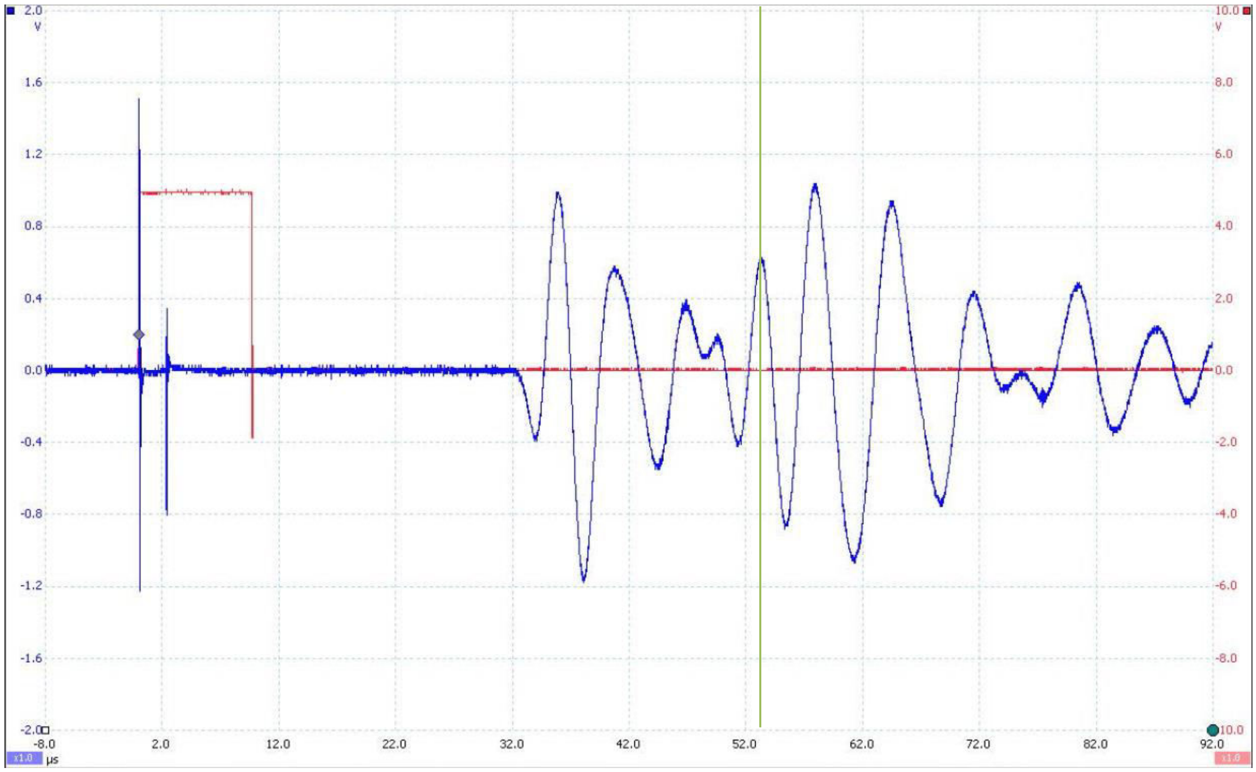

Figure B-18 – S-Wave waveform for sample 5-24-17B. Orange line indicates where travel-time was picked for calculations. Travel time: 53.27ms.

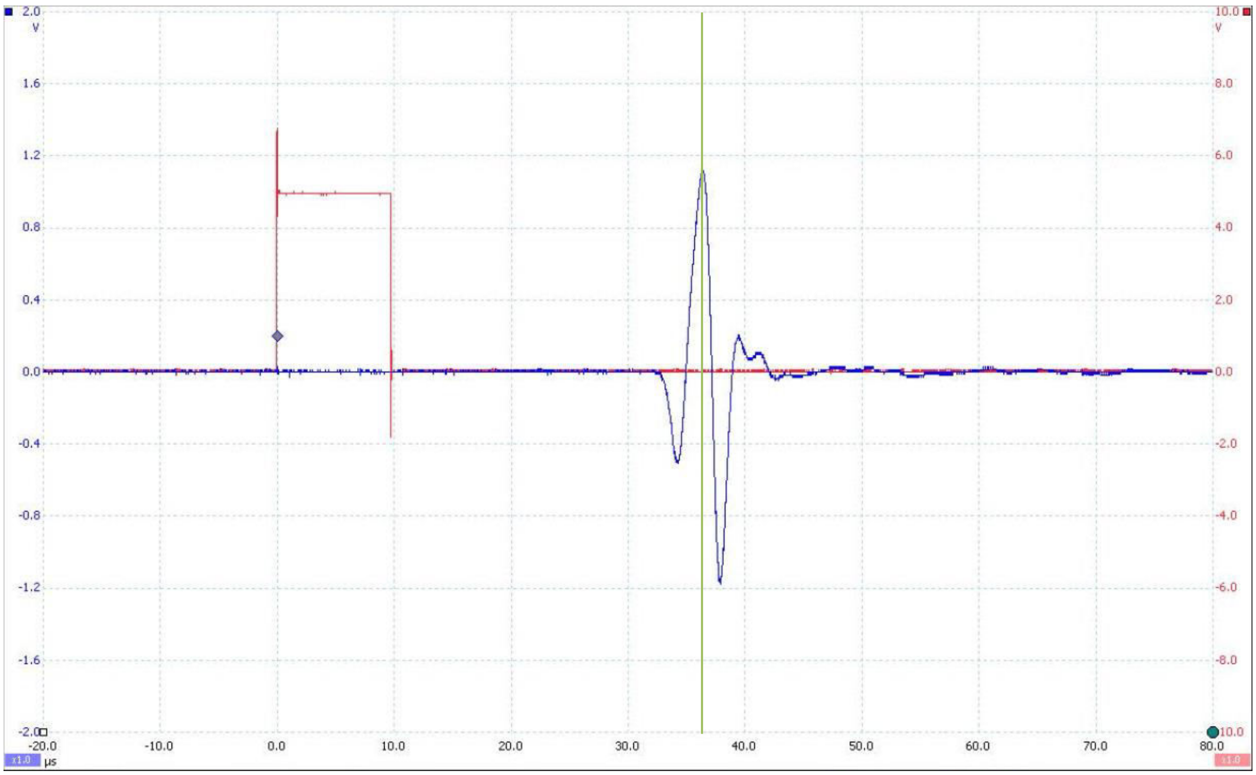

Figure B-19 – P-Wave waveform for sample 5-24-17C. Orange line indicates where travel-time was picked for calculations. Travel time: 36.33ms.

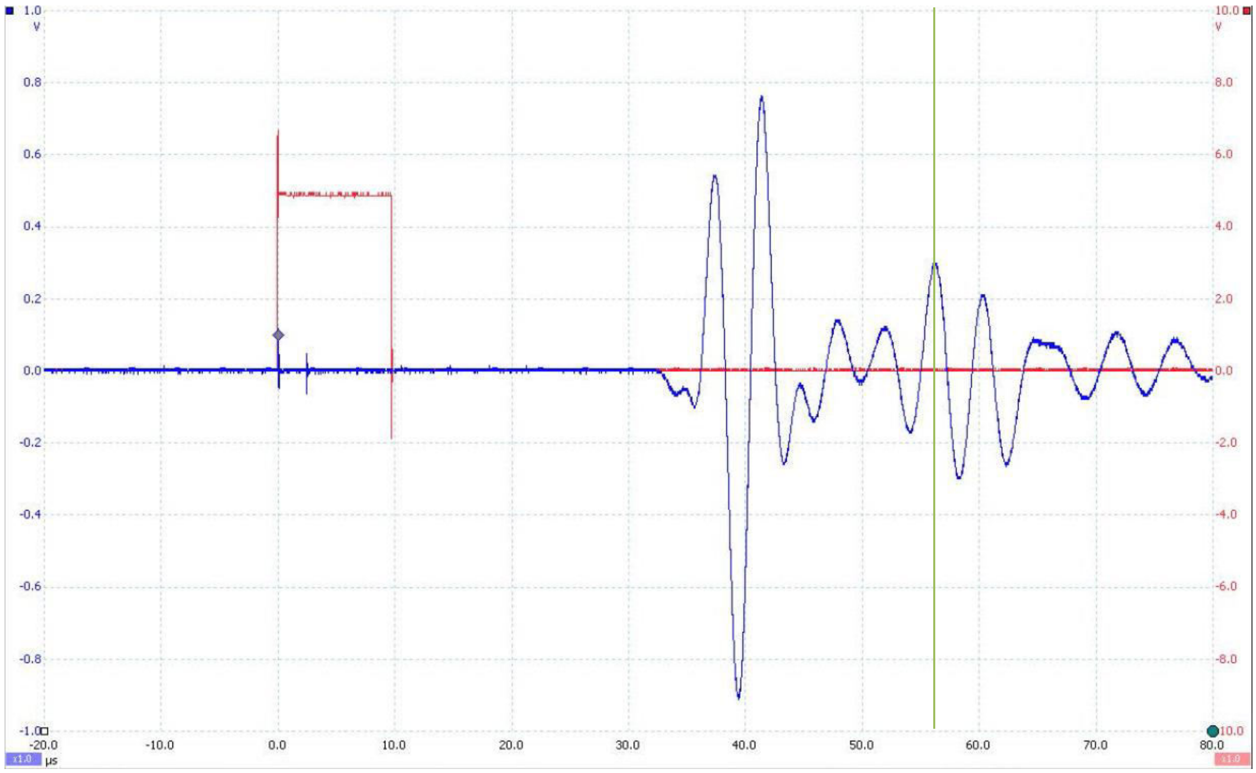

Figure B-20 – S-Wave waveform for sample 5-24-17C. Orange line indicates where travel-time was picked for calculations. Travel time: 58.06ms.

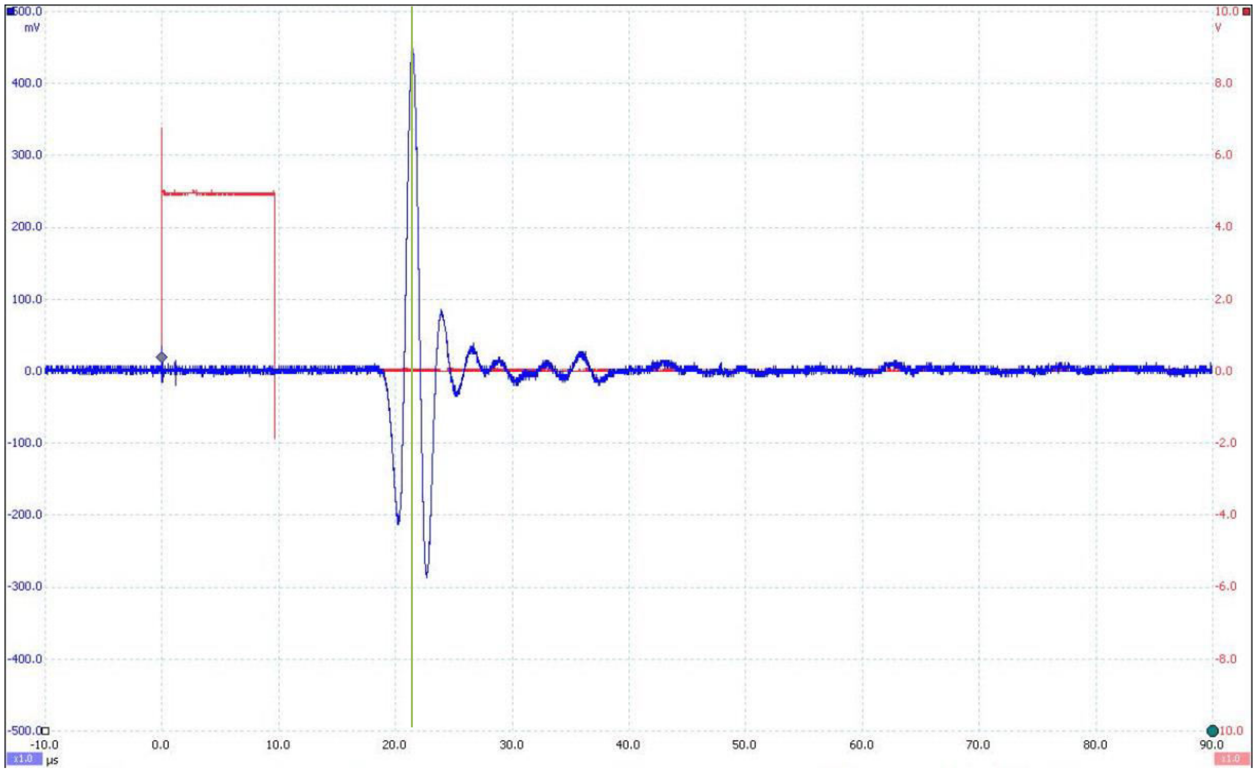

Figure B-21 – P-Wave waveform for sample 5-24-17D. Orange line indicates where travel-time was picked for calculations. Travel time: 21.47ms.

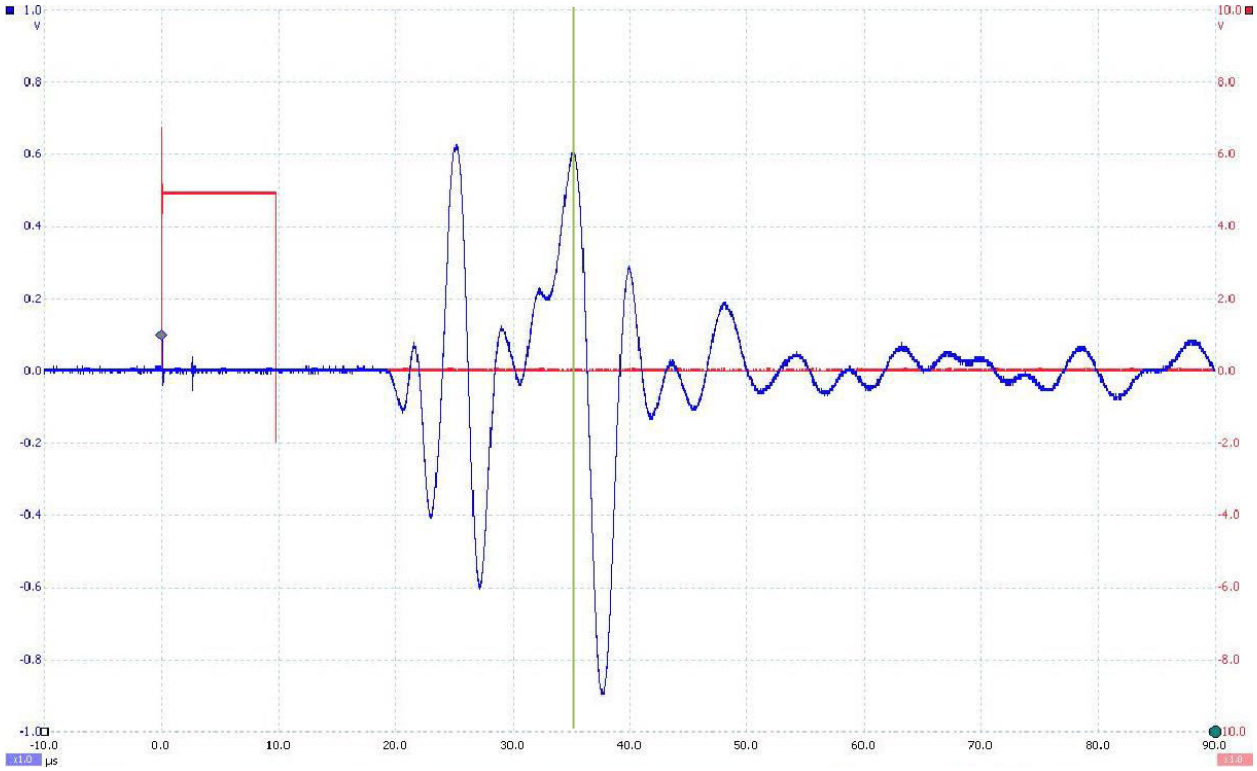

Figure B-22 – S-Wave waveform for sample 5-24-17D. Orange line indicates where travel-time was picked for calculations. Travel time: 35ms.

References

Baltz, E. H., 1972, Geologic map and cross sections of the Gallinas Creek area, Sangre de Cristo Mountains, San Miguel County, New Mexico: U.S. Geol. Survey Misc. Geol. Inv. Map 1-673 (sheet 1 of 2).

Chiles, J.P., H. Beucher, H. Wackernagel, C. Lantuejoul, P. Elion. 2008. Estimating fracture density from a linear or aerial survey. Proceedings of the VIII International Geostatistics Congress, *ed.* J. Ortiz and X. Emery. V. 1, p. 535-544. http://downloads.gecamin.cl/cierreeventos/geostats2008/prsntcns/00158 00721 p r.pdf.

Cui, Zhen-dong; Liu, Da-an; An, Guang-ming; Sun, Bo; Zhou, Miao; Cao, Fu-quan. 2009. A Comparison of two ISRM suggested chevron notched specimens for testing mode-I rock fracture toughness. International Journal of Rock Mechanics & Mining Sciences 47 (2010) 871-876.

Doolin, D.M., 1994. Fracture Toughness Testing using the Modified Ring Test, Bachelor's Thesis, University of Tennessee.

Fowell, R.J.. 1995. Suggested Method for Determining Mode I Fracture Toughness Using Cracked Chevron Notched Brazilian Disc (CCNBD) Specimens. International Journal of Rock Mechanics, Mining Science, and Geomechanics. Vol. 32, No. 1 pp. 57-64.

Fowell, R.J.; Xu, C.. 1993. The Cracked Chevron Notched Brazilian Disc Test – Geometrical Considerations for Practical Rock Fracture Toughness Measurement. International Journal of Rock Mechanics, Mining Science, and Geomechanics. Vol. 30, No. 7, pp. 821-824.

Jin, Xiaochun and Shah Subhash, 2014. A Practical Petrophysical Approach for Brittleness Prediction from Porosity and Sonic Logging in Shale Reservoirs. SPE Annual Technical Conference and Exhibition. Amsterdam, The Netherlands, 27-29 October 2014.

Lessard and Bejnar, 1976. Geology of the Las Vegas area. New Mexico Geological Society. 27th Annual Fall Field Conference Guidebook, pp. 306.

Lucas, Spencer G.; Kues, Barry S., 1985. Stratigraphic nomenclature and correlation chart for east-central New Mexico. New Mexico Geological Society 36th Annual Fall Field Conference Guidebook, 344 p.

Nara, Yoshitaka; Morimoto, Kazuya; Hiroyoshi, Naoki; Yoneda, Tetsuro; Kaneko, Katsuhiko; Benson, Phillip M. 2012. Influence of relative humidity on fracture toughness of rock: Implication for subcritical crack growth. International Journal of Solids and Structures. Vol. 49, Issue 18, 15 September 2012, pp. 2471-2481. Table 3.

Park, Namsu., 2006. Discrete Element Modeling of Rock Fracture Behavior: Fracture Toughness and Time-Dependent Fracture Growth [Ph.D. thesis]: Austin, The University of Texas. Pp. 66.

Rickman, R., M. Mullen, J. Petre, W. Grieser, and D. Kundert (2008), A practical use of shale petrophysics for stimulation design optimization: all shale plays are not clones of the barnett shale, paper presented at SPE Annual Technical Conference and Exhibition, Denver, Colorado, USA, September 21-24.

Sheriff, R.E., 1991, Encyclopedic Dictionary of Exploration Geophysics, 3rd ed. Society of Exploration Geophysics, Tulsa, OK.

Thiercelin, M. and Roegiers, J.C., 1986. Toughness Determination with the Modified Ring Test, Proceeding of 27th U.S. Symposium on Rock Mechanics: Key to Energy Production, pp. 615-622.

Thiercelin, M., 1989, Fracture Toughness and Hydraulic Fracturing International Journal of Rock Mechanics and Mining Sciences & Geomechanics Abstracts, Vol. 26, No. 3, pp. 177-183.

Wanek, A. A., 1962, Reconnaissance geologic map of parts of Harding, San Miguel, and Mora Counties, New Mexico: U.S. Geological Survey, Oil and Gas Investigations Map OM-208.

Wang, Q.Z. 2007. Formula for calculating the critical stress intensity factor in rock fracture toughness tests using cracked chevron notched Brazilian disc (CCNBD) specimens. International Journal of Rock Mechanics & Mining Sciences 47 (2010) 1006-1011.

Whittaker, Barry N.; Singh, Raghu N.; Sun, Gexin. 1992. Rock Fracture Mechanics Principles, Design and Applications. Developments in Geotechnical Engineering 71: 349-371.
Wickham, John; Yu, Xinbau; McMullen, Richard. 2013. Geomechanics of Fracture Density. Unconventional Resources Technology Conference. URTeC Control ID # 1619745.

Zhixi, Chen; Mian, Chen; Yan, Jin; Rongzun, Huang. 1997. Determination of Rock Fracture Toughness and its Relationship with Acoustic Velocity. International Journal of Rock Mechanics & Mining Sciences 34 (1997) ISSN 0148-9062.

Zoback, M.D., 1978. A Simple Hydraulic Fracturing for Determining Rock Fracture Toughness, Proceedings of 19th U.S. Symposium on Rock Mechanics, pp. 83-85.

Biographical Information

Scott Moore graduated from the University of Texas at Arlington in August of 2018 with a Master of Science in Petroleum Geoscience. During his time at UTA he worked as a geotech at Omimex Petroleum in Fort Worth and interned at Lewis Energy Group as a geology intern in San Antonio. Prior to attending UTA, he graduated from the University of Kansas where he graduated with a Bachelor of Science in Geology in December of 2015. After graduation he will move to Oklahoma City, Oklahoma where he will work as a Geoscience Intern with Baker Hughes in their Real Time Services team.